UNIVERSIDADE FEDERAL DO RIO GRANDE DO SUL
INSTITUTO DE CIÊNCIAS BÁSICAS DA SAÚDE
PROGRAMA DE PÓS-GRADUAÇÃO EM NEUROCIÊNCIAS

EFEITOS DA ADMINISTRAÇÃO INTRACEREBROVENTRICULAR DE ÁCIDO ARÚNDICO SOBRE ASPECTOS HISTOLÓGICOS, BIOQUÍMICOS E COMPORTAMENTAIS NO MODELO EXPERIMENTAL DE HEMORRAGIA INTRACEREBRAL EM RATOS

JULIANA DE LIMA CORDEIRO

Porto Alegre
2020

UNIVERSIDADE FEDERAL DO RIO GRANDE DO SUL
INSTITUTO DE CIÊNCIAS BÁSICAS DA SAÚDE
PROGRAMA DE PÓS-GRADUAÇÃO EM NEUROCIÊNCIAS

EFEITOS DA ADMINISTRAÇÃO INTRACEREBROVENTRICULAR DE ÁCIDO ARÚNDICO SOBRE ASPECTOS HISTOLÓGICOS, BIOQUÍMICOS E COMPORTAMENTAIS NO MODELO EXPERIMENTAL DE HEMORRAGIA INTRACEREBRAL EM RATOS

Orientador: Prof. Dr. Carlos Alexandre Netto

Tese apresentada ao Programa de Pós-Graduação em Neurociências da Universidade Federal do Rio Grande do Sul como requisito parcial para obtenção do título de Doutora em Neurociências.

Porto Alegre
2020

AGRADECIMENTOS

Agradeço ao Programa de Pós-Graduação em Neurociências, por proporcionar excelente formação e construção de conhecimentos aos seus alunos.

Ao meu orientador, prof. Dr. Carlos Alexandre Netto, por ter me acolhido como doutoranda e confiado no meu trabalho. Obrigada por todos os conhecimentos transmitidos, pela disponibilidade em ajudar, pelas palavras de calma e sabedoria que me guiaram ao longo de todo esse percurso.

Aos meus colegas e amigos do Laboratório 35, pela colaboração, parceria e amizade. Muito obrigada por estarmos juntos em cada etapa desse trabalho, que só foi possível com a ajuda e companheirismo de vocês.

À minha família, por ser parte indispensável da minha vida, por me proporcionar todo o suporte de que preciso e por estar sempre presente, mesmo que longe fisicamente. `

Às minhas amigas, de perto e de longe, pelo apoio e por sempre torcerem pelo meu sucesso e felicidade.

Ao meu amor, por ser o meu companheiro de vida e estar sempre ao meu lado, tornando tudo mais leve.

O presente trabalho foi realizado com apoio da Coordenação de Aperfeiçoamento de Pessoal Nivel Superior – Brasil (CAPES) – Código de Financiamento 001.

SUMÁRIO

APRESENTAÇÃO

Esta tese é constituída por:

PARTE I:

1. Introdução: contém o embasamento teórico necessário para a compreensão da proposta de trabalho e objetivos.

2. Justificativa: elucida a relevância científica do estudo realizado.

3. Hipótese: expõe os principais resultados esperados.

4. Objetivos: definem os propósitos centrais do trabalho, desenvolvidos ao longo dos capítulos 1 e 2.

PARTE II:

Capítulo 1: Artigo publicado no periódico *Neuroscience* – "Arundic acid (ONO-2506), an inhibitor of S100B protein synthesis, prevents neurological deficits and brain tissue damage following intracerebral hemorrhage in male Wistar rats".

Capítulo 2: Artigo submetido ao periódico *Cellular and Molecular Neurobiology* – "Arundic acid (ONO-2506) attenuates neuroinflammation and prevents motor impairment in rats with intracerebral hemorrhage".

PARTE III:

Discussão Geral: contém a interpretação dos resultados obtidos nos artigos 1 e 2, englobando-os em um contexto geral.

Conclusões: abordam as conclusões gerais da tese.

Referências: listam as referências citadas nas seções Introdução e Discussão.

LISTA DE ABREVIATURAS

AA = ácido arúndico

AVC = acidente vascular cerebral

BHE = barreira hemato-encefálica

ERO = espécies reativas de oxigênio

GFAP = proteína glial fibrilar ácida

GS = glutamina sintetase

GSH = glutationa

HB = hemoglobina

HIC = hemorragia intracerebral

ICV = intracerebroventricular

IL-1β = interleucina - 1β

LCE = líquido cerebrospinal

MMP = metaloproteinase de matriz

RAGE = receptor para produtos finais de glicação avançada

SNC = sistema nervoso central

TNF-α = fator de necrose tumoral – α

LISTA DE FIGURAS

Introdução

Capítulo 1

Capítulo 2

Discussão Geral

RESUMO

A hemorragia intracerebral (HIC) consiste no principal subtipo de acidente vascular cerebral (AVC) hemorrágico, sendo responsável por altas taxas de mortalidade e graves sequelas neurológicas. Até o momento, não existe nenhum tratamento específico capaz de melhorar os desfechos da doença. Níveis aumentados da proteína astrocitária S100B são reportados após a HIC e contribuem no mecanismo de lesão cerebral secundária, estando associados à exacerbação da neuroinflamação, agravamento da lesão e piores desfechos neurológicos. A inibição da síntese de S100B pelos astrócitos através do ácido arúndico (AA) tem mostrado efeitos neuroprotetores em diferentes modelos experimentais de doenças do sistema nervoso central (SNC), mas seus efeitos ainda não foram estudados na HIC. Esta tese teve como objetivos estabelecer uma concentração efetiva para a administração intracerebroventricular (ICV) de AA e analisar os seus efeitos em ratos submetidos à HIC induzida por colagenase, quanto aos níveis centrais e periféricos de S100B, reatividade astrocitária e microglial, morte neuronal, parâmetros inflamatórios e oxidativos, assim como suas consequências no volume de lesão e na função neurológica dos animais. Inicialmente, ratos Wistar machos sem lesão prévia receberam umas das seguintes concentrações de AA: 0.02, 0.2, 2 e 20 µg/µl; e a concentração mais efetiva na redução dos níveis de S100B e GFAP no estriado (2 µg/µl) foi utilizada nos experimentos seguintes. Para os próximos experimentos, os ratos foram submetidos a uma cirurgia estereotáxica para administração de AA no ventrículo esquerdo e de colagenase no estriado dorsolateral esquerdo. As análises bioquímicas foram realizadas 24h, 72h e 7 dias após a HIC, e as análises histológicas e comportamentais em 72h e 7 dias após a lesão. Os resultados mostram que o tratamento com AA reduziu os níveis de S100B no estriado, soro e liquido cerebrospinal, assim como os níveis de proteína glial fibrilar ácida (GFAP, indicador de reatividade astrocitária) no estriado. Além disso, o AA aumentou os níveis do antioxidante cerebral glutationa (GSH), reduziu a formação de espécies reativas de oxigênio (ERO), e atenuou a ativação da microglia, reduzindo os níveis das citocinas inflamatórias interleucina-1β (IL-1β) e fator de necrose tumoral-α (TNF-α). Essas ações neuroprotetoras culminaram no aumento da sobrevivência neuronal (manutenção da densidade neuronal e prevenção de apoptose) no estriado, na limitação da expansão do volume de lesão e na prevenção de déficits neurológicos nos animais tratados. Os resultados sugerem que a proteína S100B tem um importante papel no mecanismo de lesão secundária inicial da HIC, e que o Ácido Arúndico demonstrou ser um agente neuroprotetor promissor no tratamento da doença.

Palavras-chave: Hemorragia intracerebral; S100B; astrócito; ácido arúndico; neuroinflamação

ABSTRACT

Intracerebral hemorrhage (ICH) is the main subtype of hemorrhagic stroke, being responsible for high mortality rates and severe neurological impairments. To date, there is no specific treatment capable to improve the disease outcomes. Increased levels of the astrocytic protein S100B are reported after ICH and contribute to the mechanism of secondary brain injury, being associated with exacerbation of neuroinflammation and worsening of the injury and neurological deficits. Inhibition of astrocytic synthesis of S100B by arundic acid (AA) has shown neuroprotective effects in different experimental models of central nervous system (CNS) disorders, but its effects have not yet been studied in ICH. This thesis aimed to establish an effective concentration for intracerebroventricular (ICV) administration of AA and to analyze its effects in rats submitted to collagenase-induced ICH, in terms of central and peripheral levels of S100B, astrocytic and microglial reactivity, neuronal death, inflammatory and oxidative parameters, as well as its consequences in the lesion volume and functional neurological outcome. Initially, rats without previous CNS injury received one of the following concentrations of AA: 0.02, 0.2, 2 and 20 µg/µl; and the most effective concentration in reducing S100B and GFAP striatal levels (2 µg/µl) was used in the following experiments. For the next experiments, rats underwent a stereotactic surgery to AA administration in the left ventricle and collagenase in the left dorsolateral striatum. Biochemical analyzes were performed 24h, 72h and 7 days after ICH, and histological and behavioral analyzes at 72h and 7 days after the injury. Results show that the AA treatment reduced S100B levels in the striatum, serum and cerebrospinal fluid, as well as the glial fibrillar acid protein (GFAP, indicator of astrocytic reactivity) levels in the striatum. In addition, AA increased levels of the brain antioxidant glutathione (GSH), reduced the production of reactive oxygen species (ROS), and attenuated the activation of microglia, thus reducing the levels of the inflammatory cytokines interleukin-1β (IL-1β) and tumor necrosis factor-α (TNF-α). These neuroprotective effects culminated in improving neuronal survival (maintaining neuronal density and preventing apoptosis) in the striatum, limiting the expansion of the lesion volume and preventing neurological deficits in treated animals. Thus, the S100B protein has been shown to play an important role in the initial secondary injury mechanism of ICH, and AA has proved to be a promising neuroprotective agent in the treatment of the disease.

Keywords: Intracerebral hemorrhage; S100B; arundic acid; astrocyte; neuroinflammation

PARTE I

1. INTRODUÇÃO

A hemorragia intracerebral (HIC) consiste no extravasamento sanguíneo para o interior do parênquima cerebral ou espaços ventriculares (Mracsko and Veltkamp, 2014; Provencio et al., 2013). Alterações degenerativas relacionadas à hipertensão arterial ou angiopatia amilóide cerebral são responsáveis por 50% e 20% dos casos, respectivamente (Qureshi et al., 2001). A hemorragia relacionada à hipertensão, na maior parte dos casos, ocorre nas proximidades ou na bifurcação de pequenas artérias penetrantes que se originam das artérias basilares ou das artérias cerebrais anterior, média ou posterior (Campbell and Khatri, 2020). Por sua vez, a angiopatia amilóide cerebral é caracterizada pela deposição de peptídeo β-amilóide e alterações degenerativas nos vasos sanguíneos do encéfalo (Rosand et al., 2000). Outros fatores de risco relevantes são o uso oral de anticoagulantes, obesidade, diabetes mellitus, colesterol alto, tumores cerebrais, aneurismas, malformações vasculares cerebrais, angiomas cavernosos e fístulas arteriovenosas (Qureshi et al., 2009).

As internações por HIC aumentaram nas últimas décadas devido ao aumento do número de idosos, muitos dos quais não possuem um controle adequado da pressão arterial, e ao uso crescente de anticoagulantes, trombolíticos e antiagregantes plaquetários (Campbell and Khatri, 2020; Garton et al., 2020; Qureshi et al., 2009). A HIC corresponde a 15% de todos os AVCs e possui uma incidência anual de 10-30 para cada 100 mil pessoas, totalizando cerca de 2 milhões de novos casos no mundo a cada ano (Labovitz et al., 2005; van Asch et al., 2010). Constitui um importante problema de saúde pública,

sendo responsável por altas taxas de morbidade e mortalidade: 40-50% dos pacientes morrem no primeiro ano após a HIC e 70% dentro de 5 anos (Poon et al., 2014); além disso, apenas 20% dos sobreviventes recuperam sua independência funcional 6 meses após o evento (van Asch et al., 2010).

Comumente, a HIC afeta os lobos cerebrais, os núcleos da base, o tálamo, o tronco encefálico (principalmente a ponte) e o cerebelo (Qureshi et al., 2001; Xi et al., 2006), resultando em morte celular em torno da região do hematoma e consequente atrofia cerebral (Keep et al., 2012). A localização da hemorragia, o volume inicial e a expansão do hematoma podem ser preditores do prognóstico e determinantes na escolha de um potencial tratamento (Schlunk and Greenberg, 2015). As hemorragias pontinas, por exemplo, possuem a maior mortalidade e as hemorragias superficiais podem ser mais viáveis de tratar cirurgicamente (Mendelow et al., 2011). Em cerca de 20 a 40% dos casos, ocorre expansão do hematoma no primeiro dia após o dano inicial, contribuindo para o efeito de massa da HIC com consequente compressão mecânica das estruturas cerebrais (Balami and Buchan, 2012; Dowlatshahi et al., 2011). Em torno do hematoma, ocorre a formação de edema, cujo volume aumenta cerca de 75% nas primeiras 24 horas, atingindo o pico entre 5 a 6 dias e contribuindo consideravelmente para o efeito de massa e a lesão cerebral (Gebel et al., 2002; Inaji et al., 2003).

A apresentação clínica clássica do AVC hemorrágico inclui déficits neurológicos focais de início rápido, diminuição da consciência e sinais de disfunção do tronco encefálico, os quais estão relacionados ao tamanho e à localização do hematoma (Qureshi et al., 2009).

Até o momento, nenhum tratamento clínico ou cirúrgico se mostrou capaz de reduzir a mortalidade ou melhorar o desfecho clínico dos pacientes, especialmente em fases agudas da HIC. O tratamento baseia-se nos cuidados dentro da unidade de terapia intensiva, a fim de garantir controle/prevenção da hipertensão arterial, coagulopatia, aumento da pressão intracraniana (em alguns casos é necessária a colocação de um cateter de drenagem ventricular). Além disso, alguns casos podem requerer a realização de uma craniotomia ou craniectomia para evacuação da hemorragia e/ou descompressão (Fiorella et al., 2015; Thabet et al., 2017; Ziai and Carhuapoma, 2018).

1.1. Fisiopatologia da hemorragia intracerebral (HIC)

1.1.1. Lesão cerebral primária

O sangramento no interior do parênquima cerebral leva à formação de um hematoma, ocasionando o aumento da pressão intracraniana, compressão de estruturas cerebrais (podendo levar à hérnia cerebral), redução do fluxo sanguíneo (isquemia) e destruição mecânica direta de axônios e células gliais. (Keep et al., 2012; Qureshi et al., 2009).

Após o início do sangramento, a expansão do hematoma agrava os danos cerebrais em 20 a 40% dos pacientes dentro de 24 horas (Balami and Buchan, 2012). As regiões circundantes ao hematoma são caracterizadas por edema, apoptose, necrose e células inflamatórias (Qureshi et al., 2003). O edema periematomal aumenta em volume em cerca de 75% nas primeiras 24 horas após a HIC (Gebel et al., 2002), atinge o pico em torno de 5 a 6 dias e

dura até 14 dias (Inaji et al., 2003). Na presença de uma pressão intracraniana muito elevada e uma baixa pressão de perfusão cerebral, torna-se alto o risco de isquemia global (Qureshi et al., 2009).

1.1.2. Lesão cerebral secundária

A lesão secundária após a HIC pode ser causada por uma cascata de eventos iniciados pela lesão primária (por exemplo, efeito de massa e ruptura física), pela resposta fisiológica ao hematoma (por exemplo, inflamação) e pela liberação de componentes do coágulo (por exemplo, hemoglobina e ferro) (Keep et al., 2012) **(Figura 1)**.

Os produtos derivados do sangue, como a hemoglobina (Hb), heme e ferro, são altamente tóxicos ao tecido cerebral e têm sido implicados como potentes mediadores da lesão após a HIC (Lin et al., 2012a; Righy et al., 2016). A lise eritrocitária ocorre dentro de minutos e continua por vários dias após a formação do hematoma (Wu et al., 2003). Heme, o principal componente da hemoglobina, é degradada em biliverdina, monóxido de carbono e ferro, através das heme oxigenases (HO) (Righy et al., 2016). A sobrecarga de ferro no encéfalo após a hemorragia gera altos níveis de espécies reativas de oxigênio (EROs) (Xiong et al., 2014). Hb, heme e ferro são potencialmente citotóxicos e, através de uma ampla variedade de mecanismos, aumentam a resposta inflamatória e promovem a oxidação de proteínas, ácidos nucleicos, carboidratos e lipídios, interrompendo a sinalização celular e causando, finalmente, a morte celular (Dutra and Bozza, 2014; Figueiredo et al., 2007). Neste processo de lesão, o neurotransmissor excitatório glutamato é liberado em quantidades patológicas por neurônios necróticos ao redor do hematoma e

por vasos rompidos, levando ao acúmulo de subprodutos oxidativos, ainda mais necrose de células vizinhas e à formação de edema citotóxico (Sharp et al., 2008).

Outra resposta do tecido cerebral à hemorragia é a ativação de mecanismos hemostáticos para limitar o sangramento, como a liberação de trombina. A trombina, no entanto, afeta diversos tipos de células na penumbra circundante, criando condições inflamatórias e neurotóxicas (Xi et al., 2003): ativa as células microgliais, as quais liberam mediadores inflamatórios; causa proliferação de células mesenquimais e formação de tecido cicatricial; e leva à disfunção das células endoteliais, resultando em aumento da permeabilidade, rompimento da BHE e formação de edema vasogênico (Liu et al., 2010; Xi et al., 2003).

A disfunção da BHE após a HIC não apenas contribui para a inflamação, favorecendo a infiltração de leucócitos, mas é também uma consequência da resposta inflamatória, uma vez que EROs derivadas de leucócitos, citocinas pró-inflamatórias, quimiocinas e metaloproteinases de matriz (MMPs) promovem a ruptura da BHE (Keep et al., 2008). Células inflamatórias, tais como leucócitos derivados do sangue, microglia, macrófagos, astrócitos e mastócitos são vitais para a depuração do hematoma, mas também podem aumentar a lesão cerebral causada pela HIC, devido à excreção de uma variedade de citocinas e quimiocinas (Wu et al., 2010; Zhang et al., 2017).

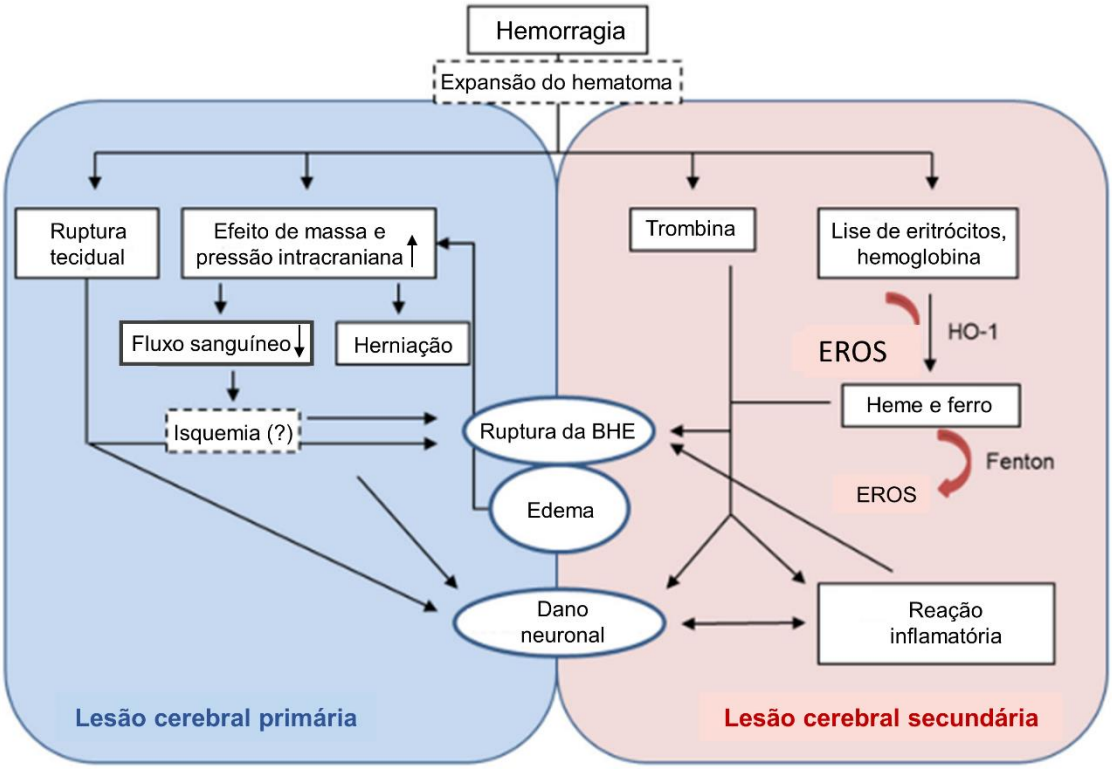

Figura 1. Representação esquemática do mecanismo de lesão cerebral primária e secundária após hemorragia intracerebral. BHE = barreira hemato-encefálica; EROs = espécies reativas de oxigênio; HO-1 = heme oxigenase-1. (Adaptada de Mraksco et al., 2014)

1.2. Modelos animais de HIC

Os modelos animais mais utilizados atualmente para estudar os efeitos da HIC espontânea consistem na infusão intraestriatal de colagenase bacteriana (tipo IV ou tipo VII) ou de sangue autólogo, usualmente em roedores. Ambos os modelos são úteis no estudo dos mecanismos e progressão da lesão, assim como na investigação de potenciais tratamentos.

A colagenase é uma enzima derivada da bactéria anaeróbica *clostridium hystolyticum* que, quando injetada no estriado, age dissolvendo a matriz extracelular periendotelial à base de colágeno, levando à ruptura da lâmina basal de vasos sanguíneos, o que resulta em hemorragia espontânea no tecido circundante (Askenase et al., 2016; MacLellan et al., 2010). O sangramento

ocorre após aproximadamente 10 minutos, com crescimento adicional do hematoma durante pelo menos 2 horas (Won et al., 2013). Esta abordagem contempla alguns elementos-chave da HIC na clínica, incluindo o dano endotelial, rompimento da barreira hematoencefálica, o sangramento / ressangramento contínuo e subsequente expansão do hematoma (James et al., 2008; Schlunk and Greenberg, 2015). Além disso, o modelo é altamente reprodutível e reproduz a fisiopatologia da morte celular secundária e do edema causado pelo hematoma (Schlunk and Greenberg, 2015).

No entanto, sabe-se que o modelo induzido por injeção estereotáxica de colagenase não simula exatamente as mesmas condições da HIC humana, em que ocorre a ruptura de um único vaso, devido à combinação de danos estruturais crônicos e efeitos intrínsecos de pulsações sanguíneas intravasculares (Schlunk and Greenberg, 2015). Outro fator que deve ser levado em consideração, sugerido por alguns autores, é que este modelo gera níveis mais altos de inflamação que outros modelos, possivelmente como resultado da presença de traços bacterianos contaminantes, da capacidade de ativar receptores de reconhecimento de padrões bacterianos ou simplesmente devido à dissolução contínua da membrana basal (Barratt et al., 2014; MacLellan et al., 2010; Xue and Del Bigio, 2003).

O modelo de HIC induzido por injeção estriatal de sangue autólogo mimetiza os efeitos de um hematoma intracerebral, possuindo a vantagem do controle preciso do tamanho do hematoma. No entanto, esta abordagem não modela efetivamente o dano endotelial, a ruptura dos vasos sanguíneos ou o sangramento sustentado associado a HIC na clínica. Acredita-se que fatores solúveis associados ao dano endotelial, incluindo ativadores da cascata do

complemento e trombina, sejam importantes sinais precoces na patologia da HIC (Babu et al., 2012).

Um estudo (Maclellan et al., 2008) comparou os dois modelos animais e concluiu que, embora tenha-se ajustado a dose de colagenase para produzir um hematoma de igual tamanho ao do modelo de infusão de sangue, o tamanho final da lesão induzida por colagenase foi substancialmente maior, resultou em maiores danos à BHE, ao estriado, substância negra, substância branca e córtex cerebral do que o modelo de sangue autólogo, o qual apresentou resolução mais rápida do hematoma e recuperação total dos déficits funcionais.

Com base nas evidências existentes na literatura e levando em consideração as vantagens e limitações de ambos os modelos, a injeção estereotáxica de colagenase foi escolhida para induzir a HIC neste trabalho, por possuir mais similaridades ao mecanismo de lesão primário e secundário que ocorre em humanos, assim como o consequente prejuízo funcional grave e, na maioria das vezes, irreversíveis que os acometem.

1.3. Neuroinflamação na HIC

Evidências crescentes sugerem que mecanismos inflamatórios estão envolvidos na progressão da lesão cerebral induzida pela HIC, sendo um fator chave na patogênese e no desfecho da doença (Righy et al., 2016; Wang, 2010; Wang and Doré, 2007; Zhang et al., 2017; Zhou et al., 2014).

A neuroinflamação é mediada por componentes celulares, como leucócitos e microglia residente, e componentes moleculares, incluindo

prostaglandinas, quimiocinas, citocinas, proteases extracelulares e EROs (Mracsko and Veltkamp, 2014; Wang and Doré, 2007).

1.3.1. Ativação microglial e citocinas pró-inflamatórias

Os distúrbios agudos e crônicos do SNC levam à ativação glial, manifestada pelo aparecimento de microglia e astrócitos ativados no local e em torno dos focos de danos nos tecidos (Wajima et al., 2013). A microglia ativada é caracterizada por alterações morfológicas, como tamanho aumentado e processos robustos, além de resposta migratória, proliferativa e comportamento fagocítico (Mracsko and Veltkamp, 2014).

Microglias são as primeiras células imunes a reagir a lesões cerebrais, incluindo a HIC, e podem ser ativadas por componentes do sangue, como eritrócitos, heme, leucócitos, proteínas plasmáticas e hemoglobina, por meio de receptores do tipo Toll (TLR – do inglês "*toll-like receptor*") (Wang et al., 2014; Zhang et al., 2017). Nos modelos animais de HIC, a microglia ativada pode ser detectada dentro de uma hora após o insulto, atingindo o pico de ativação entre 3 e 7 dias (Gong et al., 2000; Wang et al., 2003; Yang et al., 2015) e retornando ao número basal dentro de 21 dias (Wang et al., 2003).

A ativação da microglia parece ter um papel duplo na HIC: sua principal função é a fagocitose dos componentes sanguíneos e de restos celulares, a fim de manter a homeostase tecidual e promover a recuperação neurológica funcional (Zhang et al., 2017); no entanto, nesse processo, a microglia ativada produz uma variedade de citocinas pró-inflamatórias, quimiocinas, EROs, proteases, óxido nítrico (NO) sintase e prostaglandinas, os quais aumentam a

lesão cerebral após a HIC (Shiratori et al., 2010; Wu et al., 2015, 2011; Yang et al., 2014).

Diversos estudos em modelos animais de HIC evidenciam o potencial terapêutico de tratamentos com base na inibição da ativação microglial, correlacionando-a com a diminuição do edema peri-hematomal, do volume de lesão tecidual, da degeneração neuronal e com a melhora das funções neurológicas (Gao et al., 2008; Qiao et al., 2018; Wang et al., 2003; Wang and Tsirka, 2005; Wu et al., 2009, 2008). Além disso, foi demonstrado que a microglia induz a produção de EROs in vitro (Yang et al., 2015), e que a sua inibição diminui a produção de EROs em um modelo animal de ICH (Wang and Tsirka, 2005), tornando evidente a relação entre a neuroinflamação mediada pela microglia e o estresse oxidativo na lesão secundária decorrente da HIC. O estresse oxidativo é uma condição na qual a superprodução de radicais livres, principalmente EROs, excede a capacidade antioxidante e subsequentemente leva a lesão celular via oxidação direta de proteínas celulares, lipídios e DNA ou participação em vias de sinalização de morte celular (Sinha et al., 2013).

Citocinas pró-inflamatórias, como o fator de necrose tumoral α (TNF-α) e a interleucina -1β (IL-1β), são liberadas pela microglia ativada em resposta a diversos tipos de lesão cerebral, incluindo a lesão hemorrágica, na qual parecem ter papel importante na progressão da lesão secundária, sendo fortemente mediadas pela produção de trombina, através de receptores específicos de trombina presentes nas células microgliais (PARs – do inglês *protease-activated receptors*) (Wu et al., 2008). Embora essas citocinas pró-inflamatórias possam ser liberadas por diversos tipos celulares (incluindo astrócitos, neurônios e células endoteliais), sua principal fonte no encéfalo são

as microglias ativadas (Emsley and Tyrrell, 2002). As citocinas liberadas induzem ou potencializam a produção de outras citocinas; além disso, elas podem induzir uma à outra mutuamente (por exemplo, TNF-α e IL-1β) (Turrin and Plata-Salamán, 2000).

1.4. O papel dos astrócitos na patologia da HIC

Os astrócitos possuem importância fundamental na homeostase cerebral, além de fornecer suporte estrutural aos neurônios. Contribuem ativamente na formação e manutenção da BHE (Abbott et al., 1992), regulam o fluxo sanguíneo cerebral (Takano et al., 2006), transportam substâncias entre o sangue e neurônios (Matsui et al., 2002), mantêm a homeostase oxidativa e iônica (Wilson, 1997), secretam fatores neuroprotetores (Mahesh et al., 2006), modulam a transmissão sináptica, a sinaptogênese e a neurogênese (Matsui et al., 2002).

Astrócitos desempenham um papel chave tanto na produção como na regulação de neurotransmissores no SNC, produzindo, por exemplo a glutamina, precursora para os neurotransmissores glutamato e GABA, a partir da glicose (Zou et al., 2010). Além de fornecer precursores para neurotransmissores, estas células gliais realizam a captação do glutamato da fenda sináptica, por meio dos transportadores astrocitários GLT-1 (transportador de glutamato 1) e GLAST (transportador de glutamato e aspartato), a fim de evitar seu acúmulo excessivo no meio extracelular (Eid et al., 2018; Lewerenz and Maher, 2015). Na HIC, o glutamato é patologicamente liberado em quantidades excitotóxicas pelos neurônios necróticos em decorrência da lesão (Senn et al., 2014); além disso, os níveis dos

transportadores desse neurotransmissor diminuem agudamente após lesões cerebrais, exacerbando a morte neuronal devido à excitotoxicidade glutamatérgica (Eid et al., 2018; Neves et al., 2018). Além da remoção do glutamato da fenda sináptica, os astrócitos são responsáveis pela sua conversão em glutamina, através da enzima glutamina sintetase (GS) (Eid et al., 2016). Por este motivo, a atividade da GS tem sido utilizada para caracterizar a função astroglial no tecido cerebral (Eid et al., 2016; Nedergaard et al., 2002; Neves et al., 2018)

Outra importante função desempenhada pelos astrócitos diz respeito ao suporte a outras células cerebrais em defesa contra as EROs. O tripeptídeo glutationa (GSH), sintetizado e secretado pelos astrócitos, é o principal antioxidante cerebral, exercendo importante papel neuroprotetor contra danos oxidativos (Dringen et al., 2015). Estudos mostram que o conteúdo de GSH encontra-se reduzido após a HIC experimental, contribuindo para o aumento da morte neuronal em decorrência do estresse oxidativo (Diao et al., 2020; Wang et al., 2018).

1.4.1. Astrogliose reativa

A astrogliose reativa é uma resposta dos astrócitos a lesões ou processos neuropatologicos, caracterizada pela hipertrofia dos corpos e processos celulares, alteração da expressão gênica e proliferação dos astrócitos em torno do local da lesão (Sofroniew and Vinters, 2010a; Sukumari-Ramesh et al., 2012a). Diversos tipos de células podem liberar mediadores que induzem a astrogliose reativa, incluindo neurônios, microglia, células endoteliais, leucócitos e outros astrócitos, em resposta aos insultos no SNC. Citocinas

liberadas pela microglia, por exemplo são fortes indutoras da reatividade astrocitária (Wajima et al., 2013). Além disso, durante a hemorragia, fatores derivados do sangue, como a trombina, são potenciais indutores da proliferação e ativação astrocítica (Nishino et al., 1993).

Evidências indicam que os astrócitos reativos possuem um papel complexo em resposta a lesões do SNC, tendo potencial tanto para aumentar a regeneração e sobrevivência neuronal, como para contribuir com o agravamento da lesão (Sofroniew, 2009; Sofroniew and Vinters, 2010a). Os efeitos benéficos proporcionados pelos astrócitos incluem o reparo tecidual, proteção celular, captação do glutamato e liberação de neurotrofinas (Sukumari-Ramesh et al., 2012b; Wasserman and Schlichter, 2007), enquanto efeitos potencialmente prejudiciais podem ser causados pela liberação de citocinas inflamatórias como IL-1β e TNF-α (Mracsko and Veltkamp, 2014) e de radicais citotóxicos (Qu et al., 2016), levando à potencialização de respostas inflamatórias, aumento da permeabilidade da BHE , edema vasogênico e estresse oxidativo após a HIC (Barreto et al., 2011; Sukumari-Ramesh et al., 2012a). Além disso, no processo de reparo tecidual, os astrócitos formam uma cicatriz glial com a finalidade de proteger o tecido não danificado, a qual acaba por gerar uma barreira física e produção de inibidores químicos que impedem a regeneração axonal (Barreto et al., 2011).

1.4.2. Proteína glial fibrilar ácida (GFAP)

A astrogliose reativa em decorrência de lesões no SNC leva ao aumento da expressão de GFAP, membro da família de proteínas do citoesqueleto dos astrócitos, que ajuda a manter a força mecânica, bem como a forma dessas

células. Assim, o aumento dos níveis de GFAP é considerado um importante marcador biológico, sensível e específico para a rápida resposta dos astrócitos a lesões e doenças no SNC, incluindo a HIC (Kumar et al., 2015).

Após a HIC, GFAP pode ser encontrado no soro e no plasma de pacientes devido à destruição de astrócitos e à ruptura da BHE (Foerch et al., 2012; Senn et al., 2014) e seus níveis correlacionam-se ao volume do hematoma e ao desfecho clínico dos pacientes (Foerch et al., 2012; Kumar et al., 2015). Níveis elevados de GFAP também são encontrados na HIC experimental (Neves et al., 2017) e um estudo recente mostrou que a atenuação da atividade astrocítica, através da administração de um inibidor específico, reduziu o acúmulo de astrócitos e a expansão do hematoma, diminuiu a destruição da BHE e melhorou os desfechos neurológicos funcionais de ratos submetidos à HIC (Chiu et al., 2017).

1.4.3. Proteína S100B

Outra consequência da reatividade e proliferação astrocitária frente a um insulto no SNC é o aumento dos níveis da proteína S100B, uma proteína ligante de cálcio, encontrada abundantemente no cérebro, onde é expressa principalmente pelos astrócitos (Sorci et al., 2010). No caso de lesões no sistema nervoso, a concentração de S100B extracelular pode ser ainda mais alta em decorrência de danos ou necrose dos astrócitos, levando à liberação passiva da proteína e possivelmente a um "*clearance*" menos eficaz em consequência da inflamação (Sorci et al., 2010).

A S100B faz parte de uma família de proteínas ligantes de Ca^{2+} que, quando ativadas por este íon, interagem com proteínas alvo intracelulares,

cujas funções são dependentes de cálcio, regulando assim suas atividades (Sorci et al., 2010). S100B intracelular exerce atividades regulatórias nas células e, uma vez secretada/liberada, atua como um sinal extracelular. Como regulador intracelular, a S100B atua na regulação da fosforilação de proteínas, no metabolismo energético, na dinâmica dos constituintes do citoesqueleto, na homeostase do Ca^{+2} e na proliferação e diferenciação celular (Donato et al., 2009). À nível extracelular, a S100B pode atuar como fator neurotrófico ou neurotóxico, dependendo de sua concentração. Em níveis baixos, fisiológicos (nano molares – nM) protege os neurônios contra apoptose, estimula o crescimento de neuritos e a sobrevivência neuronal; no entanto, em concentrações elevadas (micro molares - mM), exerce efeito tóxico, facilitando a morte neuronal (Villarreal et al., 2014).

A S100B se liga nos receptores RAGE (receptor para produtos finais de glicação avançada), um receptor multiligante da superfamília de imunoglobulinas expresso em vários tipos de células, incluindo neurônios, astrócitos e microglia (Hofmann et al., 1999), nas quais ativa diferentes cascatas de sinalização intracelular.

A ligação de RAGE por S100B nos neurônios demonstrou ser responsável pelos efeitos neurotróficos (em doses baixas) e pró-apoptóticos (em altas doses), com consequente superprodução de EROs (Huttunen et al., 2000). A ativação da microglia devido a um dano cerebral é acompanhada pelo aumento da densidade de receptores RAGE em sua superfície (Lue et al., 2001) e, assim, a S100B torna-se capaz de atrair quimicamente as células microgliais para o local da lesão, além de aumentar a expressão e secreção de IL-1β, TNF-α, ciclo-oxigenase-2 (COX-2) e óxido nítrico sintase induzível (iNOS) por

essas células (Esposito et al., 2006; Kim et al., 2004). Nos astrócitos, concentrações elevadas de S100B demonstraram induzir astrogliose reativa, proliferação e migração para o local da lesão (Villarreal et al., 2014), aumentar a expressão de iNOS, liberação de NO e secreção de IL-1β, interleucina 6 (IL-6) e TNF- α (Ponath et al., 2007; Villarreal et al., 2014). (**Figura 2**).

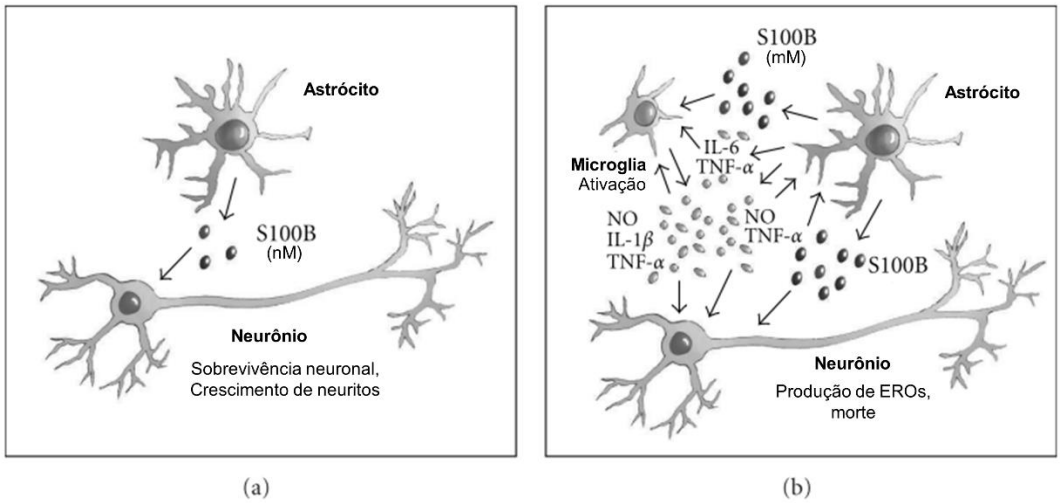

Figura 2. Representação esquemática dos efeitos extracelulares da S100B no encéfalo. (a) Em baixas concentrações, a S100B promove sobrevivência neuronal e crescimento de neuritos via estimulação da sinalização da RAGE. (b) Em altas concentrações, a S100B causa morte neuronal tanto diretamente, pela estimulação excessiva da sinalização da RAGE em neurônios, como indiretamente, via ativação dependente de RAGE da microglia e astrócitos. IL-6 = interleucina 6; TNF-α = fator de necrose tumoral alfa; NO = óxido nítrico; ERO = espécies reativas de oxigênio. (Sorci et al., 2010).

Os níveis periféricos de S100B no soro e no plasma são considerados biomarcadores de lesão no SNC, incluindo a HIC (Ferrete-Araujo et al., 2019; Senn et al., 2014; Zhou et al., 2016), na qual o dano/necrose de astrócitos, associada a ruptura da BHE podem permitir a entrada de S100B na corrente sanguínea (Kapural et al., 2002). Estudos prospectivos mostram que os níveis periféricos de S100B no sangue e no líquor em pacientes com HIC encontram-se significativamente mais altos do que nos indivíduos saudáveis nos primeiros

dias após a lesão, demonstrando ser um preditor de mortalidade (Ferrete-Araujo et al., 2019; Hu et al., 2010; Huang et al., 2010) e estar correlacionado a um maior volume hemorrágico (Huang et al., 2010; Zhou et al., 2016) e pior desfecho neurológico funcional (Delgado et al., 2006; Ferrete-Araujo et al., 2019; Huang et al., 2010; James et al., 2009; Zhou et al., 2016).

Estudos experimentais mostram que ratos submetidos à HIC induzida por colagenase também apresentam níveis elevados de S100B no soro, líquor e tecido cerebral (estriado e córtex) (Neves et al., 2017). Além disso, um estudo mostrou que o pico de S100B no soro de ratos com HIC correlacionou-se com o edema cerebral e a extensão máxima do volume do hematoma (Tanaka et al., 2009).

Diante das evidências de que o aumento dos níveis da proteína S100B em decorrência da astrogliose reativa frente a HIC possui importante papel no mecanismo de lesão secundária, resultando em aumento da morte celular e piora da função neurológica, a S100B pode ser um interessante alvo terapêutico a ser estudado na patologia e nos desfechos da HIC.

1.5. Ácido arúndico (AA)

O ácido arúndico (ONO-2506) é um agente inibidor da síntese astrocítica de S100B (Asano et al., 2005). Sua descoberta foi impulsionada por estudos *in vitro* que mostraram que astrócitos em cultura se proliferam e se ativam espontaneamente, com consequente aumento no conteúdo de S100B e GFAP, diminuição da expressão de receptores do ácido γ-aminobutírico A (GABAA) e dos transportadores gliais de glutamato (GLT-1 e GLAST) (Mori et al., 2005; Tateishi et al., 2002) . Observou-se, então, que a adição de um anticorpo

contra S100B na cultura inibiu a ativação espontânea dos astrócitos, evidenciando o papel da superexpressão de S100B na reatividade astrocitária. Assim, realizou-se uma triagem na busca de um agente que possuísse uma ação inibitória na síntese de S100B pelos astrócitos, levando à descoberta do AA (Asano et al., 2005; Tateishi et al., 2002). Verificou-se, então, que quando expostos ao AA, astrócitos resistem à ativação espontânea, mostram diminuição da expressão do RNAm de S100B e aumento da expressão do RNAm de transportadores de glutamato e receptores GABA, de forma a proteger neurônios em co-cultura (Asano et al., 2005).

Estudos experimentais têm mostrado efeitos benéficos do AA em diversas doenças no SNC, por meio de diferentes vias de administração e em variadas dosagens e protocolos de tratamento. Em modelos de isquemia cerebral, o AA reduziu o volume do infarto, melhorou a função motora (Mori et al., 2005; Tateishi et al., 2002) e reduziu os níveis de glutamato extracelular (Mori et al., 2004). Em ratos submetidos à hipoperfusão cerebral crônica, diminuiu as lesões na substância branca (Ohtani et al., 2007). Em um estudo com ratos hipertensos propensos ao AVC espontâneo, o tratamento foi capaz de diminuir a pressão arterial, aumentar a taxa de sobrevivência e o tempo médio de vida dos animais (Higashino et al., 2009). No modelo de hematoma subdural agudo, o AA diminuiu o volume da lesão e a morte celular por apoptose (Wajima et al., 2013). Ainda, a administração de AA em ratos com lesão medular levou à melhora da função motora e aumento da força de preensão, além de limitar a expansão da lesão (Hanada et al., 2014) e suprimir a dor neuropática (Ishiguro et al., 2019). Quando utilizado no modelo de doença de Parkinson, preveniu a depleção de neurônios dopaminérgicos na substância negra e o aparecimento

de disfunções motoras (Kato et al., 2004). Recentemente, a administração de AA em ratos submetidos à hipóxia-isquemia neonatal demonstrou reduzir os danos teciduais e os déficits de memória causados pela lesão (Mari et al., 2019).

Um estudo clínico (fase I) foi conduzido para avaliar a segurança e tolerabilidade da administração intravenosa de AA durante 7 dias em pacientes com AVC isquêmico agudo e verificou-se que, além de não gerar efeitos adversos importantes, o AA diminuiu os déficits neurológicos e a dependência para realização de atividades de vida diária dos pacientes até 40 dias após a lesão; além disso, os níveis séricos de S100B correlacionaram-se com o desfecho neurológico funcional (Pettigrew et al., 2006a, 2006b).

Sabe-se que a síntese astrocítica aumentada de S100B leva à ativação de múltiplas cascatas de sinalização intracelular, que induzem respostas como o aumento da produção de citocinas inflamatórias, NOS induzível e COX-2, aumento da expressão de GFAP, diminuição da expressão de transportadores de glutamato e receptores GABAA e diminuição da síntese de glutationa (Wajima et al., 2013). A microglia ativada libera citocinas inflamatórias que levam à ativação dos astrócitos, os quais promovem a síntese de S100B. A S100B liberada, por sua vez, gera ainda mais ativação da microglia, culminando em um ciclo vicioso de citocinas inflamatórias e substâncias tóxicas, resultando no agravamento da inflamação e progressão da lesão (Griffin et al., 2006). Dessa forma, os efeitos do ácido arúndico são atribuídos à sua ação inibitória na síntese de S100B, de forma a suprimir o ciclo de citocinas e as consequências prejudiciais da superexpressão da proteína (**Figura 3**).

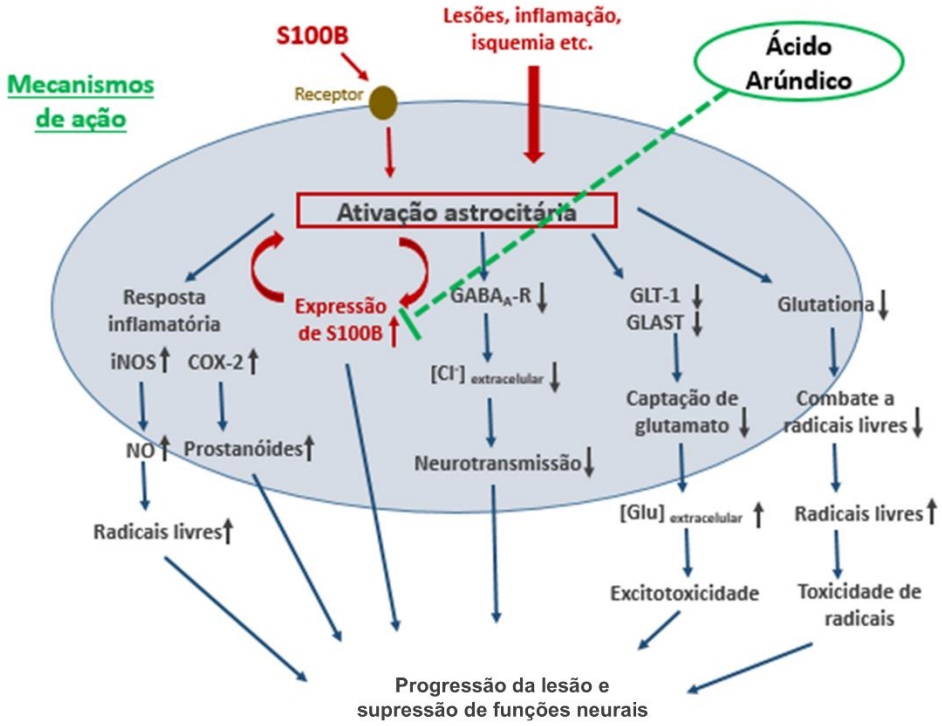

Figura 3. Mecanismo proposto pelo qual o ácido arúndico previne a progressão da lesão após ativação astrocítica devido a lesões, inflamação e isquemia. O ácido arúndico suprime o ciclo de citocinas pela inibição astrocítica da síntese de S100B. RAGE = receptor para produtos finais de glicação avançada; iNOS = óxido nítrico sintase induzível; NO = óxido nítrico; COX-2 = ciclo-oxigenase-2; $GABA_A$-R = receptor de ácido gama-aminobutírico-A; [Cl−] = concentração de íon cloro; GLT-1 = transportador de glutamato 1; GLAST = transportador de glutamato e aspartato; [Glu] = concentração de glutamato. (adaptado de Wajima et al., 2013).

2. JUSTIFICATIVA

Tendo em vista as altas taxas de mortalidade e a severidade das sequelas neurológicas causadas pela hemorragia intracerebral (HIC), torna-se evidente a necessidade da busca de novos tratamentos capazes de melhorar o prognóstico dos pacientes acometidos por esta doença.

Sabe-se, por meio de evidências experimentais e clínicas, que a proteína S100B, produzida e liberada em excesso pelos astrócitos reativos, possui efeitos prejudiciais na fisiopatologia da HIC, culminando no aumento da morte neuronal, da neuroinflamação e no agravamento da lesão.

O ácido arúndico (AA) é um agente inibidor da síntese astrocitária de S100B, cujo potencial terapêutico tem sido demonstrado em diversas doenças do sistema nervoso central, por meio da supressão dos efeitos tóxicos da proteína em níveis elevados.

Com base nestas assertivas, o estudo dos efeitos do AA sobre a fisiopatologia, a progressão da lesão e os desfechos neurológicos da HIC possui grande relevância na busca de novas condutas terapêuticas para a doença.

3. HIPÓTESE

A hipótese de trabalho é de que o tratamento intracerebroventricular com ácido arúndico, por meio de sua propriedade inibidora da síntese de S100B pelos astrócitos, seja capaz de prevenir os efeitos causados pelas concentrações aumentadas da proteína após a hemorragia intracerebral experimental, reduzindo, desta forma, a reatividade astrocitária e microglial, a produção de citocinas inflamatórias, os danos oxidativos e a morte neuronal no estriado dos animais tratados. Como resultado da supressão dos mecanismos de lesão secundária supracitados, os animais tratados com AA devem apresentar um menor volume de lesão estriatal e, consequentemente, melhores desfechos neurológicos funcionais em comparação aos animais não tratados.

4. OBJETIVOS

4.1. Objetivo geral

Investigar os efeitos da administração intracerebroventricular (ICV) de ácido arúndico (AA) no modelo experimental de hemorragia intracerebral (HIC), analisando parâmetros histológicos, bioquímicos e comportamentais.

4.2. Objetivos específicos

I. Estabelecer a dose ideal para a administração ICV de AA, a partir da análise dos níveis estriatais de S100B e GFAP em ratos não lesados;

II. Avaliar os efeitos do tratamento com AA em ratos com HIC, no que diz respeito a:

- Função motora, por meio dos testes comportamentais: escore neurológico, teste de preensão e escada horizontal, realizados em 72h e 7 dias após a lesão;

- Volume da lesão hemorrágica estriatal, por meio de coloração com hematoxilina-eosina, em 72h e 7 dias após a HIC;

- Níveis estriatais de S100B e proteína glial fibrilar ácida (GFAP), por meio da técnica de imunofluorescência, em 72h e em 7 dias após a HIC;

- Reatividade microglial, por meio da técnica de imunofluorescência, em 72h e em 7 dias após a HIC;

- Contagem neuronal, assim como a morte celular por apoptose, por meio da técnica de imunofluorescência, em 72h e em 7 dias após a HIC;

- Níveis de GFAP no estriado, e de S100B no estriado, soro e líquido cerebrospinal (LCE), por meio de ELISA, em 24h, 72h e 7 dias após a lesão;

- Atividade da enzina glutamina sintetase (GS) e conteúdo de glutationa (GSH) no estriado, em 24h, 72h e 7 dias após a HIC;

- Níveis estriatais as citocinas inflamatórias interleucina-1β (IL-1 β) e fator de necrose tumoral-α (TNF-α), em 24h, 72h e 7 dias após a HIC;

- Níveis de espécies reativas de oxigênio (EROs) no estriado através da oxidação de diclorofluoresceína (DCF), em 24h, 72h e 7 dias após a HIC.

PARTE II

CAPÍTULO 1

Arundic acid (ONO-2506), an inhibitor of S100B protein synthesis, prevents neurological deficits and brain tissue damage following intracerebral hemorrhage in male Wistar rats

Juliana de Lima Cordeiro, Juliana Dalibor Neves, Adriana Fernanda Vizuete, Dirceu Aristimunha Thales Ávila Pedroso, Eduardo Farias Sanches, Carlos Alberto Gonçalves, Carlos Alexandre Netto

Manuscrito publicado no periódico *Neuroscience* (2020); 440:97-112. doi:10.1016/j.neuroscience.2020.05.030

Arundic acid (ONO-2506), an inhibitor of S100B protein synthesis, prevents neurological deficits and brain tissue damage following intracerebral hemorrhage in male Wistar rats

J. L. Cordeiro, [a,b*]; J. D. Neves[a]; A. F. Vizuete[a]; D. Aristimunha[a]; T. A. Pedroso[a], E. F. Sanches[a,c]; C. A. Gonçalves[a] and C. A. Netto[a]

[a] Department of Biochemistry, Instituto de Ciências Básicas da Saúde, Universidade Federal do Rio Grande do Sul, Porto Alegre, RS 90035-003, Brazil

[b] Post-graduation Program of Neurosciences, Instituto de Ciências Básicas da Saúde, Universidade Federal do Rio Grande do Sul, 90035-190, Brazil

[c] Post-graduation Program of Phisiology, Instituto de Ciências Básicas da Saúde, Universidade Federal do Rio Grande do Sul, 90035-190, Brazil

Abstract

Stroke is one of the leading causes of mortality and neurological morbidity. Intracerebral hemorrhage (ICH) has the poorest prognosis among all stroke subtypes and no treatment has been effective in improving outcomes. Following ICH, the observed high levels of S100B protein have been associated with worsening of injury and neurological deficits. Arundic acid (AA) exerts neuroprotective effects through inhibition of astrocytic synthesis of S100B in some models of experimental brain injury; however, it has not been studied in ICH. The aim of this study was to evaluate the effects of intracerebroventricular (ICV) administration of AA in male Wistar rats submitted to ICH model assessing the following variables: reactive astrogliosis, S100B levels, antioxidant defenses, cell death, lesion extension and neurological function. Firstly, AA was injected at different doses (0.02, 0.2, 2 and 20 µg/µl) in the left lateral ventricle in order to observe which dose would decrease GFAP and S100B striatal levels in non-injured rats. Following determination of the effective dose, ICH damage was induced by IV-S collagenase intrastrial injection and 2 µg/µl AA was injected through ICV route immediately before injury. AA treatment prevented ICH-induced neurological deficits and tissue damage, inhibited excessive astrocytic activation and cellular apoptosis, reduced peripheral and central S100B levels (in striatum, serum and cerebrospinal fluid), improved neuronal survival and enhanced the antioxidant defenses after injury. Altogether, these results suggest that S100B is a viable target for treating ICH and highlight AA as an interesting strategy for improving neurological outcome after experimental brain hemorrhage.

Key words: intracerebral hemorrhage, arundic acid (ONO-2506), astrocyte, S100B, neuroprotection.

1.Introduction

Intracerebral hemorrhage (ICH) accounts for 15–20% of all stroke cases and is associated with high morbidity and mortality rates (Qureshi et al., 2009). ICH has the poorest prognosis among all stroke subtypes, with only 20% of survivors having independent functioning 6 months after injury (Agnihotri et al., 2011). No pharmacological or surgical intervention has been able to reduce mortality or to improve the outcome following ICH (Fiorella et al., 2015). Therefore, ICH patients usually present with sensorimotor impairments according to the site and the extent of brain damage (Cheon, 2015).

ICH injury mechanisms can be divided into two phases. The primary damage occurs due to the initial bleeding and hematoma formation into the brain parenchyma, which leads to the compression of brain regions, decrease of blood flow and direct mechanical destruction of axons and glial cells (Qureshi et al., 2009; Keep et al., 2012). Secondary brain injury occurs mainly due to the hematoma formation and clearance, which causes hemotoxicity by the blood breakdown products released (Qureshi et al., 2009; Aronowski and Zhao, 2011). These secondary mechanisms result in blood brain-barrier (BBB) disruption, neuronal loss and reactive gliosis (Hu et al., 2016).

Astrocytes contribute to neuronal metabolism and cell survival (Matsui et al., 2002). Glutamate uptake from the extracellular space is a major astrocyte function in order to prevent glutamate-induced excitotoxicity (Eid et al., 2018). Furthermore, glutamate is used in the synthesis of glutamine through the glutamine synthetase (GS) enzyme (Eid et al., 2016) and also for the synthesis of glutathione (GSH), an important brain antioxidant (Dringen et al., 2015). Astrocytes become reactive in response to a central nervous system (CNS)

damage, exhibiting characteristics such as increased size and complexity of their projections, with a consequent increase of GFAP (glial fibrillary acid protein), a member of cytoskeleton protein family that has been used as an astrocyte-specific biomarker (Kumar et al., 2015). It has been demonstrated that GFAP levels are increased after CNS injury, such as ICH (Foerch et al., 2012; Kumar et al., 2015). Reactive astrocytes may cause potentially detrimental effects due to the induction of proinflammatory responses (Mracsko and Veltkamp, 2014) and oxidative stress (OS) (Qu et al., 2016).

In addition to the increase in GFAP levels, CNS insults lead to an increase in astrocyte synthesis of S100B, a 21-kD Ca^{2+} binding protein that exerts beneficial roles at low concentrations, facilitating neuronal survival, whereas at high levels it causes neurotoxic effects and neuronal death (Hu et al., 1996; Sorci et al., 2010; Wajima et al., 2013). Following brain insults, the increased levels of S100B lead to the activation of multiple intracellular signaling cascades, resulting in the suppression of neuronal function and delayed expansion of injury (Matsui et al., 2002).

S100B has been considered a biomarker of brain damage in several CNS disorders, including ICH (Tanaka et al., 2009; Hu et al., 2010; Zhou et al., 2016; Neves et al., 2017). High S100B plasma concentration was related with hemorrhage volume, neurological deficits and functional disability in ICH patients (Hu et al., 2010; Zhou et al., 2016). In a recent preclinical study, increased levels of S100B in serum, cerebrospinal fluid (CSF), striatum and cerebral cortex were observed following ICH in a collagenase-induced model in rats (Neves et al., 2017). In addition, another study reported that the increased

serum S100B levels in ICH rats was significantly correlated with brain edema formation and with hematoma volumes (Tanaka et al., 2009).

Arundic acid (AA; (R)-(-)-2-propyloctanoic acid; ONO-2506) is a novel drug acting through the inhibition of S100B synthesis in astrocytes (Asano et al., 2005). It suppresses the intracellular signaling cascades, which triggers responses as increased production of inflammatory cytokines, increased expression of GFAP, decreased expression of glutamate transporters, decreased GSH synthesis and suppressed apoptotic mechanisms, among others (Wajima et al., 2013). AA has been tested as a potential protective agent in several experimental models of CNS injuries (Hanada et al., 2014; Kato et al., 2003; Mori et al., 2005, 2006; Oki et al., 2008; Tateishi et al., 2002; Wajima et al., 2013). Following experimental ischemic stroke, AA has been able to reduce the S100B expression in the peri-infarcted area, to decrease the infarct volume and neurological deficits, and to improve motor function (Tateishi et al., 2002; Mori et al., 2005). However, despite evidence suggesting neuroprotection following ischemic brain injury, there are no studies evaluating the effects of AA on ICH.

Considering that S100B may serve as a therapeutic target following ICH, the aims of this study were: 1 - to identify the most effective intracerebroventricular (ICV) dose of AA for adult rats considering astroglial parameters as the main outcome. 2 - to test the protective effects of the AA after ICH induced by the intrastriatal injection of collagenase in rats, by evaluating neurochemical, histological, immunofluorescence and behavioral responses up to 7 days after the injury.

2. Experimental procedures

2.1. Animals

Adult male Wistar rats (n = 176) approximately 90 daysold (300–350 g weight) were housed in groups of four animals in Plexiglas cages under standard laboratory conditions (12 h light/dark cycle, with lights off at 7:30p. m. and controlled temperature of 22 ± 2 C). Water and standard laboratory chow were provided ad libitum. All procedures were approved by the University Ethics Committee for Animal Research under the experimental protocol #30944 and were in accordance with the Guidelines for Care and Use of Laboratory Animals adopted by the National Institute of Health (USA) and with National Animal Experimentation Control Board (CONCEA-Brazil). All efforts were made to minimize animal suffering and to reduce the number of animals needed.

2.2. Experimental design

Experiment I – Effective ICV AA dose curve.

The experiment aimed to determine an effective dose for ICV administration of AA. For this purpose, the decrease in S100B and GFAP protein levels in the left striatum of healthy rats, assessed 24 h after the AA administration, were taken as the main outcome in order to determine the effective AA dose. AA was dissolved in 5 mL of saline solution and injected in the left lateral ventricle in the following concentrations: 0.02 µg/µL, 0.2 µg/µL, 2 µg/µL and 20 µg/µL. The dose was calculated based on the animal weight (weight x 0.005). Animals were randomly allocated into groups in order to receive one of the determined AA doses. Vehicle rats received saline solution

and the Naïve group had no injection. A total of 37 animals were used for this experiment. The AA dose that reduced both S100B and GFAP protein levels in the striatum was chosen to be used in the following experiments.

Experiment II – effects of AA treatment on behavioral, histological and biochemical parameters in rats submitted to ICH.

Biochemical analysis was performed 24 h (n = 18), 72 h (n = 21) and 7 days (n = 27) after ICH in order to measure the effects of AA treatment on S100B levels on striatum, CSF and serum; GFAP protein levels, quantification of brain antioxidant GSH and GS activity in the rats striatum were also determined (Fig. 1). Sensorimotor function was evaluated using the neurological score, assessed by an investigator blinded to the rat's experimental condition at 72 h (n = 21) and 7 days (n = 27) after ICH (different animals were used for each endpoint). A total of 66 rats were used for biochemical and behavioral assessments.

Histological analysis of the striatum was performed 72 h (n = 27) and 7 days (n = 21) after ICH in order to measure the effects of AA treatment on hemorrhage and injured hemisphere volumes. Immunofluorescence analysis was performed 7 days (n = 16–19) after ICH to quantify the fluorescence intensity of S100B, GFAP, NeuN (neuron marker) and cleaved caspase-3 (cell apoptosis marker) in the striatum. A total of 48 rats were used for histological and immunofluorescence assessments.

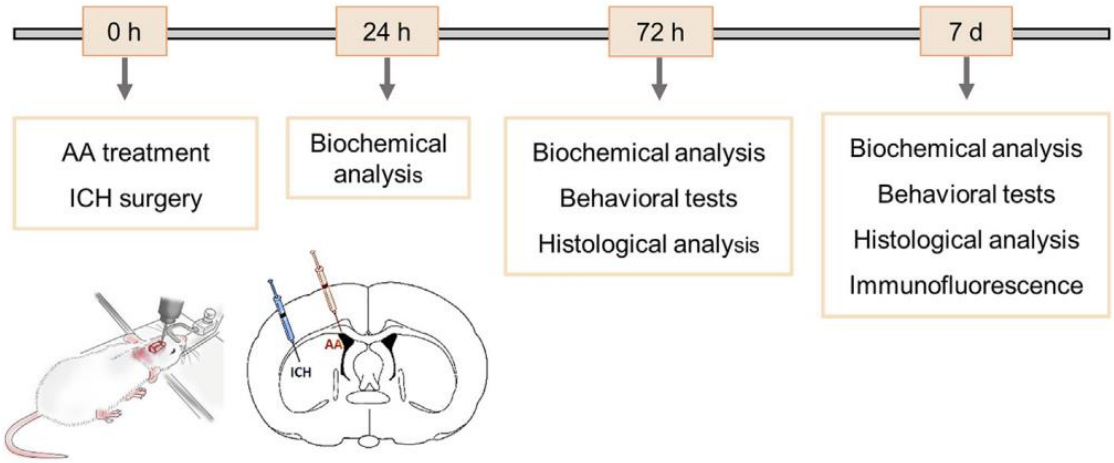

Figure 1. Timeline of experiment II showing ICH surgery, AA treatment and the subsequent biochemical, behavioral, histological and immunofluorescence analysis.

2.3. Surgical procedures – ICH and AA administration

Animals were anesthetized with isoflurane (4% induction, 2% maintenance in 70% N_2O and 30% O_2) and placed in a stereotaxic frame. For AA administration, a burr hole was drilled in the skull and a 26-G needle (Hamilton, Reno, NV, USA) was inserted into the left lateral ventricle according to the following stereotactic coordinates: 0.80 mm anterior, 1.50 mm lateral and 3.50 mm ventral to Bregma in the left side (Paxinos and Watson, 2007). In experiment I, a single dose of AA (concentrations: 0.02 µg/µl, 0.2 µg/µl, 2 µg/µl or 20 µg/µl; dose: weight x 0.005; Tocris®) or saline solution (dose: weight x 0.005) was infused and the needle was kept in the position for additional 5 min period to prevent backflow. In the experiment II, the most effective dose (2 µg/µl) was injected under the same conditions, immediately before ICH induction.

ICH was produced by injecting 0.5 mL of bacterial collagenase type-IVs (Sigma-Aldrich, USA) into the rat's striatum at a concentration of 0.2 U per 1.0 µL of saline buffer into the dorsolateral striatum, at the following coordinates: 0 mm anterior, 3.6 mm lateral and 6.0 mm ventral to Bregma (Paxinos and

Watson, 2007). The needle was kept in position for an additional 5 min period and then slowly removed to prevent backflow. In the Vehicle group, sterile saline (0.5 µL) was injected rather than collagenase. After surgery, the incision was sutured, the animals were housed in a biologically clean room and monitored daily. The total mortality rate (including the Vehicle group) was around 15%, with no statistical difference between treated (20.75%) and untreated groups (21.15%).

2.4. Experimental groups

Animals were randomly divided into three experimental groups: ICH (rats that underwent ICH and received saline solution); ICH + AA (rats that underwent ICH and treated with AA); Vehicle (surgical and treatment controls that received only saline solution). Based on results of Experiment I, in which there were no differences between Naive and Vehicle groups, and in order to reduce the number of animals used, only vehicle-treated rats were used as controls in Experiment II.

2.5. Behavioral assessment

Neurological score

The neurological score was used to evaluate motor function and included the assessment of spontaneous ipsilateral circling and beam walk ability. Spontaneous ipsilateral rotation was assessed with the rat being held by the tail for 10 s and the behavior was rated into five degrees of severity: 0 – normal symmetric rotation; 1 – a tendency to ipsilateral rotation; 2 – ipsilateral rotation with occasional contralateral turns; 3- frequent ipsilateral rotation

without contralateral rotation; and 4 – continuous ipsilateral rotation. The beam walk ability was performed to assess the animal capability to traverse a narrow, elevated beam till the home cage and was also rated according to the degree of severity in: 0 – normal walking to home cage; 1 – minor dysfunction such as long stride or unbalanced walking; 2 – mild dysfunction with frequent slip of the limb from the beam; 3 – moderate dysfunction with inability to walk on a beam; and 4 – severe dysfunction, falling from beam within 10 s. Beam walk was run twice for animal habituation and the third trial was scored. The final neurological score was obtained by summing up the points of both spontaneous rotation and the beam walk ability (Altumbabic et al., 1998; Imamura et al., 2003; Neves et al., 2017).

2.6. Histological assessment

Rats were subjected to transcardiac perfusion under deep anesthesia with isoflurane. Saline solution followed by 4% paraformaldehyde were injected through the animals' circulation (Reagen, Rio de Janeiro, Brazil) through the left cardiac ventricle. Brains were removed from the skull, stored in the same fixative solution overnight and crioprotected with sucrose 30% solution until sink. Brains were frozen in liquid nitrogen and stored at 20º C before sectioning.

Coronal sections (30 µm) were obtained using a cryostat (one slice every 210 µm), from +1.70 to -1.40 mm from Bregma (Paxinos and Watson, 2007). The slices were mounted on gelatin-coated slides and stained with hematoxylin–eosin (HE).

The striatal hemorrhage volume and the brain hemispheres were measured using the software NIH – Image J. The striatal hemorrhage volume

(mm^3) was defined as follows: lesion area of all coronal sections X interval between sections X number of sections analyzed (Mestriner et al., 2013). The hemisphere volume was calculated in the formula: area of all sections X interval between sections X number of sections analyzed, and the hemisphere volume ratio was calculated by the equation: ipsilateral volume (mm^3) / contralateral volume (mm^3).

The presence of hemorrhage in the coronal section located at the bregma 0.20 mm (interaural 9.20 mm – according to Paxinos' Atlas coordinates) after HE staining was used to check whether the injection site was correct (Paxinos and Watson, 2007).

2.7. Immunofluorescence analysis

For the immunofluorescence analysis, frozen brain slices were washed with PBS, permeabilized in PBS-Triton X (0.25%), and then blocked with goat serum (5%) for 45 min. In order to perform astrocytes and calciumbinding protein S100B co-labeling, sections were incubated with the primary antibodies against glial fibrillary acidic protein (anti-GFAP, mouse IgG, 1:200, Thermo Fisher – MA5-12023) and against S100B (antiS100B, rabbit IgG, 1:200, Dako – Z0311). In order to identify neurons and cleaved caspase-3, the primary antibodies anti-NeuN (mouse IgG, 1:250, Merck Millipore – MAB377) and anti-cleaved caspase-3 (rabbit IgG, 1:250, Cell Signaling – 9661 S) were used. This procedure was carried out in 1% goat serum and PBSTx at 4ºC overnight. Following PBS washes, sections were incubated with secondary antibody anti-mouse Alexa 555 (1:500, Molecular Probes, Invitrogen, USA) and secondary antibody anti-rabbit Alexa 488 (1:500, Molecular Probes, Invitrogen, USA).

Slices were covered in aqueous mounting medium with DAPI (Fluoroshield F6057, Sigma-Aldrich) and coverslipped.

Images of the peri-hematomal area of the left striatum and corresponding area of the right striatum (Fig. 2) were captured using a microscope (EVOS® FL Auto Imaging System). Four brain slices per animal were used and all analyses were made using high magnification images (x20). An area of interest (AOI) was determined (400 x 400 µm) to assess the staining intensity (integrated densities/mm^2), the total immunostained surface (percent of the immunostained surface/mm^2) and the number of stained cells. Assessments were performed through the capture and analysis of images in the software Image J v. 1.46. The analyzes were performed on the left (ipsilateral) and right (contralateral) striatum and the data are reported as the left/right ratio of as previously described (Nicola et al., 2016).

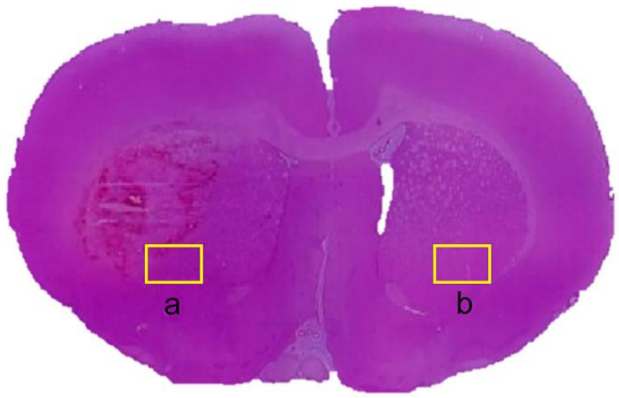

Figure 2. Image of a brain slice illustrating the location of the perihematomal area in the left hemisphere (A) and the corresponding striatal region in the contralateral hemisphere (B) that were captured under the microscope for immunofluorescence analysis.

2.8. Biochemical analysis

ELISA

The immunocontent of S100B in the striatum, serum and CSF, as well as immunocontent of GFAP in the striatum were measured by ELISA assays 24 h, 72 h and 7 days after ICH surgery.

For this purpose, animals from Experiment II were deeply anesthetized with isoflurane (4%; Cristália, Brazil), and placed in a stereotaxic frame. Then, a maximum volume of 30 µL of CSF was obtained by puncturing the cisterna magna using an insulin syringe, in a period of 3 min to minimize risk of brainstem damage. Serum samples of approximately 1 mL of blood were obtained via cardiac puncture. The samples were centrifuged and the supernatant was removed. Serum and CSF fluid samples were frozen (-80º C) until use. For striatum samples, rats were decapitated, brains were removed from the skull and the ipsilateral striatum was dissected on ice. Transverse slices of 0.3 mm (Bregma, +1.7–4.8 mm) were obtained using a McIlwain Tissue Chopper and the samples were frozen (-80º C) until they were used for the biochemical analysis.

S100B quantification

Microtiter plates (96-well flatbottom) were coated for 12–18 h with the samples diluted (PBS) from striatum, CSF and serum to give a final quantity between 5 and 500 ng of protein. Slices were then, homogenized in PBS (50 mM NaCl, 18 mM Na_2HPO_4, 83 mM $NaH_2PO_4H_2O$, pH 7.4), containing 1 mM EGTA and 1 mM phenylmethyl-sulphonyl fluoride (PMSF). The S100B content in the CSF, serum and brain tissue were measured by ELISA, as previously described (Leite et al., 2008). Briefly, polyclonal primary antibody (anti-S100B rabbit – Dako – Z0311) was incubated for 30 min and then, the secondary

antibody (anti-rabbit peroxidase-conjugated anti-IgG-GE Amersham-NA934 V) was added for 30 min both, at final concentration of 1:5000. The color reaction with o-phenylenediamine dihydrochloride (OPD), a detection reagent, was measured at 492 nm. The standard S100B curve ranged from 0.02 to 1 ng/mL.

GFAP quantification

Microtiter plates (96-well flatbottom) were coated for 12–18 h with the samples diluted (PBS) from striatum to give a final quantity between 5 and 500 ng of protein. Slices were then, homogenized in PBS (50 mM NaCl, 18 mM Na_2HPO_4, 83 mM $NaH_2PO_4H_2O$, pH 7.4), containing 1 mM EGTA and 1 mM PMSF. GFAP content was measured by ELISA, as previously described (Tramontina et al., 2007). Briefly, the homogenate was blocked for 2 h followed by an incubation with a polyclonal primary antibody (anti-GFAP rabbit-Sigma Aldrich-G9269) for 1 h and an incubation with a secondary antibody (anti-rabbit peroxidase-conjugated anti-IgG-NA934 V, GE Amersham) for 1 h, at room temperature both, at final concentration of 1:1000. The color reaction with OPD was measured at 492 nm. The standard GFAP curve ranged from 0.1 to 10 ng/mL. Antibody characterization is presented in Table 1.

Table 1. Characterization of antibodies used in biochemical and histological analyzes.

Antibody name	Immunogen	Manufacturer	Concentration
Anti-S100B	Anti-mouse monoclonal	Sigma – S2532	1:1000
	Anti-rabbit polyclonal	Dako – Z0311	1:5000
			1:200
Anti-IgG	Anti-rabbit peroxidase-conjugated	GE Amersham – NA934 V	1:5000
Anti-GFAP	Anti-rabbit polyclonal	Dako – Z0334	1:1000
		Sigma Aldrich – G9269	1:1000
	Anti-mouse monoclonal	Thermo Fisher – MA512023	1:200
Anti-IgG	Anti-rabbit peroxidase-conjugated	GE Amersham – NA934 V	1:1000
Anti-NeuN	Anti-mouse monoclonal	Merck Millipore – MAB377	1:250
Anti-Cleaved-caspase-3	Anti-rabbit polyclonal	Cell Signaling – 9661 S	1:250

GS activity

The enzymatic assay was performed as previously described (Minet et al., 1997). Briefly, homogenized tissue samples were added to a reaction mixture containing (in mM): 10 $MgCl_2$, 50 mM L-glutamate, 100 imidazole-HCl buffer (pH 7.4), 10 2-mercaptoethanol, 50 hydroxylamine-HCl and 10 ATP and incubated for 15 min at 37º C. The reaction was stopped by the addition of 0.4 mL of a solution containing (in mM): 370 ferric chloride; 670 HCl; 200 trichloroacetic acid. After centrifugation, the supernatant was measured at 530 nm and compared to the absorbance generated by standard quantities of γ-glutamylhydroxamate treated with ferric chloride reagent. The standard γ-glutamylhydroxamate acid (Sigma-Aldrich, St. Louis, MO. USA) curve ranged from 0.1 to 10 mmol/ml.

GSH content assay

Total GSH content was determined as previously described (Tietze, 1969; Allen et al., 2000) in order to detect the reduced GSH content. Briefly, striatal slices were homogenized in sodium phosphate buffer (0.1 M, pH 8.0), and protein was precipitated in 1.7% metaphosphoric acid. Supernatant was assayed with o-phthaldialdehyde (1 mg/mL methanol) at room temperature for 15 min. Fluorescence was measured using excitation and emission wave lengths of 350 and 420 nm, respectively. A calibration curve was performed with standard GSH solution (0–500 µM).

Protein assessment

Protein concentration was measured by Lowry's method, modified by Peterson, using bovine serum albumin as standard (Peterson, 1977).

2.9. Statistics

All statistical analysis was performed using SPSS 22.0 for Windows (SPSS Inc., Chicago, IL, USA). Normality of data distribution was confirmed by Shapiro-Wilk test and the variance equality by the Levene's test. Parametric data were analyzed by one-way ANOVA (data are expressed as mean ± SD) followed by Duncan's post hoc test. As for non-parametric data (neurological score) Kruskal-Wallis analysis of variance, followed by Dunn's post hoc tests whenever indicated, were used (data are expressed as median and 25th-75th percentiles). Significance was accepted when $p < 0.05$. Sample size calculation was based on previous studies with similar methodology for biochemical analysis (Neves et al., 2017) in order to reach the statistical power of 80% calculated with the software PEPI for-windows 4.0.

3. Results

3.1. AA dose response curve

A dose–response curve of AA (from 0.02 to 20 µg/µL) was carried out in order to quantify, in non-injured rats, striatal S100B and GFAP immunocontent (Fig. 3). After receiving 0.2 µg/µL and 2 µg/µL, S100B levels decreased compared to controls groups (Naïve and Vehicle) (Fig. 3A) ($F_{(5,36)} = 4.009$, $p = 0.006$; $n = 5–7$). The dosing of 2 µg/µL was used in the Experiment II because of its marked inhibitory effect on GFAP levels (Fig. 3B) ($F_{(5,36)} = 2.919$, $p =$

0.028; n = 5–7). Interestingly, animals exposed to the highest AA concentration (20 µg/µL) had no inhibitory effects on the evaluated parameters at all.

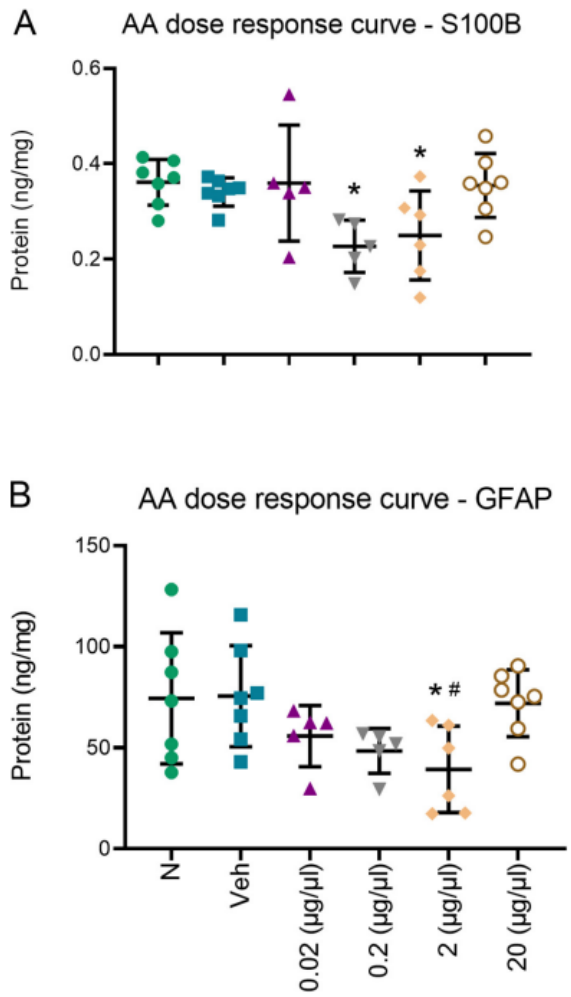

Figure 3. Effects of intracerebroventricular injection of different doses of AA on striatal levels of S100B (A) and glial fibrillary acid protein – GFAP (B), measured 24 h after injection in Naïve rats. n = 5–7 per group. Data are expressed as mean ± SD. *Different from the control group and # different from 20 µg/µL group.

3.2. Behavioral assessment

Seventy-two hours after surgery, both ICH and ICH + AA animals presented neurological deficits, as compared to the control group ($X^2_{(2)}$ = 13.792, p = 0.001) (Fig. 4A). However, 7 days after injury, ICH group showed motor dysfunction compared to the Vehicle group, while ICH + AA had better

performance than ICH group and was not different from controls, indicating the total reversion of ICH motor dysfunction by AA ($X^2_{(2)}$ = 13.368, p = 0.001) (Fig. 4B).

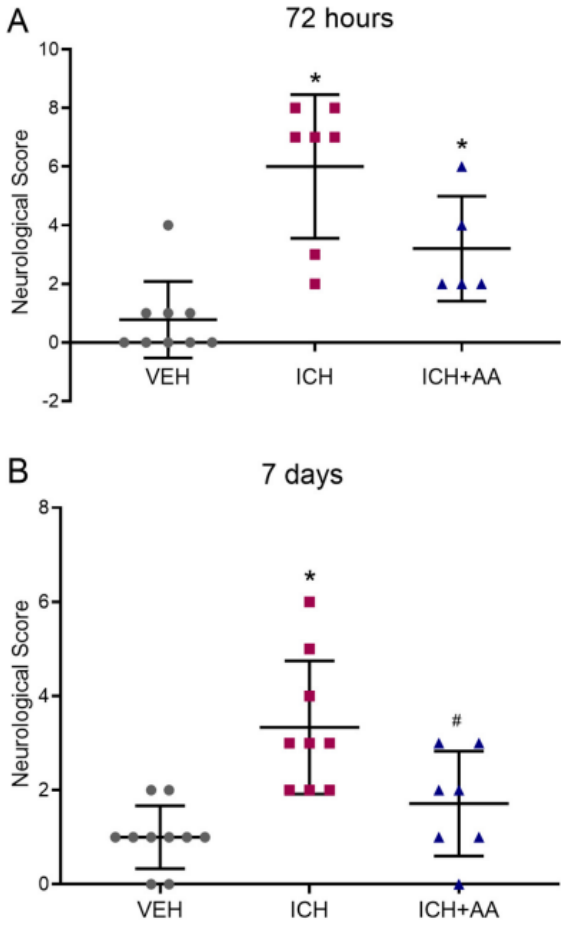

Figure 4. Effects of AA on motor impairment caused by ICH, as assessed by the neurological score at 72 h (A) and 7 days (B) post injury. n = 5–9 and 7–10 per group 72 h and 7 days after injury, respectively. Data are expressed as median (25th and 75th percentiles). *Different from the control group and # different from the ICH group.

3.3. Histological assessment

Collagenase injection into the dorsolateral striatum caused intrastriatal hemorrhage, as expected. Seventy two hours following injury, ICH and ICH + AA groups presented striatal lesion compared to the Vehicle group and AA treatment was not able to reduce the lesion volume at this time point ($F_{(2,26)}$ = 29.923, p < 0.001; n = 8–10) (Fig. 5A, E). However, 7 days after injury, the AA

injected group showed a decrease in the striatal lesion volume as compared to ICH group, being similar to the Vehicle group ($F_{(2,20)}$ = 10.686, p = 0.001; n = 5–8) (Fig. 5B, F). Hemispheric ratio was increased both in the ICH and ICH + AA groups compared to the Vehicle group at 72 h after injury ($F_{(2,26)}$ = 14.675, p < 0.001; n = 8–10) (Fig. 5C). Nonetheless, there was a decrease in the volume of the injured hemispheres and the left/right ratio became similar among all groups 7 days after ICH ($F_{(2,20)}$ = 2.309, p = 0.128; n = 5–8) (Fig. 5D).

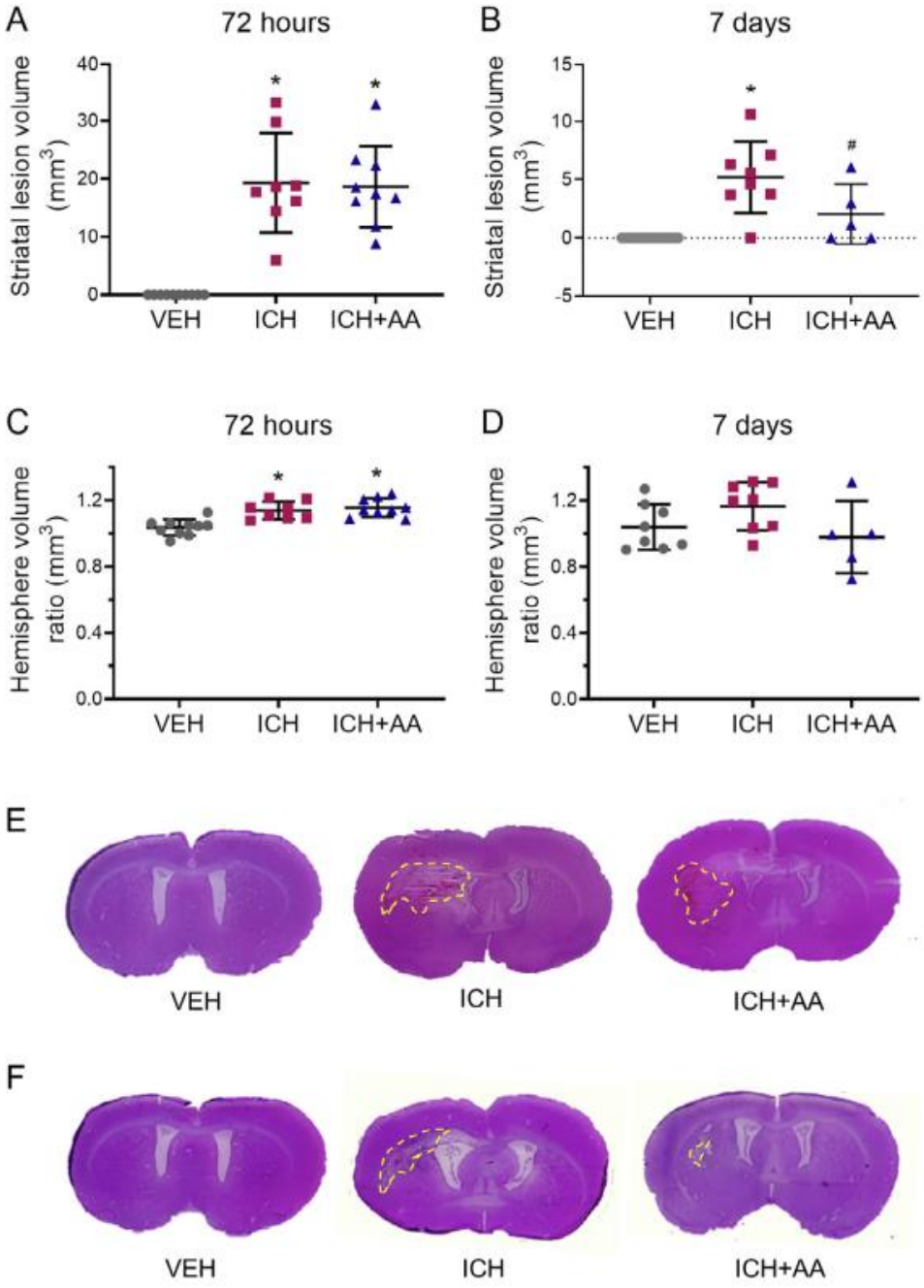

Figure 5. Effects of ICH surgery and AA treatment on hemorrhage and hemisphere volumes. Hemorrhage volume 72 h (A) and 7 days (B) post ICH; n = 8–10 and 5–8 per group 72 h and 7 days after injury, respectively. Volume of hemispheres 72 h (C) and 7 days (D) post ICH; n = 8–10 and 5–8 per group at 72 h and 7 days after injury, respectively. Lesion volume representative images at 72 h (E) and 7 days (F) after ICH. Data are expressed as mean ± SD. *Different from the control group and #different from the ICH group.

3.4. Immunofluorescence

Immunofluorescence analysis performed 7 days after injury showed high levels of GFAP and S100B protein in striatum of ICH compared to Vehicle rats, as shown by the fluorescence intensity (Fig. 6A, B, E) (GFAP: $F_{(2,18)} = 4.312$, $p = 0.032$, n = 6–7; S100B: $F_{(2,18)} = 4.899$, $p = 0.022$, n = 6–7) and the immunostained surface (Fig. 6C, D) (GFAP: $F_{(2,18)} = 18.604$, $p < 0.001$, n = 6–7; S100B: $F_{(2,18)} = 11.459$, $p = 0.001$, n = 6–7), suggesting reactive astrogliosis and increased S100B synthesis/ release in injured animals. AA treated rats had significantly lower levels of striatal GFAP and S100B as compared to the untreated group, being similar to the Vehicle.

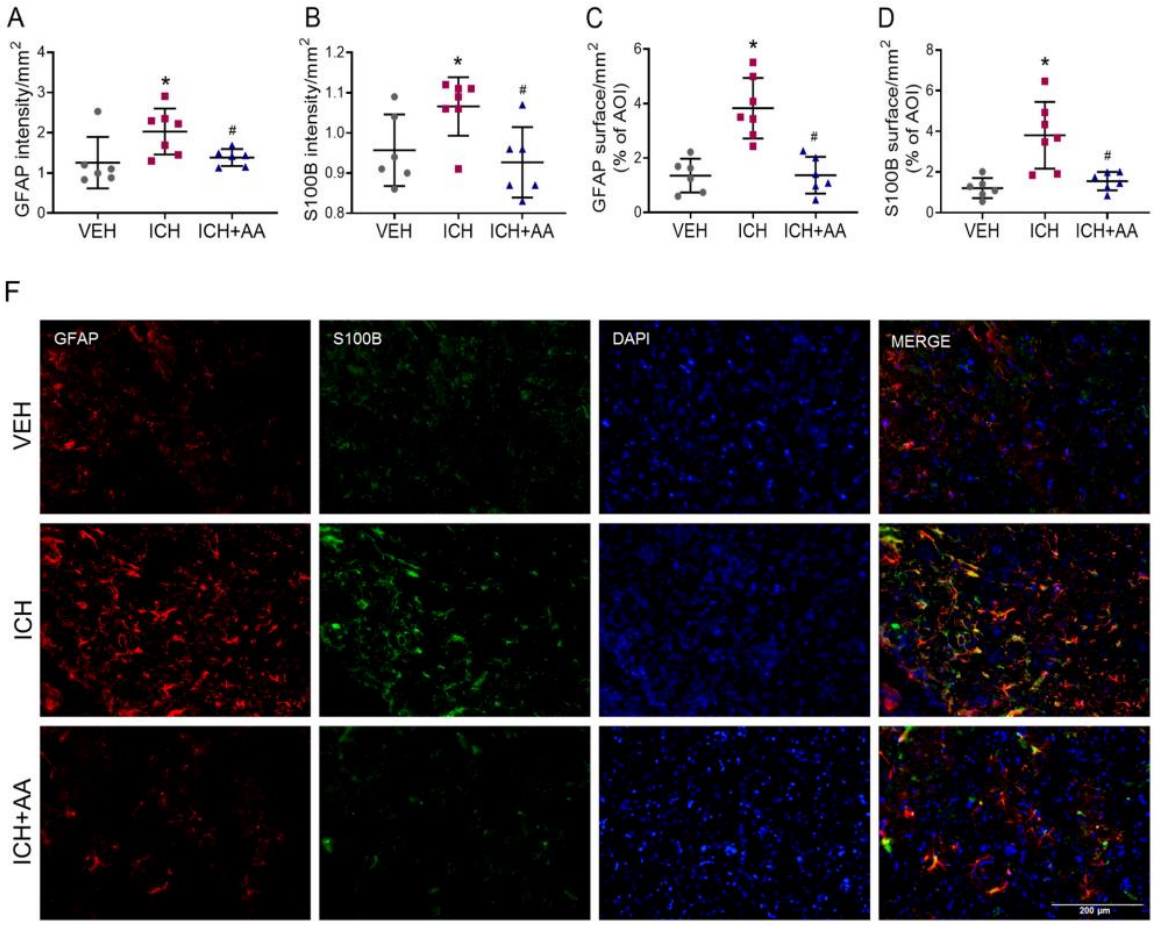

Figure 6. Effects of ICH injury and AA treatment on glial fibrillary acid protein (GFAP) and S100B levels measured by immunofluorescence analysis in the striatum, 7 days after injury. (A) Fluorescence intensity for GFAP (n = 6–7); (B) Fluorescence intensity for S100B (n = 6–7); (C) Immunostained surface for GFAP (n = 6–7); (D) Immunostained surface for GFAP (n = 6–7); (E) Representative images of immunofluorescence. Data are expressed as mean ± SD of ipsilateral/contralateral fluorescence intensity and immunostained surface ratio *different from the Vehicle group and #different from the ICH group. Statistical difference was considered when $p < 0.05$. One-way ANOVA followed by Duncan test. Scale is equivalent to 200 µm.

The number of NeuN positive cells (Fig. 7C) as well as the NeuN fluorescence intensity (Fig. 7A) were reduced in ICH rats compared to the Vehicle group ($F_{(2,15)} = 9.170$, $p = 0.003$, n = 5–6; $F_{(2,15)} = 7.617$, $p = 0.006$; n = 5–6, respectively), suggesting striatal neuronal death caused by injury, which occurred in parallel to the increase in cleaved Caspase-3 positive cells (Fig. 7D) and fluorescence intensity (Fig. 7B), a marker of cell apoptosis ($F_{(2,15)} = 7.011$, $p = 0.009$, n = 5–6; $F_{(2,15)} = 4.808$, $p = 0.027$; n = 5–6, respectively). Further,

double stained Neun^{+} and cleaved caspase-3^{+} cells was increased in ICH group compared to Vehicle ($F_{(2,15)}$ = 3.801, p = 0.05, n = 5–6) confirming the occurrence of striatal neuronal death as a result of the injury. Still, ICH + AA animals had NeuN and cleaved Caspase-3 levels similar to the Vehicle group and significantly lower than ICH group, suggesting that AA treatment prevented striatal cell death (Fig. 7).

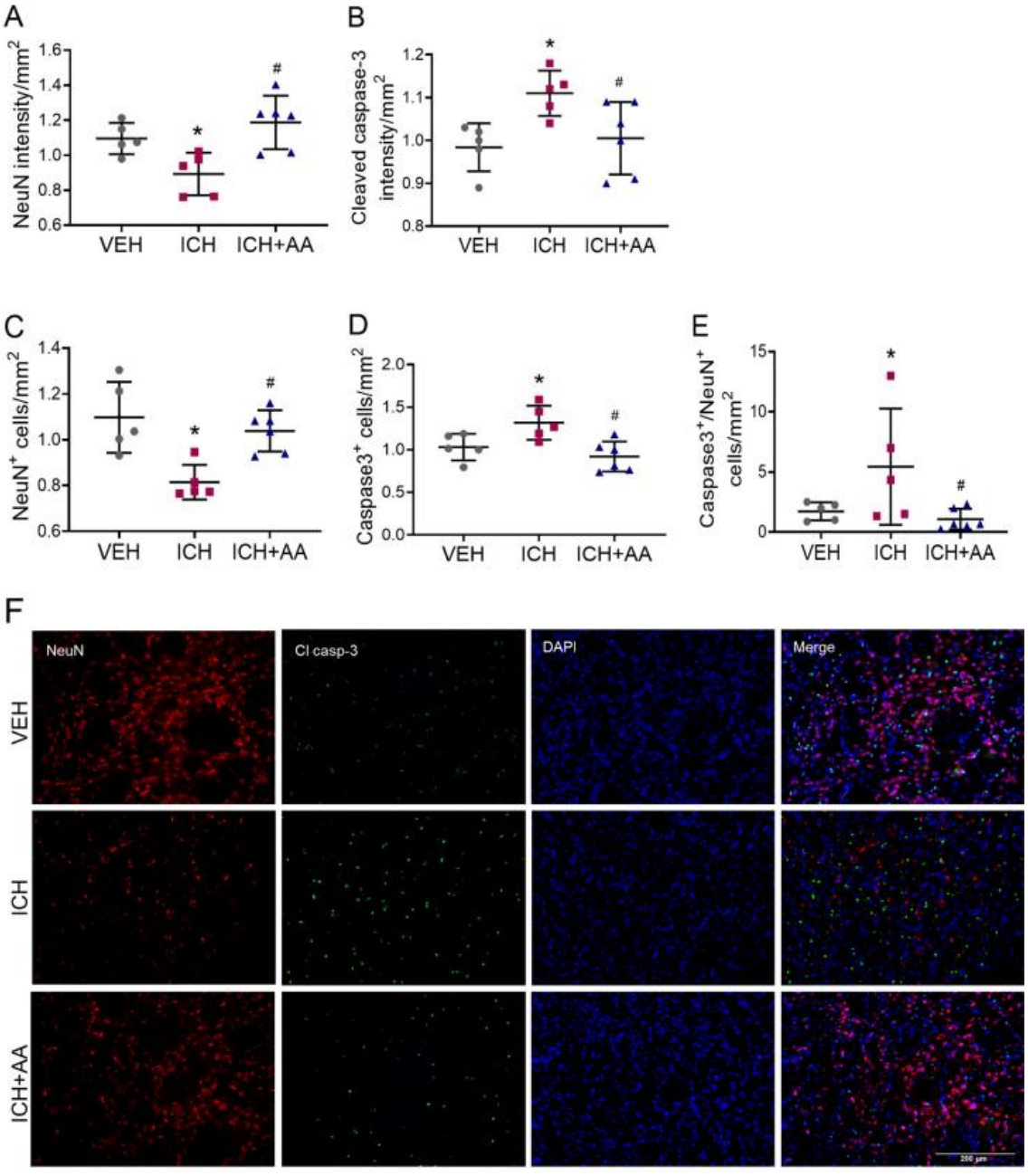

Figure 7. Effects of ICH injury and AA treatment in neuronal survival and in cell apoptosis measured by immunofluorescence analysis in the striatum, 7 days after injury. (A) NeuN levels measured by fluorescence intensity (n = 5–6). (B) Cleaved Caspase-3 levels measured by fluorescence intensity (n = 5–6). (C) Number of NeuN positive cells (n = 5–6). (D) Number of cleaved caspase-3 positive cells (n = 5–6). (E) Number of double stained NeuN and cleaved caspase-3 positive cells (n = 5–6). (F) Representative images of immunofluorescence. Data are expressed as mean ± SD of ipsilateral/contralateral ratio *different from the Vehicle group and #different from the ICH group. Statistical difference was considered when $p < 0.05$. One-way ANOVA followed by Duncan test. Scale is equivalent to 200 µm.

3.5. Biochemical analysis

As shown in Fig. 8, striatal levels of GFAP increased in the ICH group 7 days following injury, whereas AA treated group kept protein levels similar to the control group ($F_{(2,23)} = 3.490$; $p = 0.049$).

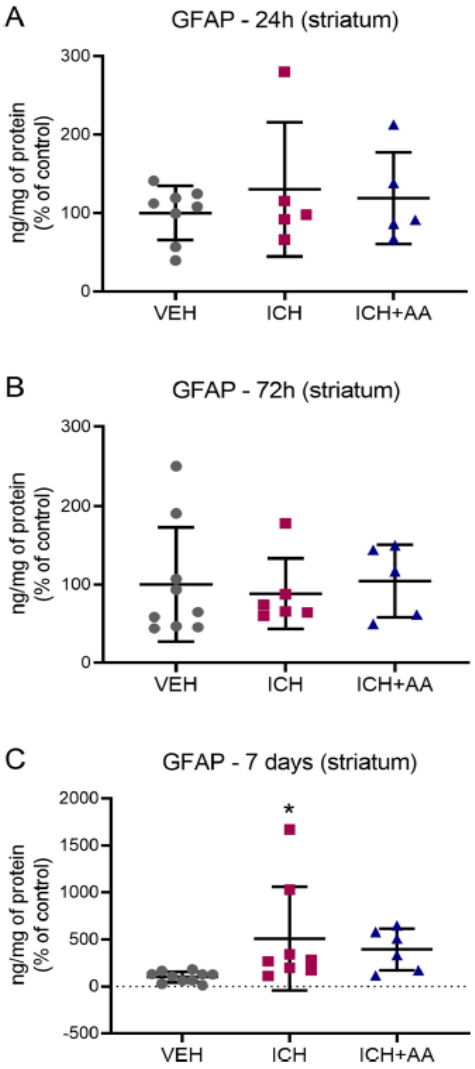

Figure 8. Effects of ICH surgery and AA treatment on striatal levels of GFAP 24 h (A), 72 h (B) and 7 days (C) post ICH; n=5–8, 5–9 and 6–10 per group, respectively. Data are expressed as percentage of control values (mean±SD). *Different from the control group.

S100B protein content in the striatum increased 7 days after injury in the ICH group compared to the control. However, ICH + AA group presented a decrease in S100B levels compared to ICH group ($F_{(2,26)}$ = 3.592; p = 0.043) (Fig. 9C), confirming results of immunofluorescence analysis. In the CSF, S100B levels were increased 72 h after injury in the ICH group, while rats treated with AA kept S100B levels similar to the Vehicle group and significantly lower than injured group ($F_{(2,17)}$ = 4.045; p = 0.039) (Fig. 9E). In the serum, S100B levels were increased 24 h after injury in the ICH group, whereas in the ICH + AA group the levels were reduced compared to the untreated group and similar to the Vehicle group ($F_{(2,17)}$ = 18.537; p < 0.001) (Fig. 9G). At 72 h, S100B levels of both injured groups returned to the baseline, presenting no difference compared to the controls ($F_{(2,20)}$ = 0.219; p = 0.806) (Fig. 9H). Seven days after injury, S100B levels returned to increase in the ICH group, but did not increase in the AA treated group ($F_{(2,19)}$ = 3.599; p = 0.050) (Fig. 9I).

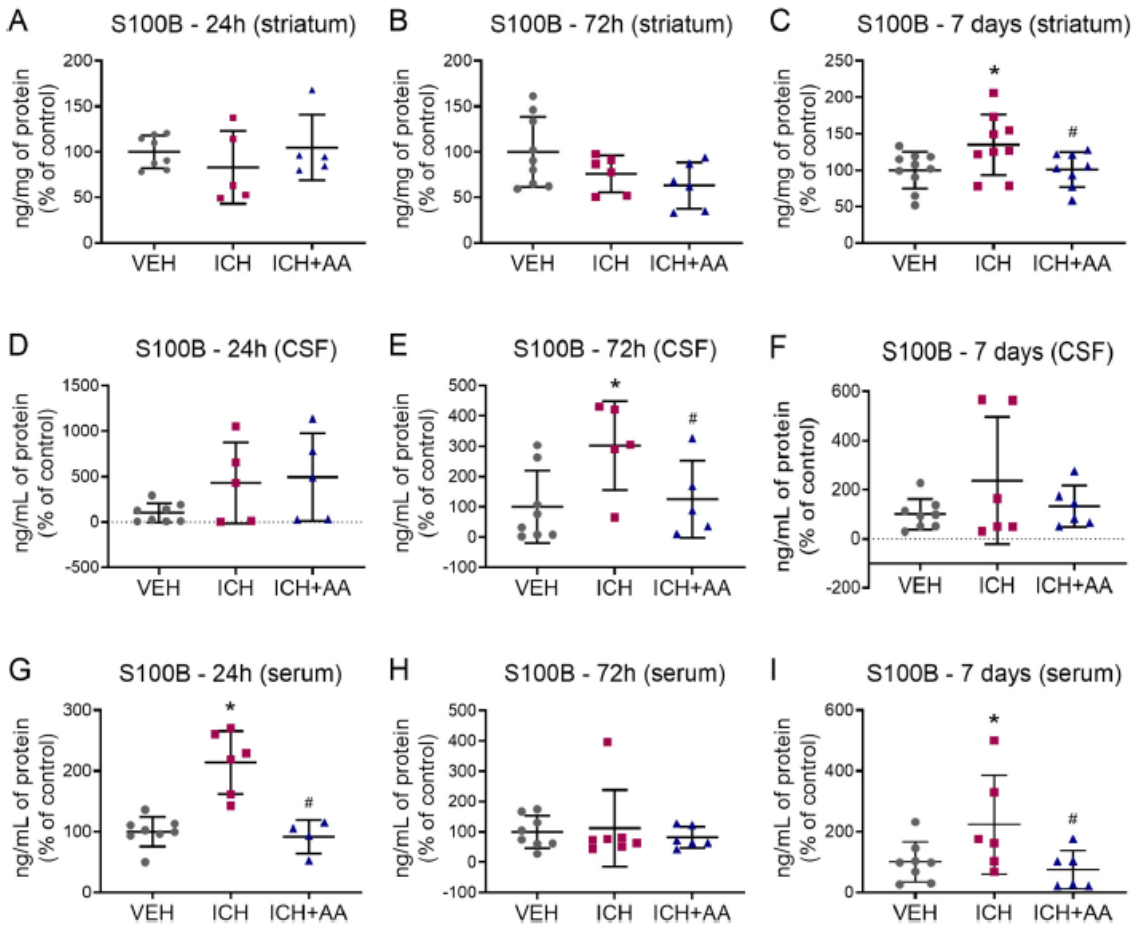

Figure 9. Effects of ICH surgery and AA treatment on central and peripheral levels of S100B. S100B levels on striatum 24 h (A; n=5–8), 72 h (B; n=6–9) and 7 days (C; n=8–10) post ICH; S100B levels on cerebrospinal fluid (CSF) 24 h (D; n=5–8), 72 h (E; n=5–8) and 7 days (F; n=6–8) post ICH; S100B levels on serum 24 h (G; n=5–8), 72 h (H; n=6–8) and 7 days (I; n=6–8) post ICH. Data are expressed as percentage of control values (mean±SD). *Different from the control group and #different from the ICH group.

GSH levels showed an increase in striatum 24 h after injury in the ICH + AA group compared to the ICH and Vehicle groups ($F_{(2,17)}$ = 4.232; p = 0.033) (Fig. 10A). Seventy-two hours (Fig. 10B) and 7 days post ICH (Fig. 10C), there were no differences in GSH levels among groups ($F_{(2,18)}$ = 0.558; p = 0.583 and $F_{(2,23)}$ = 1.411; p = 0.266, respectively).

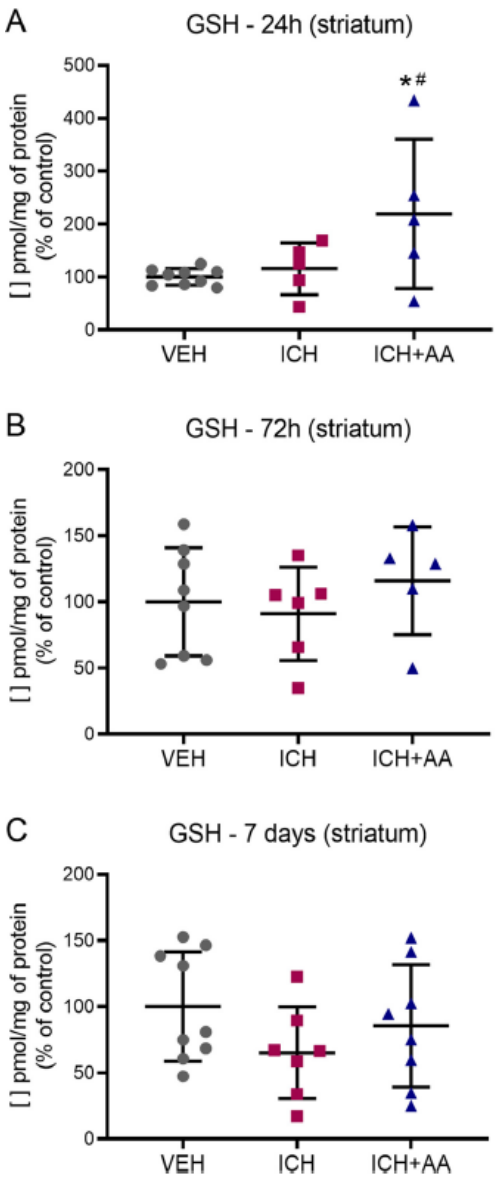

Figure 10. Striatal levels of glutathione (GSH) in response to ICH surgery and AA treatment 24 h (A), 72 h (B) and 7 days (C) following ICH. n=5–8, 5–8 and 7–9 per group in 24 h, 72 h and 7 days, respectively. Data are expressed as percentage of control values (mean±SD). *Different from the control group and #different from the ICH group.

GS activity was decreased in ICH + AA group 24 h post injury compared to the ICH and control groups ($F_{(2,17)}$ = 3.697; p = 0.050) (Fig. 11A). Seventy-two hours (Fig. 11B) and 7 days after ICH (Fig. 11C), GS activity was similar among groups ($F_{(2,17)}$ = 0.482; p = 0.627 and $F_{(2,25)}$ = 1.601; p = 0.223, respectively).

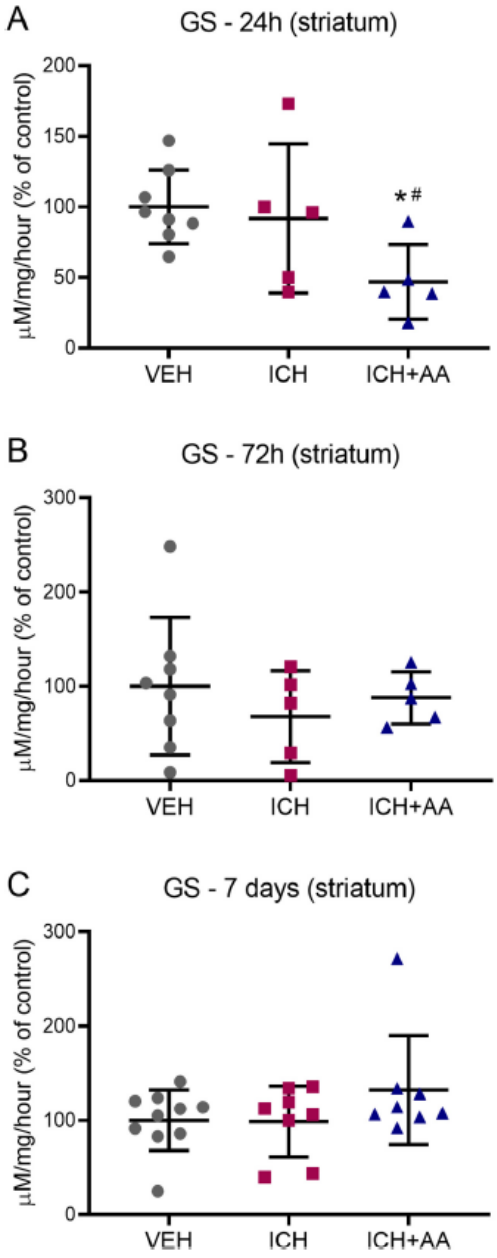

Figure 11. Activity of the glutamine synthetase (GS) enzyme in the striatum 24 h (A), 72 h (B) and 7 days (C) post ICH. n=5–8, 5–8 and 8–10 per group, respectively. Data are expressed as percentage of control values (mean±SD). *Different from the control group and #different from the ICH group.

4. Discussion

Present study aimed to analyze the beneficial effects of AA for treating ICH in rats. It is shown that AA injection exerted protective effects in injured animals, that is, it prevented neurological deficits caused by the ICH, possibly

by inhibiting the astrocytic synthesis of S100B thereby reducing glial activation and cell death, and increasing brain antioxidant defenses.

Firstly, we tested different doses of AA to define an effective dose (Experiment I) for further studies. The 2 μg/μL dose markedly reduced GFAP and S100B levels in the striatum of Naïve rats (Fig. 3) and was chosen to be used as treatment for animals undergoing ICH surgery in the further experiment (Experiment II). The advantages of ICV administration is that drugs do not need to pass through the BBB and are not metabolized before reaching the CNS, thus ensuring that the amount of drug is all delivered to brain tissue (Atkinson, 2017). However, there are some difficulties and complications have been related to this route of administration. The scarcity of studies that carry out ICV drug administration makes it difficult to establish the ideal dose (Atkinson, 2017). Furthermore, the risks of ICV catheter placement include post-operative infection, hemorrhage and malpositioning (Glascock et al., 2011). As we performed a single administration of the agent, it was not necessary to place a catheter, reducing the chances of adverse effects. Interestingly, one study compared the intraperitoneal (IP) versus stereotactic injection (SI) of Edaravone into the hematoma cavity in rats with ICH and found that the SI had superior effects than IP injection, improving the neurological deficits and decreasing the hemorrhage volume, brain edema and BBB damage (Zhang et al., 2016).

Striatum is widely known to be an important structure in motor function control (Graybiel and Grafton, 2015). Hematoma resulting from ICH in this area may directly compress brain tissue, which leads to further mechanical damage and additional secondary brain injury, as well as neurological deterioration due to excitotoxicity and cell death (Enatsu et al., 2012). We showed that striatal

injection of IV-S collagenase caused striatal hemorrhage and significant neurological impairments in rats submitted to ICH, as previously described (Mestriner et al., 2011; Zhang et al., 2016; Neves et al., 2017). Animals treated with AA had a total reversal of striatal lesion volume and neurological deficits compared to the untreated group 7 days post injury (Figs. 4 and 5). AA half-life is 2 to 3 h in patients with acute ischemic stroke (Ishibashi et al., 2007), and although only one dose of AA was administered, we believe that the prolonged effect of AA treatment was due to inhibition of deleterious events of the insult in the first hours after ICH.

Previous reports in ischemic brain injury models have also shown that AA treatment was able to mitigate the delayed expansion of infarct volume and the neurologic deficits (Tateishi et al., 2002; Asano et al., 2005; Mori et al., 2005). In addition to experimental studies, a multicenter phase I trial in patients suffering from acute ischemic stroke showed that AA treatment during 7 days was associated with lower serum levels of S100B and improvement of neurological function until 40 days after stroke (Pettigrew et al., 2006a,b).

S100B is passively released from damaged/necrotic astrocytes (Sorci et al., 2010). Peripheral S100B levels has been considered a biomarker of ICH brain damage in basic (Tanaka et al., 2009; Neves et al., 2017) and clinical research (Hu et al., 2010; Senn et al., 2014; Zhou et al., 2016). S100B plays an important role in the mechanism of secondary brain injury and its levels are associated with higher mortality rates (Hu et al., 2010) and poorer neurological outcomes (James et al., 2009) in ICH patients; in the ICH rat model, high levels of S100B are associated with cerebral edema and maximal extent of hematoma volume (Tanaka et al., 2009). In present study we observed that serum S100B

levels had an early increase within 24 h after injury (Fig. 9G), whereas the increase of S100B central levels (in the CSF and in the striatum) occurred later, at 72 h and 7 days post ICH, respectively (Fig. 9E, C). Other studies using the ICH rat model also reported increased levels of S100B in serum (Tanaka et al., 2009; Neves et al., 2017), CSF and striatum at different time-point post-ICH (Neves et al., 2017). Interestingly, S100B levels in serum had an additional increase 7 days after injury (Fig. 9I), following the increase of S100B content in the striatum. We tend to interpret such increase as a S100B leaking from the CNS into the peripheral blood through the disrupted BBB due to ICH, as previously described (Kanner et al., 2003). However, we must be careful with this assumption, since extracerebral sources such as adipocytes chondrocytes contribute to the serum S100B content (Gonçalves et al., 2010).

Importantly, AA treatment was able to reduce peripheral and central S100B levels of ICH-submitted rats at all time-points in which they were increased, as demonstrated by ELISA and immunofluorescence analysis (Figs. 9 and 6B, D). In agreement, previous studies have shown that AA reduces S100B levels in permanent middle cerebral artery occlusion (Tateishi et al., 2002; Mori et al., 2005), chronic cerebral hypoperfusion (Ohtani et al., 2007), acute subdural hematoma (Wajima et al., 2013), spinal cord injury (Hanada et al., 2014), Parkinson (Kato et al., 2004; Oki et al., 2008) and Alzheimer's disease models (Mori et al., 2006), as well as improves neurological outcomes and / or decreases tissue injury.

The increase observed in striatal S100B concentration occurred in parallel with the increase in GFAP content within 7 days after ICH in animals that did not receive AA treatment (Fig. 8C), suggesting intense reactive

astrogliosis in the region. Supporting our findings, a previous ICH study showed elevated GFAP levels in striatum, measured by ELISA, on the 7th day after ICH (Neves et al., 2017). Besides that, other studies using AA treatment have observed a reduction in GFAP tissue levels following CNS injuries (Tateishi et al., 2002; Mori et al., 2005; Higashino et al., 2009; Hanada et al., 2014), corroborating with our results. Here, the animals treated with AA had lower levels of GFAP compared to the ICH group, showing a partial decrease in reactive astrogliosis. Increases in GFAP levels following ICH are well documented (Sukumari-Ramesh et al., 2012) and, recently, Chiu et al., (2017) observed that the suppression in astrocytic activity of rats submitted to ICH resulted in a decrease in hematoma expansion, less BBB destruction, reduced astrocyte accumulation in perihematomal regions, and better neurological outcomes. This supports the idea that astrocytes play a key role in the pathological development of ICH and makes them an interesting therapeutic target in brain injury.

Immunofluorescence analysis confirmed the elevated GFAP levels in striatum of ICH rats observed by ELISA 7 days after injury (Fig. 6A, C, E), and also exhibited the morphological changes of reactive astrocytes, a process that was accompanied by the increase of S100B levels (Fig. 6B, D, E). The efficacy of AA injection could be observed by the remarkable reduction in the fluorescence of these two proteins in treated animals (Fig. 6). Reactive astrogliosis in ICH can be triggered by several factors. During brain hemorrhage, blood-derived factors such as thrombin can leak into the brain parenchyma and serve as an inducer of astrocytic activation and proliferation (Nishino et al., 1993). Also, when BBB is damaged following brain injury, a

variety of neurochemical factors are released and have been shown to induce astrogliosis (Sukumari-Ramesh et al., 2012). High S100B concentrations can also promote astroglial hypertrophy, turning astrocytes into a pro-inflammatory phenotype and activating RAGE (Receptor for Advanced Glycation End products) receptors expression, thus configuring a feed-forward loop that may potentiate and expand S100B effects (Villarreal et al., 2014), which must have happened in our study.

ICH causes significant perihematomal cell death and brain atrophy through cell death pathways that include necrosis, apoptosis and autophagy (Keep et al., 2012). This work showed that untreated injured animals had a decrease in the number of striatal neurons and an increase in cleaved caspase-3 positive neural cells, indicating apoptotic cell death, whereas AA-treated animals had neuron preservation (Fig. 7). It is well known that high concentrations of S100B lead to neuronal apoptosis, which can occur via direct action on neurons by binding to RAGE receptors, and via stimulation of nitric oxide release by astrocytes (Fanò et al., 1993; Hu et al., 2002; Sorci et al., 2010). Thus, decreased S100B protein concentration by AA action must have been an important factor in preventing neuronal death, since at low concentrations, S100B protects neurons against apoptosis, stimulates neurite growth and downregulates astrocytic response to neurotoxic agents (Sorci et al., 2010).

Another consequence of brain damage is the pathological release of glutamate in excitotoxic quantities by necrotic perihematomal neurons (Senn et al., 2014). An important function of astrocytes is the extracellular glutamate uptake, that may be targeted for conversion to glutamine by action of GS

enzyme (Eid et al., 2016), or to the synthesis of GSH (Dringen et al., 2015). Our study demonstrated an elevated GSH content in AA treated animals compared to the untreated and control group 24 h after ICH (Fig. 10A); interestingly, this increase was followed by a decrease inGSactivity at the same time point (Fig. 11A), indicating that glutamate uptake by astrocytes was directed to GSH synthesis rather than to glutamine production. This finding suggests that AA may have a potential antioxidant action, protecting the brain against OS, a metabolic challenge that plays a pivotal role in cerebral injury following ICH (Hu et al., 2016; Neves et al., 2018).

Our study has some limitations: (1) not considering sexual dimorphism in the experimental design, since the sex of animals may have an effect on behavioral, biochemical and histological variables here measured. We chose to use only male rats in order to avoid the influence of the estrous cycle and female sex hormones, especially estrogen, which exerts neuroprotective effects and modulates the immune response after experimental stroke and other acute CNS injuries (Engler-Chiurazzi et al., 2017; Ce´ spedes Rubio et al., 2018; Kim et al., 2019); (2) the correlation analysis between biochemical variables and behavioral outcomes did not reach statistical significance, probably due to the small sample size used. However, it is necessary to admit that AA could have other mechanisms of action that are influencing neurological improvement; (3) regarding the ICH model, it is possible that the collagenase itself causes an inflammatory reaction independent of the inflammation due to the components of the hematoma (Vargaftig et al., 1976), so AA could have an effect on inflammation induced by collagenase rather than inflammation resulting from the ICH lesion; (4) only one AA injection was performed immediately before the

ICH injury, so it is necessary to conduct studies to assess the effects of delayed AA administration for modelling clinical populations; (5) other limitation is that rats were evaluated only up to 7 days post-injury, so further studies assessing the AA long-term effects on this injury model are needed.

In conclusion, ICV AA injection showed neuroprotective action following ICH in rats, as demonstrated by: (1) reduction of intracellular and extracellular S100B levels; (2) prevention of excessive reactive astrogliosis in the damaged striatum; (3) reduction of cellular apoptosis and neuronal death; (4) increase in brain antioxidants concentration; (5) attenuation of striatal lesion extension and (6) improvement of neurological function. ICH is a complex pathology and, to date, there is no effective treatment for improving neurological outcome. Acting on distinct points of the injury cascade, AA was shown to be an effective neuroprotective agent after experimental ICH.

ACKNOWLEDGEMENTS

This work was supported by Coordenação de Aperfeiçoamento de Pessoal de Nível Superior (CAPES), Conselho Nacional de Desenvolvimento Científico e Tecnológico (CNPq), Fundação de Amparo à Pesquisa do Estado do Rio Grande do Sul (FAPERGS).

DECLARATIONS OF INTEREST

None.

References

Agnihotri S, Czap A, Staff I, Fortunato G, McCullough LD (2011) Peripheral leukocyte counts and outcomes after intracerebral hemorrhage. J Neuroinflammation 8:160. https://doi.org/10.1186/1742-2094-8-160.

Allen S, Shea JM, Felmet T, Gadra J, Dehn PF (2000) A kinetic microassay for glutathione in cells plated on 96-well microtiter plates. Methods Cell Sci 22:305–312. https://doi.org/10.1023/A:1017585308255.

Altumbabic M, Peeling J, Del Bigio MR (1998) Intracerebral hemorrhage in the rat: effects of hematoma aspiration. Stroke 29:1917–1922. https://doi.org/10.1161/01.STR.29.9.1917.discussion1922-1923.

Aronowski J, Zhao X (2011) Molecular pathophysiology of cerebral hemorrhage: secondary brain injury. Stroke 42:1781–1786. https://doi.org/10.1161/STROKEAHA.110.596718.

Asano T, Mori T, Shimoda T, Shinagawa R, Satoh S, Yada N, Katsumata S, Matsuda S, Kagamiishi Y, Tateishi N (2005) Arundic acid (ONO-2506) ameliorates delayed ischemic brain damage by preventing astrocytic overproduction of S100B. Curr Drug Targets CNS Neurol Disord 4:127–142. https://doi.org/10.2174/1568007053544084.

Atkinson AJ (2017) Intracerebroventricular drug administration. Transl Clin Pharmacol 25:117–124. Available from: https://doi.org/10.12793/tcp.2017.25.3.117.

Céspedes Rubio ÁE, Pérez-Alvarez MJ, Lapuente Chala C, Wandosell F (2018) Sex steroid hormones as neuroprotective elements in ischemia models. J Endocrinol 237:R65–R81. https://doi.org/10.1530/JOE-18-0129.

Cheon S-H (2015) The effect of a skilled reaching task on hippocampal plasticity after intracerebral hemorrhage in adult rats. J Phys Ther Sci 27:131–133. https://doi.org/10.1589/jpts.27.131.

Chiu C-D, Yao N-W, Guo J-H, Shen C-C, Lee H-T, Chiu Y-P, Ji H-R, Chen X, Chen C-C, Chang C (2017) Inhibition of astrocytic activity alleviates sequela in acute stages of intracerebral hemorrhage. Oncotarget 8:94850–94861. Available from: https://doi.org/10.18632/oncotarget.22022.

Dringen R, Brandmann M, Hohnholt MC, Blumrich E-M (2015) Glutathione-dependent detoxification processes in astrocytes. Neurochem Res 40:2570–2582. https://doi.org/10.1007/s11064-014-1481-1.

Eid T, Gruenbaum SE, Dhaher R, Lee T-SW, Zhou Y, Danbolt NC (2016) The glutamate-glutamine cycle in epilepsy. Adv Neurobiol:351–400. https://doi.org/10.1007/978-3-319-45096-4_14.

Eid T, Lee T-SW, Patrylo P, Zaveri HP (2018) Astrocytes and glutamine synthetase in epileptogenesis. J Neurosci Res. https://doi.org/10.1002/jnr.24267.

Enatsu R, Asahi M, Matsumoto M, Hirai O (2012) Prognostic factors of motor recovery after stereotactic evacuation of intracerebral hematoma. Tohoku J Exp Med 227:63–67. https://doi.org/10.1620/tjem.227.63.

Engler-Chiurazzi EB, Brown CM, Povroznik JM, Simpkins JW (2017) Estrogens as neuroprotectants: Estrogenic actions in the context of cognitive aging and brain injury. Prog Neurobiol 157:188. https://doi.org/10.1016/J.PNEUROBIO.2015.12.008.

Fanò G, Mariggiò MA, Angelella P, Nicoletti I, Antonica A, Fulle S, Calissano P (1993) The S-100 protein causes an increase of intracellular calcium and death of PC12 cells. Neuroscience 53:919–925. https://doi.org/10.1016/0306-4522(93)90477-w.

Fiorella D, Zuckerman SL, Khan IS, Ganesh Kumar N, Mocco J (2015) Intracerebral hemorrhage: a common and devastating disease in need of better treatment. World Neurosurg 84:1136–1141. https://doi.org/10.1016/J.WNEU.2015.05.063.

Foerch C, Niessner M, Back T, Bauerle M, De Marchis GM, Ferbert A, Grehl H, Hamann GF, Jacobs A, Kastrup A, Klimpe S, Palm F, Thomalla G, Worthmann H, Sitzer M, BE FAST Study Group (2012) Diagnostic accuracy of plasma glial fibrillary acidic protein for differentiating intracerebral hemorrhage and cerebral ischemia in patients with symptoms of acute stroke. Clin Chem 58:237–245. https://doi.org/10.1373/clinchem.2011.172676.

Glascock JJ, Osman EY, Coady TH, Rose FF, Shababi M, Lorson CL (2011) Delivery of therapeutic agents through intracerebroventricular (ICV) and intravenous (IV) injection in mice. J Vis Exp 2968. https://doi.org/10.3791/2968.

Gonçalves CA, Leite MC, Guerra MC (2010) Adipocytes as na important source of serum S100B and possible roles of this protein in adipose tissue. Cardiovasc Psychiatry Neurol 2010. https://doi.org/10.1155/2010/790431790431.

Graybiel AM, Grafton ST (2015) The striatum: where skills and habits meet. Cold Spring Harb Perspect Biol 7. https://doi.org/10.1101/cshperspect.a021691a021691.

Hanada M, Shinjo R, Miyagi M, Yasuda T, Tsutsumi K, Sugiura Y, Imagama S, Ishiguro N, Matsuyama Y (2014) Arundic acid (ONO-2506) inhibits secondary injury and improves motor function in rats with spinal cord injury. J Neurol Sci 337:186–192. https://doi.org/10.1016/j.jns.2013.12.008.

Higashino H, Niwa A, Satou T, Ohta Y, Hashimoto S, Tabuchi M, Ooshima K (2009) Immunohistochemical analysis of brain lesions using S100B and glial fibrillary acidic protein antibodies in arundic acid- (ONO-2506) treated stroke-

prone spontaneously hypertensive rats. J Neural Transm 116:1209–1219. https://doi.org/10.1007/s00702-009-0278-x.

Hu J, Castets F, Guevara JL, Van Eldik LJ (1996) S100 beta stimulates inducible nitric oxide synthase activity and mRNA levels in rat cortical astrocytes. J Biol Chem 271:2543–2547. https://doi.org/10.1074/JBC.271.5.2543.

Hu Y-Y, Dong X-Q, Yu W-H, Zhang Z-Y (2010) Change in plasma S100B level after acute spontaneous basal ganglia hemorrhage. Shock 33:134–140. https://doi.org/10.1097/SHK.0b013e3181ad5c88.

Hu J, Ferreira A, Van Eldik LJ (2002) S100b Induces Neuronal Cell Death Through Nitric Oxide Release from Astrocytes. J Neurochem 69:2294–2301. https://doi.org/10.1046/j.1471-4159.1997.69062294.x.

Hu X, Tao C, Gan Q, Zheng J, Li H, You C (2016) Oxidative stress in intracerebral hemorrhage: sources, mechanisms, and therapeutic targets. Oxid Med Cell Longev 2016:3215391. https://doi.org/ 10.1155/2016/3215391.

Imamura N, Hida H, Aihara N, Ishida K, Kanda Y, Nishino H, Yamada K (2003) Neurodegeneration of substantia nigra accompanied with macrophage/microglia infiltration after intrastriatal hemorrhage. Neurosci Res 46:289–298. https://doi.org/10.1016/S0168-0102(03)00065-8.

Ishibashi H, Creed Pettigrew L, Funakoshi Y, Hiramatsu M (2007) Pharmacokinetics of arundic acid, an astrocyte modulating agent, in acute ischemic stroke. J Clin Pharmacol 47:445–452. https://doi.org/10.1177/0091270006299090.

James ML, Blessing R, Phillips-Bute BG, Bennett E, Laskowitz DT (2009) S100B and brain natriuretic peptide predict functional neurological outcome after intracerebral haemorrhage. Biomarkers 14:388–394. https://doi.org/10.1080/13547500903015784.

Kanner AA, Marchi N, Fazio V, Mayberg MR, Koltz MT, Siomin V, Stevens GHJ, Masaryk T, Ayumar B, Vogelbaum MA, Barnett GH, Janigro D, Janigro D (2003) Serum S100beta: a noninvasive marker of blood-brain barrier function and brain lesions. Cancer 97:2806–2813. https://doi.org/10.1002/cncr.11409.

Kato H, Araki T, Imai Y, Takahashi A, Itoyama Y (2003) Protection of dopaminergic neurons with a novel astrocyte modulating agent (R)-(_)-2-propyloctanoic acid (ONO-2506) in an MPTP-mouse model of Parkinson's disease. J Neurol Sci 208:9–15. https://doi.org/10.1016/S0022-510X(02)004112.

Kato H, Kurosaki R, Oki C, Araki T (2004) Arundic acid, an astrocyte modulating agent, protects dopaminergic neurons against MPTP neurotoxicity in mice. Brain Res 1030:66–73. https://doi.org/10.1016/j.brainres.2004.09.046.

Keep RF, Hua Y, Xi G (2012) Intracerebral haemorrhage: Mechanisms of injury and therapeutic targets. Lancet Neurol 11:720–731. https://doi.org/10.1016/S1474-4422(12)70104-7.

Kim T, Chelluboina B, Chokkalla AK (2019) Age and sex differences in the pathophysiology of acute CNS injury. Neurochem Int 127:22–28. https://doi.org/10.1016/J.NEUINT.2019.01.012.

Kumar A, Kumar P, Misra S, Sagar R, Kathuria P, Vibha D, Vivekanandhan S, Garg A, Kaul B, Raghvan S, Gorthi SP, Dabla S, Aggarwal CS, Prasad K (2015) Biomarkers to enhance accuracy and precision of prediction of short-term and long-term outcome after spontaneous intracerebral haemorrhage : a study protocol for a prospective cohort study. BMC Neurol 4–9. https://doi.org/10.1186/s12883-015-0384-3.

Leite MC, Galland F, Brolese G, Guerra MC, Bortolotto JW, Freitas R, de Almeida LMV, Gottfried C, Gonc¸ alves CA (2008) A simple, sensitive and widely applicable ELISA for S100B: Methodological features of the

measurement of this glial protein. J Neurosci Methods 169:93–99. https://doi.org/10.1016/j.jneumeth.2007.11.021.

Matsui T, Mori T, Tateishi N, Kagamiishi Y, Satoh S, Katsube N, Morikawa E, Morimoto T, Ikuta F, Asano T (2002) Astrocytic activation and delayed infarct expansion after permanent focal ischemia in rats. Part I: enhanced astrocytic synthesis of S-100b in the periinfarct area precedes delayed infarct expansion. J Cereb Blood Flow Metab 22:711–722. https://doi.org/10.1097/00004647-200206000-00010.

Mestriner RG, Pagnussat AS, Boisserand LSB, Valentim L, Netto CA (2011) Skilled reaching training promotes astroglial changes and facilitated sensorimotor recovery after collagenase-induced intracerebral hemorrhage. Exp Neurol 227:53–61. https://doi.org/10.1016/j.expneurol.2010.09.009.

Mestriner RG, Miguel PM, Bagatini PB, Saur L, Boisserand LSB, Baptista PPA, Xavier LL, Netto CA (2013) Behavior outcome after ischemic and hemorrhagic stroke, with similar brain damage, in rats. Behav Brain Res 244:82–89. https://doi.org/10.1016/j.bbr.2013.02.001.

Minet R, Villie F, Marcollet M, Meynial-Denis D, Cynober L (1997) Measurement of glutamine synthetase activity in rat muscle by a colorimetric assay. Clin Chim Acta 268:121–132. https://doi.org/10.1016/s0009-8981(97)00173-3.

Mori T, Town T, Tan J, Tateishi N, Asano T (2005) Modulation of astrocytic activation by arundic acid (ONO-2506) mitigates detrimental effects of the apolipoprotein E4 isoform after permanent focal ischemia in apolipoprotein E knock-in mice. J Cereb Blood Flow Metab 25:748–762. https://doi.org/10.1038/sj.jcbfm.9600063.

Mori T, Town T, Tan J, Yada N, Horikoshi Y, Yamamoto J, Shimoda T, Kamanaka Y, Tateishi N, Asano T (2006) Arundic Acid ameliorates cerebral amyloidosis and gliosis in Alzheimer transgenic mice. J Pharmacol Exp Ther 318:571–578. https://doi.org/10.1124/jpet.106.105171.

Mracsko E, Veltkamp R (2014) Neuroinflammation after intracerebral hemorrhage. Front Cell Neurosci 8:1–13. https://doi.org/10.3389/fncel.2014.00388.

Neves JD, Aristimunha D, Vizuete AF, Nicola F, Vanzela C, Petenuzzo L, Mestriner RG, Sanches EF, Gonc¸ alves CA, Netto CA (2017) Glial-associated changes in the cerebral cortex after collagenase-induced intracerebral hemorrhage in the rat striatum. Brain Res Bull 134:55–62. https://doi.org/10.1016/j.brainresbull.2017.07.002.

Neves JD, Vizuete AF, Nicola F, Da Re´ C, Rodrigues AF, Schmitz F, Mestriner RG, Aristimunha D, Wyse ATS, Netto CA (2018) Glial glutamate transporters expression, glutamate uptake, and oxidative stress in an experimental rat model of intracerebral hemorrhage. Neurochem Int 116:13–21. https://doi.org/10.1016/j.neuint.2018.03.003.

Nicola FC, Rodrigues LP, Crestani T, Quintiliano K, Sanches EF, Willborn S, Aristimunha D, Boisserand L, Pranke P, Netto CA, Nicola FC, Rodrigues LP, Crestani T, Quintiliano K, Sanches EF, Willborn S, Aristimunha D, Boisserand L, Pranke P, Netto CA (2016) Human dental pulp stem cells transplantation combined with treadmill training in rats after traumatic spinal cord injury. Brazilian J Med Biol Res 49. https://doi.org/10.1590/1414-431x20165319.

Nishino A, Suzuki M, Ohtani H, Motohashi O, Umezawa K, Nagura H, Yoshimoto T (1993) Thrombin may contribute to the pathophysiology of central nervous system injury. J Neurotrauma 10:167–179. https://doi.org/10.1089/neu.1993.10.167.

Ohtani R, Tomimoto H, Wakita H, Kitaguchi H, Nakaji K, Takahashi R (2007) Expression of S100 protein and protective effect of arundic acid on the rat brain in chronic cerebral hypoperfusion. Brain Res 1135:195–200. https://doi.org/10.1016/j.brainres.2006.11.084.

Oki C, Watanabe Y, Yokoyama H, Shimoda T, Kato H, Araki T (2008) Delayed treatment with arundic acid reduces the MPTP-induced neurotoxicity in mice. Cell Mol Neurobiol 28:417–430. https://doi.org/10.1007/s10571-007-9241-2.

Paxinos G, Watson C (2007) The rat brain in stereotaxic coordinates. Elsevier.

Peterson GL (1977) A simplification of the protein assay method of Lowry et al. which is more generally applicable. Anal Biochem 83:346–356.

Pettigrew LC, Kasner SE, Gorman M, Atkinson RP, Funakoshi Y, Ishibashi H (2006b) Effect of arundic acid on serum S-100b in ischemic stroke. J Neurol Sci 251:57–61. https://doi.org/10.1016/j.jns.2006.09.002.

Pettigrew LC, Kasner SE, Albers GW, Gorman M, Grotta JC, Sherman DG, Funakoshi Y, Ishibashi H (2006a) Safety and tolerability of arundic acid in acute ischemic stroke. J Neurol Sci 251:50–56. https://doi.org/10.1016/j.jns.2006.09.001.

Qu J, Chen W, Hu R, Feng H (2016) The injury and therapy of reactive oxygen species in intracerebral hemorrhage looking at mitochondria. Oxid Med Cell Longev 2016:1–9. https://doi.org/10.1155/2016/2592935.

Qureshi AI, Mendelow AD, Hanley DF (2009) Intracerebral haemorrhage. Lancet (London, England) 373:1632–1644. https://doi.org/10.1016/S01406736(09)60371-8.

Senn R, Elkind MSV, Montaner J, Christ-Crain M, Katan M (2014) Potential role of blood biomarkers in the management of nontraumatic intracerebral hemorrhage. Cerebrovasc Dis 38:395–409. https://doi.org/10.1159/000366470.

Sorci G, Bianchi R, Riuzzi F, Tubaro C, Arcuri C, Giambanco I, Donato R (2010) S100B protein, a damage-associated molecular pattern protein in the brain and heart, and beyond. Cardiovasc Psychiatry Neurol 2010. https://doi.org/10.1155/2010/656481.

Sukumari-Ramesh S, Alleyne CH, Dhandapani KM (2012) Astrogliosis: a target for intervention in intracerebral hemorrhage? Transl Stroke Res 3:80–87. https://doi.org/10.1007/s12975-012-0165-x.

Tanaka Y, Marumo T, Shibuta H, Omura T, Yoshida S (2009) Serum S100B, brain edema, and hematoma formation in a rat model of collagenase-induced hemorrhagic stroke. Brain Res Bull 78:158–163. https://doi.org/10.1016/j.brainresbull.2008.10.012.

Tateishi N, Mori T, Kagamiishi Y, Satoh S, Katsube N, Morikawa E, Morimoto T, Matsui T, Asano T (2002) Astrocytic activation and delayed infarct expansion after permanent focal ischemia in rats. Part II: suppression of astrocytic activation by a novel agent (R)-(_)-2-propyloctanoic acid (ONO-2506) leads to mitigation of delayed infarct expansion and early. J Cereb Blood Flow Metab 22:723–734. https://doi.org/10.1097/00004647-200206000-00011.

Tietze F (1969) Enzymic method for quantitative determination of nanogram amounts of total and oxidized glutathione: applications to mammalian blood and other tissues. Anal Biochem 27:502–522. https://doi.org/10.1016/0003-2697(69)90064-5.

Tramontina F, Leite MC, Cereser K, de Souza DF, Tramontina AC, Nardin P, Andreazza AC, Gottfried C, Kapczinski F, Gonçalves CA (2007) Immunoassay for glial fibrillary acidic protein: antigen recognition is affected by its phosphorylation state. J Neurosci Methods 162:282–286. https://doi.org/10.1016/j.jneumeth.2007.01.001.

Vargaftig BB, Lefort J, Giroux EL (1976) Haemorrhagic and inflammatory properties of collagenase from C. histolyticum. Agents Actions 6:627–635. https://doi.org/10.1007/BF01971582.

Villarreal A, Seoane R, Torres AG, Rosciszewski G, Angelo MF, Rossi A, Barkert PA, Ramos AJ (2014) S100B protein activates a RAGE-dependent

autocrine loop in astrocytes: implications for its role in the propagation of reactive gliosis. J Neurochem 131:190–205. https://doi.org/10.1111/jnc.12790.

Wajima D, Nakagawa I, Nakase H, Yonezawa T (2013) Neuroprotective effect of suppression of astrocytic activation by arundic acid on brain injuries in rats with acute subdural hematomas. Brain Res 1519:127–135. https://doi.org/10.1016/j.brainres.2013.05.002.

Zhang Y, Yang Y, Zhang G-Z, Gao M, Ge G-Z, Wang Q-Q, Ji X-C, Sun Y-L, Zhang H-T, Xu R-X (2016) Stereotactic administration of edaravone ameliorates collagenase-induced intracerebral hemorrhage in rat. CNS Neurosci Ther 22:824–835. https://doi.org/10.1111/cns.12584.

Zhou S, Bao J, Wang Y, Pan S (2016) S100b as a biomarker for differential diagnosis of intracerebral hemorrhage and ischemic stroke. Neurol Res 38:327–332. https://doi.org/10.1080/01616412.2016.1152675.

CAPÍTULO 2

Arundic acid (ONO-2506) attenuates neuroinflammation and prevents motor impairment in rats with intracerebral hemorrhage

Juliana de Lima Cordeiro; Juliana Dalibor Neves; Fabrício Nicola; Adriana Fernanda Vizuete; Eduardo Farias Sanches; Carlos Alberto Gonçalves; Carlos Alexandre Netto

Manuscrito aceito para publicação no periódico *Cellular and Molecular Neurobiology.*

DOI: 10.1007/s10571-020-00964-6

Arundic acid (ONO-2506) attenuates neuroinflammation and prevents motor impairment in rats with intracerebral hemorrhage

Cordeiro, J.L.[1,2 *]; Neves, J.D.[1]; Nicola, F.[1]; Vizuete, A.F.[1]; Sanches, E.F.[1,3]; Gonçalves, C.A.[1]; Netto C.A.[1]

[1]Department of Biochemistry, Instituto de Ciências Básicas da Saúde, Universidade Federal do Rio Grande do Sul, Porto Alegre, RS, 90035-003, Brazil.

[2]Post-graduation Program of Neurosciences, Instituto de Ciências Básicas da Saúde, Universidade Federal do Rio Grande do Sul, 90035-190, Brazil.

[3]Post-graduation Program of Phisiology, Instituto de Ciências Básicas da Saúde, Universidade Federal do Rio Grande do Sul, 90035-190, Brazil.

* Corresponding author at: Juliana de Lima Cordeiro, Department of Biochemistry, Instituto das Ciências Básicas da Saúde (ICBS), Universidade Federal do Rio Grande do Sul, Rua Ramiro Barcelos, 2600. Mail code: 90035-003. Porto Alegre, RS, Brazil.

Phone/FAX: 0055-051 33085568. E-mail: ju.julianacordeiro@gmail.com

Abstract

Intracerebral hemorrhage (ICH) is a severe stroke subtype caused by the rupture of blood vessels within the brain. Increased levels of S100B protein may contribute to neuroinflammation after ICH through activation of astrocytes and resident microglia, with the consequent production of proinflammatory cytokines and reactive oxygen species (ROS). Inhibition of astrocytic synthesis of S100B by arundic acid (AA) has shown beneficial effects in experimental central nervous system disorders. In present study, we administered AA in a collagenase-induced ICH rodent model in order to evaluate its effects on neurological deficits, S100B levels, astrocytic activation, inflammatory and oxidative parameters. Rats underwent stereotactic surgery for injection of collagenase in the left striatum and AA (2 μg/μl; weight x 0.005) or vehicle in the left lateral ventricle. Neurological deficits were evaluated by the Ladder rung walking and Grip strength tests. Striatal S100B, astrogliosis and microglial activation were assessed by immunofluorescence analysis. Striatal levels of interleukin 1β (IL-1β) and tumor necrosis factor α (TNF-α) were measured by ELISA, and the ROS production was analyzed by dichlorofluorescein (DCF) oxidation. AA treatment prevented motor dysfunction, reduced S100B levels, astrogliosis and microglial activation in the damaged striatum, thus decreasing the release of proinflammatory cytokines IL-1β and TNF-α, as well as ROS production. Taken together, present results suggest that AA could be a pharmacological tool to prevent the harmful effects of increased S100B, attenuating neuroinflammation and secondary brain damage after ICH.

Keywords: Intracerebral hemorrhage; S100B; Arundic acid (ONO-2506); astrocyte; microglia; neuroinflammation.

1. Introduction

Intracerebral hemorrhage (ICH) is a particularly severe stroke subtype that results from rupture of blood vessels in the brain (Qureshi et al., 2009). It affects 24.6 per 100,000 person per year (van Asch et al., 2010) and is associated with a thirty-day mortality between 30% and 50% (Manno, 2012). Moreover, most of the surviving patients remain functionally dependent 12 months after the stroke (van Asch et al., 2010).

Primary brain injury after ICH is caused by the parenchymal blood accumulation, which directly compresses brain tissue, affects blood flow, and leads to mechanical injury due to the mass effect (Mracsko and Veltkamp, 2014; Xi et al., 2006). Secondary damage occurs due to the presence and clearance of hematoma (Qureshi et al., 2009). Thrombin is produced to limit the bleeding, but also activates astrocytes and microglial cells to release inflammatory mediators, and leads to endothelial cell dysfunction, causing hyperpermeability, vasogenic edema and disruption of blood brain barrier (BBB) (Xi et al., 2003) . Furthermore, hemoglobin and its degradation products, such as heme and iron, are highly toxic to the brain tissue and contribute to the production of reactive oxygen species (ROS) and inflammation (Dutra and Bozza, 2014; Lin et al., 2012b).

Neuroinflammation induced by intracerebral blood is increasingly recognized as a key factor in the pathophysiology of secondary brain damage in ICH (Wang and Doré, 2007) and involves the activation of astrocytes and resident microglia, as well as the infiltration of systemic immune cells (Mracsko and Veltkamp, 2014). The main role of activated microglia is the phagocytosis

of blood components released into the brain parenchyma and the clearance of cell debris (Aronowski and Zhao, 2011; Zhang et al., 2017). However, these immune cells can also produce a variety of proinflammatory cytokines, chemokines, ROS, nitric oxide (NO) and other potentially toxic factors, suggesting that activated microglia might contribute to increase brain damage after ICH (Mracsko and Veltkamp, 2014; Wang and Doré, 2007; Zhang et al., 2017).

In central nervous system (CNS) injuries, including ICH, astrocytes work in synergy with microglia. The release of cytokines such as tumor necrosis factor α (TNF-α) and interleukin 1β (IL-1β) by the activated microglia, triggers and increases astrocytic activation (Wajima et al., 2013). In addition, cell death or injury and blood-derived factors (such as thrombin) can also be potent inducers of reactive astrogliosis, characterized by proliferation and activation of astrocytes surrounding the hematoma (Nishino et al., 1993; Sofroniew and Vinters, 2010b; Sukumari-Ramesh et al., 2012a). Reactive astrocytes may exert some detrimental effects in ICH lesion, such as inducing proinflammatory responses and ROS production (Mracsko and Veltkamp, 2014).

Astrogliosis as a result of brain damage also leads to an increased expression of S100B, a 21-kD Ca^{2+} binding protein that is expressed primarily by astrocytes (Sorci et al., 2010). Intracellular S100B exerts regulatory functions and, once secreted/released, it acts as an extracellular signal, exerting trophic and toxic effects depending on its concentration and the density of RAGE (receptor for advanced glycation end products) molecules expressed on the surface of different cell types (Sorci et al., 2010). At low (nanomolar), physiological concentrations, extracellular S100B protects neurons against

apoptosis and stimulates neurite outgrowth (Huttunen et al., 2000; Sorci et al., 2010). At high (micromolar) concentrations, S100B causes neuronal apoptosis and consequent overproduction of ROS (Huttunen et al., 2000), induces reactive gliosis and a pro-inflammatory phenotype in astrocytes (Villarreal et al., 2014), and leads to microglial activation and migration with the consequent increase in the release of pro-inflammatory factors, thus actively contributing to neuroinflammation (Bianchi et al., 2011, 2010; Kim et al., 2004).

S100B plays an important role in the mechanisms of secondary brain injury and its levels has been considered a biomarker of CNS lesions (Kanner et al., 2003), including ICH (Senn et al., 2014; Zhou et al., 2016). In ICH patients, high peripheral levels of S100B are associated with the hemorrhage volume, functional neurological outcomes and mortality rates (Delgado et al., 2006; Hu et al., 2010; James et al., 2009; Zhou et al., 2016), thus showing diagnostic and prognostic value (Sen and Belli, 2007). Comparatively, in ICH rat model, S100B levels were found increased in brain tissue, serum and cerebrospinal fluid (CSF) (Cordeiro et al., 2020; Neves et al., 2017) and a previous study reported that the increased serum S100B levels was related to hematoma volume and brain edema (Tanaka et al., 2009).

Arundic acid (AA; (R)-(−)-2-propyloctanoic acid; ONO-2506) is an astrocyte-modulating agent suggested to inhibit S100B synthesis (Asano et al., 2005) and suppress the subsequent activation of multiple intracellular signaling pathways arising from S100B overexpression by the reactive astrocytes in the damaged area (Asano et al., 2005; Wajima et al., 2013). Experimental evidence demonstrates that AA inhibited the overexpression of S100B, decreased astrocytic activation, reduced the delayed infarct expansion and improved

neurologic deficits in experimental models of cerebral ischemia (Mori et al., 2005; Ohtani et al., 2007; Tateishi et al., 2002). A recent study of our group showed that intracerebroventricular administration of AA immediately before ICH surgery had neuroprotective effects, preventing neuronal death, the expansion of hemorrhagic volume and motor impairments (Cordeiro et al., 2020).

Considering the suggested benefits of AA in CNS lesions and the need for effective treatments for ICH, the aim of this study was to evaluate the effects of AA treatment on S100B levels, astrocytic activation, inflammatory and oxidative parameters and motor function impairment in rats submitted to intracerebral hemorrhage.

2. Materials and methods

2.1. Animals

Adult male Wistar rats (n = 122) approximately 90 days-old (300–350 g weight) were housed in groups of 4 animals in Plexiglas cages. They were maintained in a temperature controlled room (21 ± 2 °C) on a 12/12 h light/dark cycle, with food and water available *ad libitum.* All procedures were approved by the Research Ethics Committee of the University (#30944) and were in accordance with the Guidelines for Care and Use of Laboratory Animals adopted by the National Institute of Health (USA) and with National Animal Experimentation Control Board (CONCEA-Brazil). All efforts were made to minimize animal suffering and to reduce the number of animals needed.

2.2. Experimental design

Animals underwent surgery for the induction of the ICH model by collagenase injection in the striatum and for the intracerebroventricular (ICV) administration of AA.

Rats were randomly divided into three experimental groups: VEH (Vehicle - surgical and treatment controls that received only saline solution, n=48), ICH (rats that underwent intracerebral hemorrhage and received saline solution rather than arundic acid treatment, n=37) and ICH+AA (rats that underwent intracerebral hemorrhage and were treated with arundic acid, n=37).

To evaluate the effects of ICH injury and AA treatment on motor function, the Ladder rung walking test and the Grip strength test were performed 72 hours and 7 days after the ICH injury. At the same time points, immunofluorescence analyzes were performed in order to measure the levels of S100B, GFAP (glial fibrillary acid protein; astrocytes marker) and CD11b (microglia and macrophages marker) in the striatum. Biochemical analyzes were performed 24 hours, 72 hours and 7 days after ICH induction to measure the levels of proinflammatory cytokines, such as tumor necrosis factor α (TNF-α) and interleukin 1β (IL-1β), and the production of reactive oxygen species (ROS). The sample number for each assessment and time point is described in the Results section. The experimental design is shown in **figure 1**.

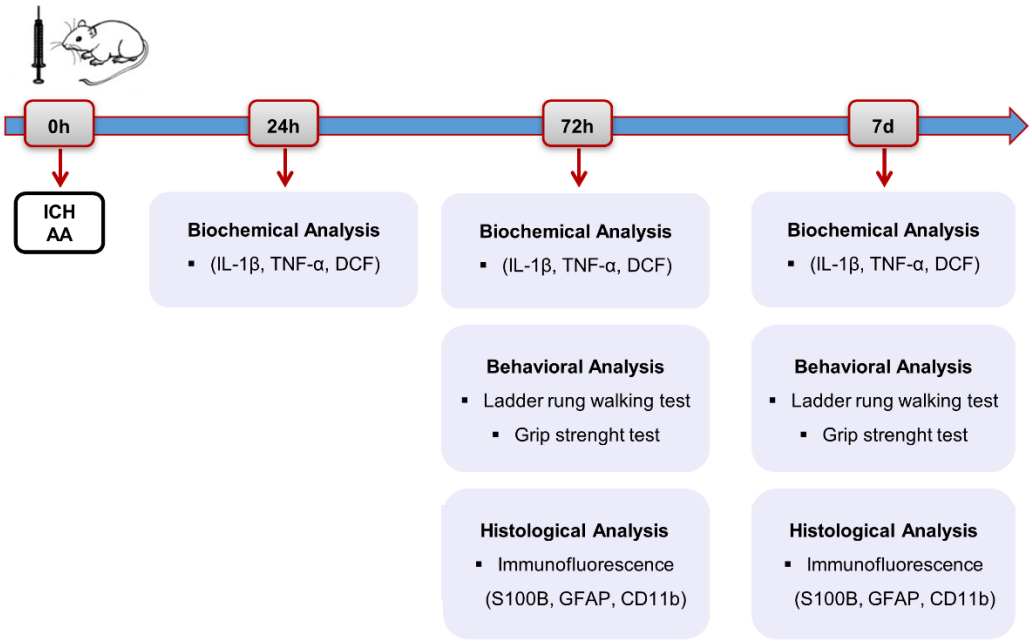

Figure 1. Timeline of the experiments performed 24 hours, 72 hours and 7 days after experimental intracerebral hemorrhage (ICH) and arundic acid injection (AA) (time 0h) in rats.

2.3. Experimental ICH and AA treatment

AA was injected via ICV, immediately before ICH induction. For this purpose, animals were anesthetized with isoflurane (4% induction, 2% maintenance in 70% N_2O and 30% O_2) and positioned in a stereotaxic frame. For AA injection, a burr hole was drilled in the skull and a 26-G needle (Hamilton, Reno, NV, USA) was inserted into the left lateral ventricle according to the following stereotactic coordinates: 0.80 mm anterior, 1.50 mm lateral and 3.50 mm ventral to Bregma (Paxinos and Watson, 2007) in the left side. Thus, a single dose of AA (concentration: 2 µg of AA per µl of saline solution; dose: weight x 0.005; Tocris®) or saline solution (dose: weight x 0.005) was infused and the needle was kept in the position for additional 5 min period to prevent backflow. The AA concentration was chosen based on our previous study (Cordeiro et al., 2020).

Subsequently, ICH was induced by infusing 0.5 µl of bacterial collagenase type-IVs (concentration: 0.2 U per 1.0 µL of saline buffer; Sigma-Aldrich, USA) into the dorsolateral striatum, at the following coordinates: 0 mm anterior, 3.6 mm lateral and 6.0 mm ventral to Bregma (Paxinos and Watson, 2007). In Vehicle surgery, sterile saline (0.5 µL) was injected rather than collagenase. The needle was kept in position for an additional 5 min period and then slowly removed to prevent backflow. After surgery, the incision was sutured and the rats were housed in a biologically clean room.

2.4. Behavioral analysis

2.4.1. Ladder rung walking test

The gait skills, hindlimb and forelimb function were evaluated by the ladder rung walking test. The apparatus consisted of two transparent acrylic walls (width: 1 m; high: 20 cm) with metal rungs (diameter: 3 mm) which could be inserted into the walls in variable arrangements. The ladder was elevated 30 cm above the ground with a dark cage at the end.

Animals underwent a training session (before surgery), using a regular pattern (1 cm of distance between rungs). On test day, animals were required to walk along the ladder with an irregular pattern (from 1 to 4 cm of distance between rungs) that was changed from trial to trial, so that the same patterns were applied to all animals to standardize the difficulty of the test. The test was video-recorded from an inferior view and paw placement on the rung was rated as follows: 0 = Total miss: deep fall after limb missed the rung; 1 = Deep slip: deep fall after limb slipped off the rung; 2 = Slight slip: slight fall after limb slipped off the rung; 3 = Replacement: limb replaced from one rung to another;

4 = Correction: limb aimed for one rung but was placed on another, or limb position on same rung was corrected; 5 = Partial placement: limb placed on rung with either digits/toes or wrist/heel; and 6 = Correct placement: the midportion of the palm of the limb was placed on the rung with full weight support) (Metz and Whishaw, 2002).

The mean number of errors per step and paws placement quality of contralateral forelimb and hind limb were analyzed. An error was considered as each limb placement that received a score of 0, 1 or 2 points (any kind of paw slip or total miss) and was calculated and averaged for three trials, according to the equation: number of erros / number of steps X 100. Paws placement and accuracy of the paws position on the rung on consecutive steps was rated from 0 to 6 and averaged for three trials (Antonow-Schlorke et al., 2013).

2.4.2. Grip strength test

In order to measure the grasping strength of the forepaws, the grip strength test was performed as previously described (Jeyasingham et al., 2001). A digital force gauge instrument (TEC-04422 Instrutherm DD-500, Brazil) was used. The forepaws were put on the metal bar attached to a strain gauge. Then, the animal was gently pulled by the tail until it released the bar. The value of three trials were recorded in grams (g) and the mean value for each animal was calculated.

2.5. Immunofluorescence analysis

Rats were deeply anaesthetized with isoflurane and subsequently subjected to transcardiac perfusion. Saline solution followed by 4%

paraformaldehyde were injected through the animals' circulation (Reagen, Rio de Janeiro, Brazil) through the left cardiac ventricle. Brains were removed from the skull, stored in the same fixative solution overnight and crioprotected with sucrose 30% diluted in phosphate buffer saline (PBS)., After cryoprotection, the samples were frozen in liquid nitrogen and stored at -20ºC until slicing. Coronal sections of 30 µm thick were taken every 210 µm using a cryostat (Leica, Germany), from +1.70 to −1.40 mm from Bregma (Paxinos and Watson, 2007) and were mounted on gelatin-coated slides..

For the immunofluorescence analyzes, the slices were washed with PBS, permeabilized in PBS-Triton X (0.25%), and then blocked with goat serum (5%) for 45 min. In order to identify astrocytes and calcium-binding protein S100B, sections were incubated with the primary antibodies against glial fibrillary acidic protein (anti-GFAP, mouse IgG, 1:200, Thermo Fisher – MA5-12023) and against S100B (anti-S100B, rabbit IgG, 1:200, Dako-Z0311). In order to identify microglia/macrophages, the primary antibody against CD11B was used (anti-CD11B, mouse IgG, 1:200, Millipore - CBL 1512). This procedure was carried out in 1% goat serum and PBS-Tx at 4°C overnight. Following PBS washes, sections were incubated with secondary antibody anti-mouse Alexa 488 (1:500, Molecular Probes, Invitrogen, USA) and secondary antibody anti-rabbit Alexa 555 (1:500, Molecular Probes, Invitrogen). Slices were covered in aqueous mounting medium with DAPI (Fluoroshield F6057, Sigma-Aldrich) and coverslipped.

Images of the peri-hematomal area of the left striatum and corresponding area of the right striatum were captured using a microscope (EVOS ® FL Auto Imaging System). All analyses were made using high magnification images

(X20). An area of interest (AOI) was determined (180X180 μm) to assess the staining intensity. The integrated density value per unit of area was obtained through the capture and analysis of images in the software Image J v. 1.46. Data are reported as the left/right ratio of integrated densities/mm^2, as previously described (Nicola et al., 2016).

2.6. Biochemical analysis

Rats under deep anesthesia with isoflurane (4%; Cristália, Brazil) were decapitated for the removal of the brains from the skull and dissection of the ipsilateral striatum on ice. Transverse slices of 0.3 mm (Bregma, +1.7 to 4.8 mm) were obtained using a Mcllwain Tissue Chopper and the samples were frozen and kept in -80°C until the analysis.

2.6.1. Quantification of TNF-α and IL-1β

Striatal soluble extracts were prepared by a phosphate buffer saline (PBS) (mM) (50 NaCl, 18 Na_2HPO_4, 83 $NaH_2PO_4.H_2O$, pH 7.4), containg 1 mM EGTA and 1 mM PMSF followed by centrifugation at 1000 ×g for 5 min at 4 °C. These assays were carried out in 100 μL of supernatant, using a rat TNF-α and IL-1β ELISA (eBioscience, Ref. 88-7340, San Diego, USA) (Vizuete et al., 2013).

2.6.2. 2',7'- dichlorofluorescein (H_2DCF) oxidation assay

The method of LeBel et al., (1992) was used to measure reactive species production based on the oxidation of 2',7'- dichlorofluorescein (H_2DCF). Samples of ipsilateral striatum (60 μl) were incubated for 30 min at 37ºC in the

dark with 240 µL of 100 mM 2',7'-dichlorofluorescein diacetate (H_2DCF-DA) solution in a 96 wells plate. H_2DCF-DA was cleaved by cellular esterases and the resultant H_2DCF was eventually oxidized by reactive species present in the samples. The last reaction produces the fluorescent compound dichlorofluorescein (DCF) which was measured at 485 nm excitation and 520 nm emission wave lengths.

2.7. Statistics

Statistical analysis was performed using SPSS 22.0 for Windows (SPSS Inc., Chicago, IL, USA). Normality of data distribution was confirmed by Shapiro-Wilk test. Parametric data were analyzed by one-way ANOVA followed by Duncan's post hoc test. Data are expressed as mean ± SEM. Differences were considered significant when $P \leq 0.05$. Sample size calculation was based on previous studies with similar methodology for biochemical analysis (Neves et al., 2017) in order to reach the statistical power of 80% calculated with the software PEPI for-windows 4.0. Artwork was made in Graphpad Prism 8.

3. Results

3.1. Behavioral assessment

3.1.1. Ladder rung walking test

In the ladder rung walking test, 72 hours after injury, ICH group showed motor impairment, having a higher percentage of right forelimb and hindlimb placement errors per number of paw steps than the VEH group (**Fig 2a**, **b**). ICH+AA had a better performance in the test, presenting less errors than the

ICH group in both assessments (F(2,20)=9.463, p=0.002 for forelimb and F(2,20)=16.024, p<0.001 for hindlimb, respectively; n=5-9 per group). Similarly, the ICH+AA showed a higher forelimb and hindlimb step quality than the ICH group (**Fig 2c**, **d**), being similar to the VEH (F(2,20)=10.380, p=0.001 and F(2,20)=11.972 and p<0.001, respectively; n=5-9 per group). At 7 days after injury, the ICH group had more right forelimb (**Fig 2e**) and hindlimb erros (**Fig 2f**) than VEH, and the ICH+AA group presented a reversal of motor deficit compared to ICH, not differing from the VEH group (F(2,26)=12.296, p=0.000 and F(2,26)=3.381, p=0.051, respectively; n=8-10 per group). The step quality was better in the ICH+AA than the ICH group in the forelimbs (F(2,26)=7.824, p=0.002; n=8-10 per group) and hindlimbs (F(2,26)=4.056, p=0.030; n=8-10 per group), being similar to VEH, at 7 days post-injury.

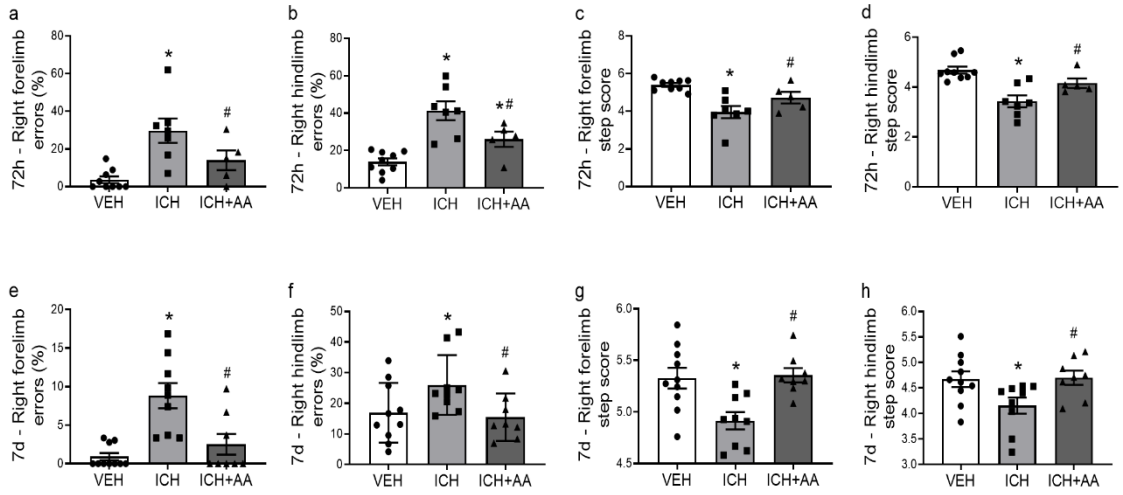

Figure 2. The Ladder rung walking test assessing the percentage of step errors (a, b, e, f) and the step placement quality (c, d, g, h) applied in right forelimb and hindlimb at 72h and 7 days after injury. N=5-9 and 8-10 per group in 72 hours and 7 days after injury, respectively. Data expressed as mean ± SEM of foot placement score and percentages of limb placement errors per number of paw steps. *different from the VEH group and #different from the ICH group. Statistical difference was considered when p <0.05. One-way ANOVA followed by Duncan test.

3.1.2. Grip strength test

The ICH group had significant loss of forelimbs strength compared to VEH group 72 hours after injury (Fig **3a**) and the ICH+AA group showed no loss of strength, remaining similar to the VEH group ($F(2,17)=8.584$, $p=0.003$; n=5-8 per group). At 7 days (Fig **3b**), a total recovery of both groups submitted to ICH was observed, with no difference between groups ($F(2,26)=2.239$, $p=0.128$; n=8-10 per group).

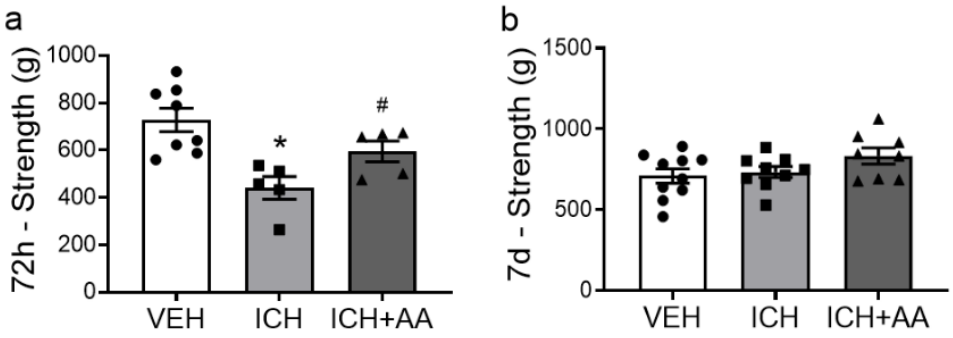

Figure 3. Grasping test assessing the forelimbs strength 72 hours (a) and 7 days (b) post-injury. N=5-8 and 8-10 per group in 72 hours and 7 days post-injury, respectively. Data are expressed as mean ± SEM of forepaw strength (g). *different from the VEH group and #different from the ICH group. Statistical difference was considered when $p < 0.05$. One-way ANOVA followed by Duncan test.

3.2. GFAP, S100B and CD11b levels

GFAP levels increased in both ICH and ICH+AA groups compared to VEH with no difference between them in 72 hours after injury (**Fig 4a, c**) ($F(2,29)=81.397$, $p<0.001$; n=8-12 per group), suggesting that there was a process of reactive astrogliosis in the striatum caused by the lesion. S100B levels also increased in both ICH and ICH+AA groups 72 hours after injury compared to VEH (**Fig 4b and c**), but the AA-treated animals had lower levels compared to the untreated group ($F(2,29)=77.718$, $p<0.001$; n=8-12 per group).

Seven days after injury, GFAP levels remained increased in the ICH group, but there was a reduction of the levels in the AA treated animals (**Fig 5a, c**), with no difference when compared to the VEH ($F(2,26)=4.982$, $p=0.015$; n=8-10 per group). Similarly, S100B levels also remained high in the ICH group, but the AA-treated animals had a decrease in S100B levels compared to the untreated group (**Fig 5b and c**), showing similar levels to the VEH group ($F(2,26)=3.781$, $p=0.037$; n=8-10 per group).

CD11b levels were also increased in both groups submitted to ICH compared to the VEH group 72 hours after injury (**Fig 6a, c**), demonstrating microglial/macrophage activation in the damaged striatum. The ICH+AA had lower levels compared to ICH group ($F(2,28)=36.928$, $p<0.001$; n=8-12 per group). At 7 days, the ICH group had increased CD11b levels, while the AA treated animals presented lower levels, similar to the Vehicle group (**Fig 6b, c**) ($F(2,26)=5.089$, $p=0.014$; n=8-10 per group).

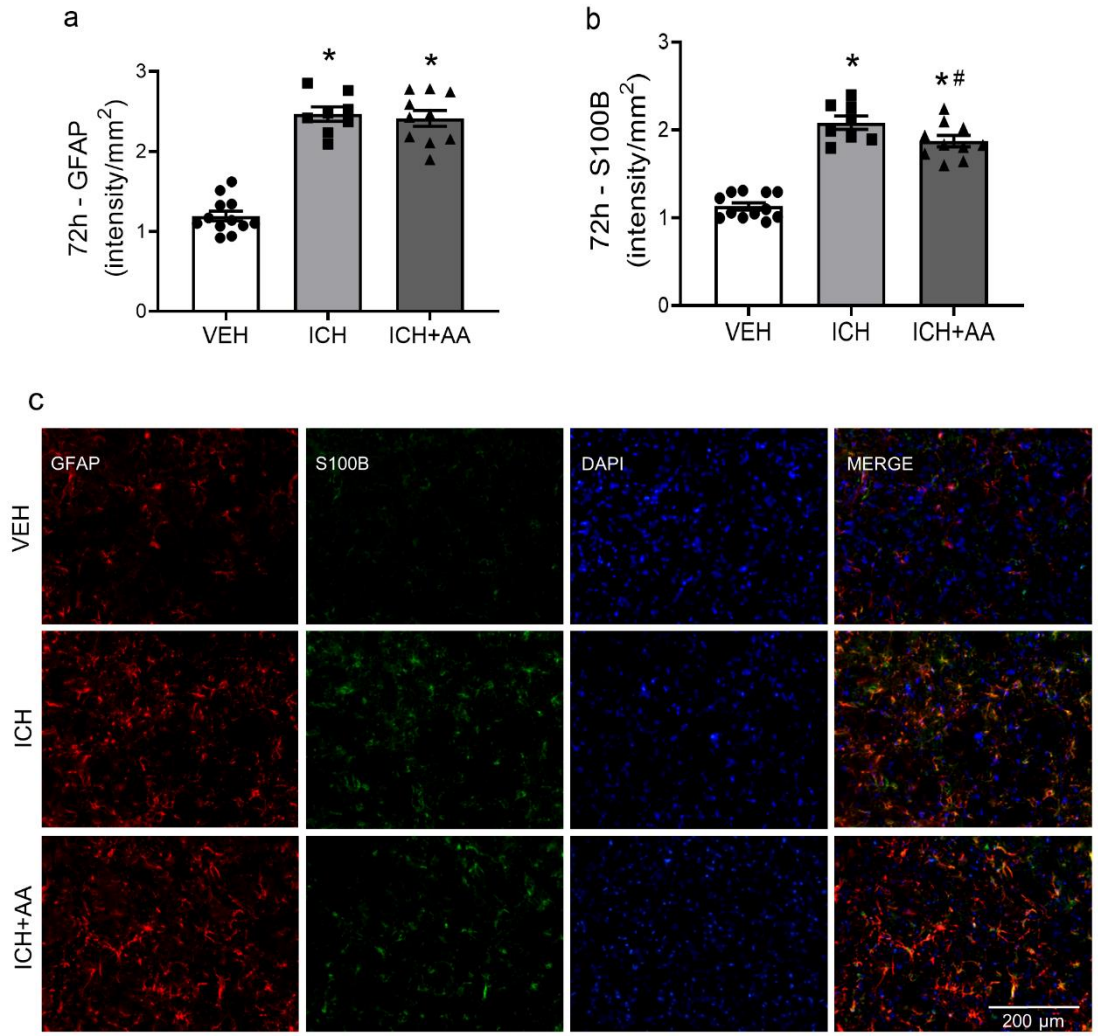

Figure 4. Effects of ICH injury and AA treatment on glial fibrillary acid protein (GFAP) and S100B levels measured by immunofluorescence analysis in the striatum, 72 hours after injury. a) GFAP levels (n=8-12 per group); b) S100B levels (n=8-12 per group); c) Representative images of immunofluorescence. Data are expressed as mean ± SEM of ipsilateral/contralateral fluorescence intensity ratio *different from the VEH group and #different from the ICH group. Statistical difference was considered when $p<0.05$. One-way ANOVA followed by Duncan test.

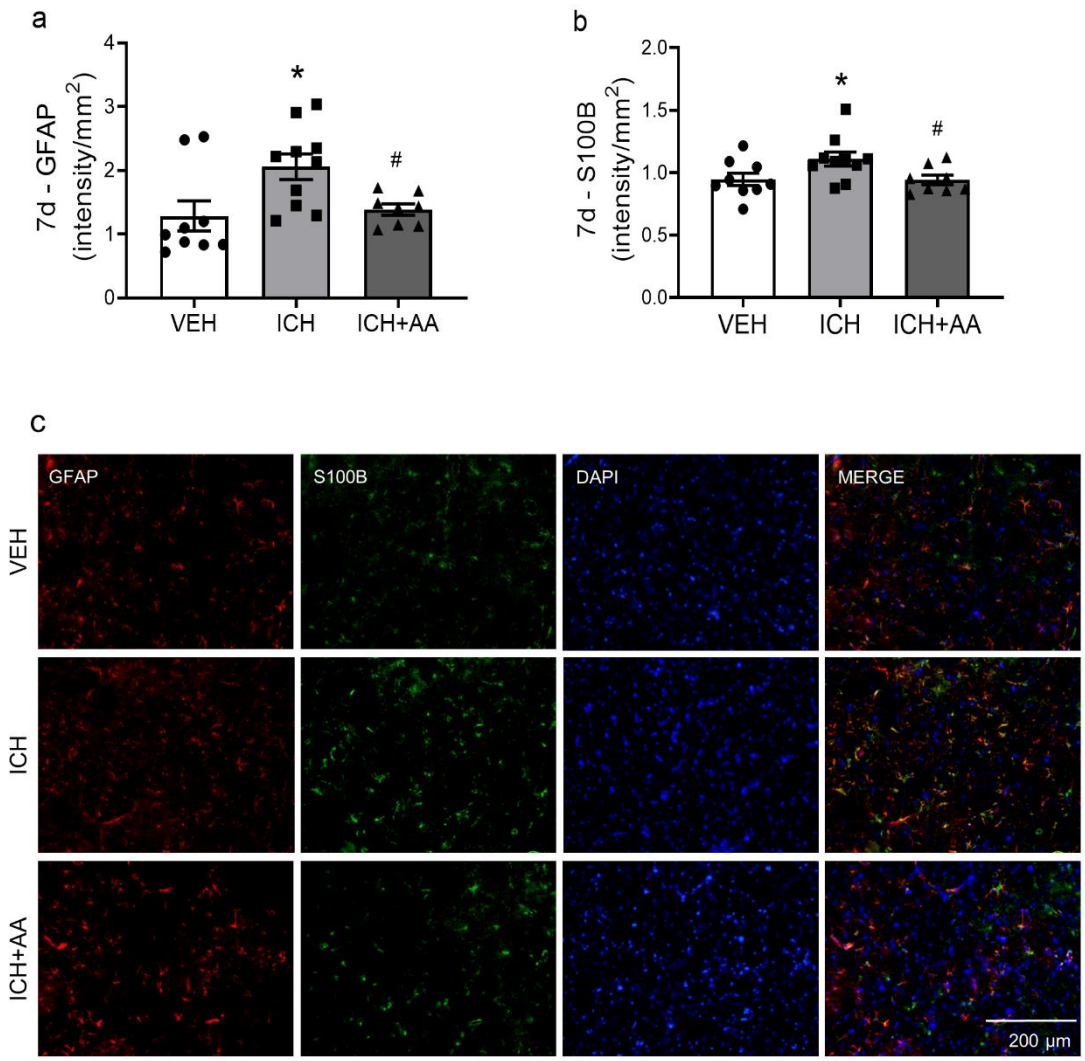

Figure 5. Effects of ICH injury and AA treatment on glial fibrillary acid protein (GFAP) and S100B levels measured by immunofluorescence analysis in the striatum, 7 days after injury. a) GFAP levels (n=8-10 per group); b) S100B levels (n=8-10 per group); c) Representative images of immunofluorescence. Data are expressed as mean ± SEM of ipsilateral/contralateral fluorescence intensity ratio *different from the VEH group and #different from the ICH group. Statistical difference was considered when $p < 0.05$. One-way ANOVA followed by Duncan test.

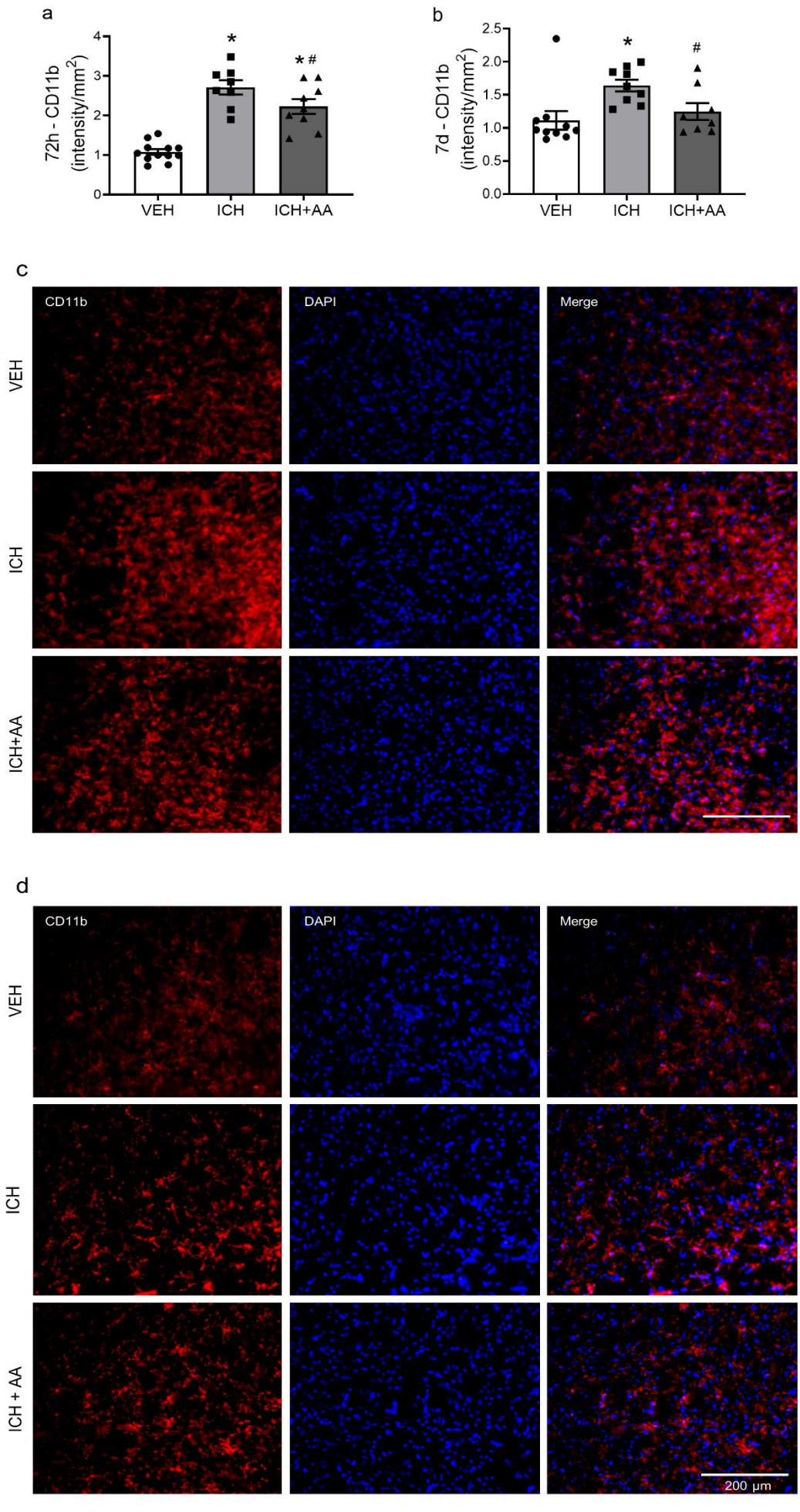
a
72h - CD11b (intensity/mm2)
VEH
ICH
ICH+AA
b
7d - CD11b (intensity/mm2)
c
CD11b
DAPI
Merge
d
200 μm

.00

Figure 6. Effects of ICH injury and AA treatment on microglia/macrophage activation measured by immunofluorescence analysis in the striatum, 72 hours and 7 days post-injury. a) CD11b levels at 72 hours (n=8-12 per group); b) CD11b levels at 7 days (n=8-10 per group); c) Representative images of immunofluorescence at 72 hours; d) Representative images of immunofluorescence at 7 days. Data are expressed as mean ± SEM of ipsilateral/contralateral fluorescence intensity ratio *different from the VEH group and #different from the ICH group. Statistical difference was considered when $p < 0.05$. One-way ANOVA followed by Duncan test.

3.3. TNF-α and IL-1β levels

TNF-α levels were not different between groups 24 hours (**Fig 7a**) ($F(2,17)=0.089$; n=5-8 per group) and 72 hours (**Fig 7b**) ($F(2,18)=2.266$; n=6-7 per group) after injury. At 7 days (**Fig 7c**), the ICH group had increased levels compared to the Vehicle, and the ICH + AA group had a reduction of TNF- α levels in relation to the ICH group ($F(2,20)=3.856$, $p=0.040$; n=6-8 per group), being similar to the control.

IL-1β levels were also not different between groups in 24 hours (**Fig 7d**) ($F(2,17)=2.148$; n=5-8 per group), had a tendency to increase in ICH group in 72 hours (**Fig 7e**) ($F(2,17)=2.633$; n=5-8 per group) and increased significantly 7 days after injury (**Fig 7f**) in ICH but not in ICH + AA group, which remained at levels similar to those in the Vehicle group ($F(2,23)=3.581$, $p=0.046$; n=7-10 per group). These results show that AA treatment prevented increased levels of proinflammatory cytokines, possibly controlling neuroinflammation in the damaged striatum.

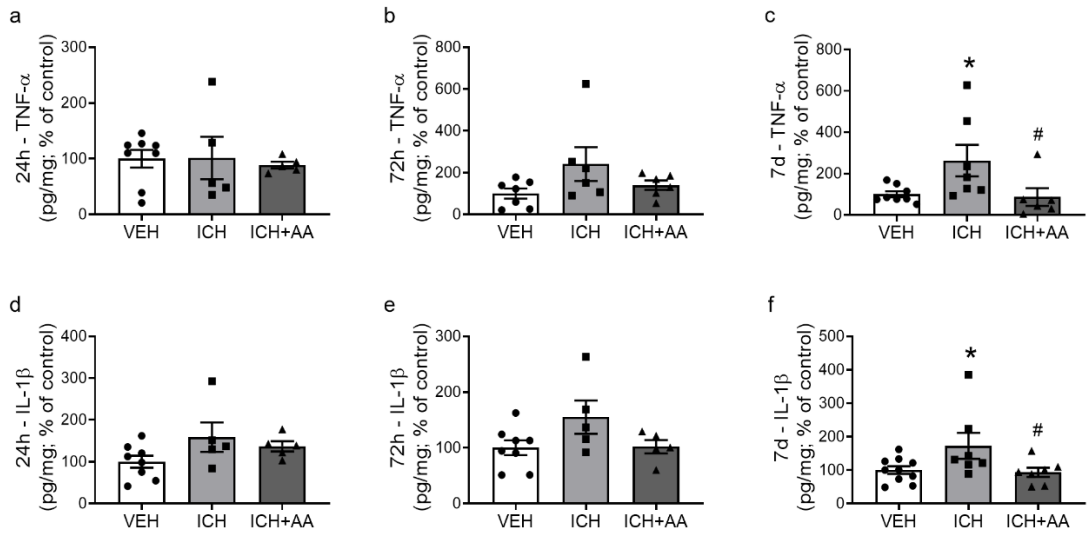

Figure 7. Striatal levels of the pro-inflammatory cytokines tumor necrosis factor α (TNF-α) and interleukin 1β (IL-1β) in response to ICH surgery and AA treatment. a) TNF-α levels at 24 hours (n=5-8 per group); b) TNF-α at 72 hours (n=6-7 per group); c) TNF-α levels at 7 days (n=6-8 per group); d) IL-1β levels at 24 hours (n=5-8 per group); e) IL-1β levels at 72 hours (n=5-8 per group); f) IL-1β levels at 7 days (f; n=7-10 per group) post-injury. Data are expressed as percentage of control values (mean ± SEM). *different from the VEH group and #different from the ICH group. Statistical difference was considered when $p < 0.05$. One-way ANOVA followed by Duncan test.

3.4. DCF assay

The analysis of DCF oxidation revealed that there was no significant increase in reactive oxygen species (ROS) production within 24 hours after injury (**Fig 8a**) ($F(2,17)=0.584$; n=5-8 per group). In 72 hours (**Fig 8b**), both ICH and ICH+AA groups presented increase of ROS compared to VEH ($F(2,19)=5.132$, $p=0.018$; n=6-8 per group) indicating oxidative stress in damaged striatal tissue. At 7 days post-injury (**Fig 8c**), only the ICH group had increased ROS levels, while the AA treated group had a reduction of the levels compared to the ICH group ($F(2,25)=4.388$, $p=0.024$; n=8-10 per group), being similar to the VEH group.

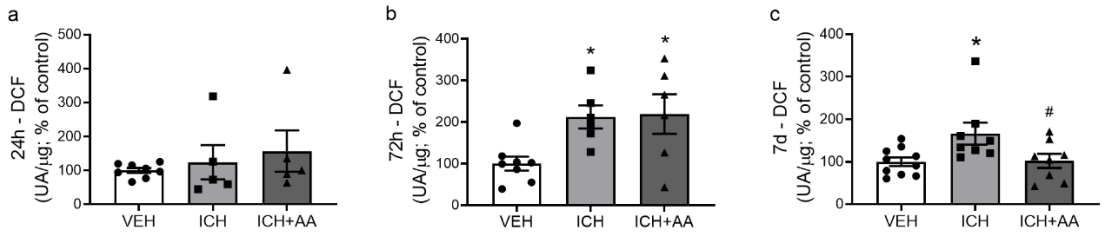

Figure 8. Levels of reactive oxygen species (ROS) in striatum assessed by DCF oxidation in 24 hours (a; n=5-8 per group), 72 hours (b; n=6-8 per group) and 7 days (c; n=8-10 per group) post-injury. Data are expressed as percentage of control values (mean ± SEM). *different from the VEH group and #different from the ICH group. Statistical difference was considered when $p < 0.05$. One-way ANOVA followed by Duncan test.

4. Discussion

Present study investigated the effects of intracerebroventricular administration of arundic acid in rats with experimental intracerebral hemorrhage. As expected, ICH caused severe neurological deficits, evidenced by impairment in gait ability and loss of limb strength and function. AA treatment was effective in reversing motor impairment, possibly due to the reduction of S100B levels, reactive astrogliosis and microglial activation in the damaged striatum, thus decreasing the release of proinflammatory cytokines and oxidative stress in treated rats.

Motor impairment is well-documented in experimental ICH (Mestriner et al., 2011; Neves et al., 2017; Zhang et al., 2016). Herein, behavioral assessments showed that AA treated animals had a lower percentage of errors (falls) and a better quality of foot placement on the rungs in the ladder rung walking test (**Fig 2**) and more forelimb strength in the grasping test (**Fig 3**) than the untreated animals. Previous studies have also shown the potential of AA in

reducing neurological deficits and motor impairments in experimental models of ischemic stroke (Mori et al., 2005; Tateishi et al., 2002), spinal cord injury (Hanada et al., 2014) and Parkinson's disease (Kato et al., 2004).

In the immunofluorescence analysis, we found that animals with ICH had increased levels of S100B and GFAP (suggesting astrogliosis), as well as an increase of microglia/macrophages in the damaged striatum (**Figs 4, 5 and 6**), which were reversed by AA administration. This findings are particularly important, since S100B expression is enhanced in astrogliosis and is passively released from damaged and/or necrotic cells (Sorci et al., 2010), having potential for affect astrocytic, neuronal and microglial activities (Bianchi et al., 2010). Given the ability of S100B to alter cellular functions, participate in the inflammatory response and cause cell death, it can been considered as damage-associated molecular pattern (DAMP) (Sorci et al., 2010) and its levels are reported to have diagnostic and/or prognostic value (Sen and Belli, 2007; Zhou et al., 2016).

In the present study, AA treatment reduced GFAP expression in the perihematomal tissue. Increased levels of this protein are reported in clinical and experimental ICH (Neves et al., 2017; Sukumari-Ramesh et al., 2012a). It has been shown that high extracellular S100B concentration after brain injury leads to astroglial migration to the injured site and induces reactive gliosis by activating a number of intracellular cascades via RAGE ligation (Villarreal et al., 2014). This may explain why an S100B inhibitor was able to reduce reactive gliosis in the injured site. Moreover, evidence suggests that suppression in astrocytic activity in rats submitted to ICH resulted in a decreased size of hematoma, less BBB destruction and better neurobehavioral function (Chiu et

al., 2017). The harmful effects of reactive astrocytes might be caused by the release of proinflammatory cytokines such as IL-1β and TNF-α (Mracsko and Veltkamp, 2014), ROS production (Qu et al., 2016) and inhibition of axonal regeneration (Barreto et al., 2011).

Extracellular S100B also stimulates microglia migration and activation, which shows an increase in the density of RAGE molecules on its surface (Lue et al., 2001), contributing to the propagation of inflammation after the insult. In this study, microglia/macrophage was found increased in the damaged striatum 72 hours and 7 days after ICH injury in untreated animals (**Fig 6**). Although the primary role of activated microglia after ICH is to clear the hematoma, numerous evidence suggests it is the major cell type responsible for secondary damage after ICH (Wang and Doré, 2007). In this study, ICV administration of AA prevented the increase in microglial activation in injured rats. AA has been previously reported inhibiting microglial activation in other SNC injuries (Mori et al., 2006; Oki et al., 2008). Evidences have shown that inhibition of microglial activation in experimental ICH leads to decrease in brain injury, edema and neuronal degeneration, thus improving functional neurological outcomes (Gao et al., 2008; Wang et al., 2003; Wang and Tsirka, 2005; Wu et al., 2009, 2008).

One of the detrimental effects of microglial activation on ICH pathology is the increased expression and release of proinflammatory cytokines, such as IL-1β and TNF-α (Bianchi et al., 2011, 2010; Sorci et al., 2010), as observed in this study (**Fig 7**). Interestingly, AA administration was effective in reducing the levels of these two major inflammatory cytokines, possibly due to reduced expression of microglia/macrophages as well as reactive astrogliosis. Experimental studies have provided evidence that inhibition or reduction in

levels of proinflammatory cytokines IL-1β and TNF-α may decrease brain damage and improve functional outcomes after ICH (Li et al., 2018; Ren et al., 2018). Intrastriatal infusion of anti-TNF-α agents and the consequent downregulation of TNF-α expression reduced hematoma volume, cell death, and improved the neurobehavioral deficits in rat model of ICH (Lei et al., 2013; Mayne et al., 2001a, 2001b). In clinical studies, high plasma concentrations of TNF-α were associated with increased risk of mortality, hematoma growth and poor functional outcome in ICH patients (Fang et al., 2007; Silva et al., 2005). IL-1β inhibition has also been reported to attenuate brain edema formation and intracerebral inflammation in a rat model of ICH (Masada et al., 2003, 2001). In this context, modulation of microglial activation and inflammatory cytokine levels appears to be one of the possible therapeutic targets to mitigate the deleterious effects of ICH, and AA has the potential to decrease microglia activation and inflammatory cytokine production, possibly attenuating neuroinflammation due to ICH.

In addition to inflammatory factors, we found an increase in ROS production 72h and 7 days after injury (**Fig 8**). Overproduction of free radicals can lead to oxidative stress (OS), which causes cell injury via direct oxidation of cellular protein, lipid, and DNA or participating in cell death signaling pathways (Sinha et al., 2013). Hemoglobin and its degradation products are potent mediators of increased ROS release in ICH pathology (Hu et al., 2016). Furthermore, activated microglia, in addition to proinflammatory factors, also contributes to a large release of ROS (Hu et al., 2016). Inflammation and OS are closely related, since they can stimulate each other forming a positive feedback loop (Hu et al., 2015; Khaper et al., 2010). Moreover, the inhibition of

microglia was reported to decrease the ROS production, injury volume, and to improve the neurological functional outcome in an ICH animal model (Wang and Tsirka, 2005). Herein, AA treatment was able to reduce ROS, microglial activation and proinflammatory factors, corroborating with the literature.

High extracellular S100B concentration can also contribute to OS-related injury, since it leads to neuronal apoptosis (and consequent overproduction of ROS) via a direct action on neurons through RAGE ligation and via stimulation of nitric oxide (NO) release by astrocytes (Hu et al., 2002). By inducing neuronal death, increased S100B stimulates inflammation and dispersion of interleukins, such as IL-1β and TNF-α (Kim et al., 2004; Ponath et al., 2007). This helps to explain why AA treated animals had reduced free radical generation and proinflammatory cytokines levels in the damaged striatum.

This study has some limitations: 1) In order to avoid other invasive procedures, such as brain cannulation, treatment was performed with only one stereotaxic injection of AA, during ICH surgery. However, we recognize the need to study late administration, as well as continued AA treatments; 2) The effects of AA were assessed only up to 7 days after the injury, therefore the investigation of the long-term treatment effectiveness is necessary. 3) Only male rats were used, in order to avoid the influence of the estrous cycle and female sex hormones, which are reported to exert neuroprotective effects after experimental stroke and other acute CNS injuries (Céspedes Rubio et al., 2018; Engler-Chiurazzi et al., 2017; Kim et al., 2019). However, we recognize the importance of considering sex dimorphism in future studies, since the sex of animals may affect behavioral, biochemical and histological variables.

In conclusion, this study provides interesting findings that contribute to the understanding of the mechanism by which AA exerts neuroprotective effects in the pathology of experimental ICH. Firstly, AA decreased S100B protein expression in the damaged tissue, avoiding the excessive astrocyte and microglia activation and, consequently, decreasing the release of proinflammatory cytokines and ROS production (possibly attenuating the neuroinflammation that leads to cell injury and death). Altogether, the results suggest that AA treatment inhibited the cascade of events secondary to S100B overexpression in ICH, thus preventing neurological impairment in treated animals. The identification of new potential therapeutic targets and drugs in the treatment of ICH is of great importance, given the scarcity of effective treatments and the poor prognosis of this type of stroke.

Acknowledgments: This work was supported by Coordenação de Aperfeiçoamento de Pessoal de Nível Superior (CAPES), Conselho Nacional de Desenvolvimento Científico e Tecnológico (CNPq), Fundação de Amparo à Pesquisa do Estado do Rio Grande do Sul (FAPERGS).

References

Abbott, N.J., Revest, P.A., Romero, I.A., 1992. Astrocyte-endothelial interaction: Physiology and pathology, in: Neuropathology and Applied Neurobiology. Neuropathol Appl Neurobiol, pp. 424–433. https://doi.org/10.1111/j.1365-2990.1992.tb00808.x

Alexandrova, M.L., Danovska, M.P., 2011. Serum C-reactive protein and lipid hydroperoxides in predicting short-term clinical outcome after spontaneous intracerebral hemorrhage. J. Clin. Neurosci. 18, 247–252. https://doi.org/10.1016/j.jocn.2010.07.125

Antonow-Schlorke, I., Ehrhardt, J., Knieling, M., 2013. Modification of the ladder rung walking task-new options for analysis of skilled movements. Stroke Res. Treat. 2013, 418627. https://doi.org/10.1155/2013/418627

Aronowski, J., Zhao, X., 2011. Molecular pathophysiology of cerebral hemorrhage: secondary brain injury. Stroke 42, 1781–6. https://doi.org/10.1161/STROKEAHA.110.596718

Asano, T., Mori, T., Shimoda, T., Shinagawa, R., Satoh, S., Yada, N., Katsumata, S., Matsuda, S., Kagamiishi, Y., Tateishi, N., 2005. Arundic acid (ONO-2506) ameliorates delayed ischemic brain damage by preventing astrocytic overproduction of S100B. Curr. Drug Targets. CNS Neurol. Disord. 4, 127–42. https://doi.org/10.2174/1568007053544084

Askenase, M.H., Sansing, L.H., Author, S.N., 2016. Stages of the Inflammatory Response in Pathology and Tissue Repair after Intracerebral Hemorrhage HHS Public Access Author manuscript. Semin Neurol 36, 288–297. https://doi.org/10.1055/s-0036-1582132

Babu, R., Bagley, J.H., Di, C., Friedman, A.H., Adamson, C., 2012. Thrombin and hemin as central factors in the mechanisms of intracerebral hemorrhage-induced secondary brain injury and as potential targets for intervention. Neurosurg. Focus 32. https://doi.org/10.3171/2012.1.FOCUS11366

Balami, J.S., Buchan, A.M., 2012. Complications of intracerebral haemorrhage. Lancet Neurol. https://doi.org/10.1016/S1474-4422(11)70264-2

Barratt, H.E., Lanman, T.A., Carmichael, S.T., 2014. Mouse intracerebral hemorrhage models produce different degrees of initial and delayed

damage, axonal sprouting, and recovery. J. Cereb. Blood Flow Metab. 34, 1463–1471. https://doi.org/10.1038/jcbfm.2014.107

Barreto, G.E., Gonzalez, J., Torres, Y., Morales, L., 2011. Astrocytic-neuronal crosstalk: Implications for neuroprotection from brain injury. Neurosci. Res. 71, 107–113. https://doi.org/10.1016/j.neures.2011.06.004

Bianchi, R., Giambanco, I., Donato, R., 2010. S100B/RAGE-dependent activation of microglia via NF-κB and AP-1: Co-regulation of COX-2 expression by S100B, IL-1β and TNF-α. Neurobiol. Aging 31, 665–677. https://doi.org/10.1016/J.NEUROBIOLAGING.2008.05.017

Bianchi, R., Kastrisianaki, E., Giambanco, I., Donato, R., 2011. S100B Protein Stimulates Microglia Migration via RAGE-dependent Up-regulation of Chemokine Expression and Release. J. Biol. Chem. 286, 7214–7226. https://doi.org/10.1074/jbc.M110.169342

Céspedes Rubio, Á.E., Pérez-Alvarez, M.J., Lapuente Chala, C., Wandosell, F., 2018. Sex steroid hormones as neuroprotective elements in ischemia models. J. Endocrinol. 237, R65–R81. https://doi.org/10.1530/JOE-18-0129

Chen, Y.C., Chen, C.M., Liu, J.L., Chen, S.T., Cheng, M.L., Chiu, D.T.Y., 2011. Oxidative markers in spontaneous intracerebral hemorrhage: Leukocyte 8-hydroxy-2′-deoxyguanosine as an independent predictor of the 30-day outcome: Clinical article. J. Neurosurg. 115, 1184–1190. https://doi.org/10.3171/2011.7.JNS11718

Chiu, C.-D., Yao, N.-W., Guo, J.-H., Shen, C.-C., Lee, H.-T., Chiu, Y.-P., Ji, H.-R., Chen, X., Chen, C.-C., Chang, C., 2017. Inhibition of astrocytic activity alleviates sequela in acute stages of intracerebral hemorrhage. Oncotarget 8, 94850–94861. https://doi.org/10.18632/oncotarget.22022

Cordeiro, J.L., Neves, J.D., Vizuete, A.F., Aristimunha, D., Pedroso, T.A., Sanches, E.F., Gonçalves, C.A., Netto, C.A., 2020. Arundic Acid (ONO-2506), an Inhibitor of S100B Protein Synthesis, Prevents Neurological Deficits and Brain Tissue Damage Following Intracerebral Hemorrhage in Male Wistar Rats. Neuroscience 440, 97–112. https://doi.org/10.1016/j.neuroscience.2020.05.030

Delgado, P., Alvarez Sabin, J., Santamarina, E., Molina, C.A., Quintana, M., Rosell, A., Montaner, J., 2006. Plasma S100B Level After Acute Spontaneous Intracerebral Hemorrhage. Stroke 37, 2837–2839.

https://doi.org/10.1161/01.STR.0000245085.58807.ad

Diao, X., Zhou, Z., Xiang, W., Jiang, Y., Tian, N., Tang, X., Chen, S., Wen, J., Chen, M., Liu, K., Li, Q., Liao, R., 2020. Glutathione alleviates acute intracerebral hemorrhage injury via reversing mitochondrial dysfunction. Brain Res. 1727. https://doi.org/10.1016/j.brainres.2019.146514

Donato, R., Sorci, G., Riuzzi, F., Arcuri, C., Bianchi, R., Brozzi, F., Tubaro, C., Giambanco, I., 2009. S100B's double life: Intracellular regulator and extracellular signal. Biochim. Biophys. Acta - Mol. Cell Res. 1793, 1008–1022. https://doi.org/10.1016/J.BBAMCR.2008.11.009

Dowlatshahi, D., Demchuk, A.M., Flaherty, M.L., Ali, M., Lyden, P.L., Smith, E.E., 2011. Defining hematoma expansion in intracerebral hemorrhage: Relationship with patient outcomes. Neurology 76, 1238–1244. https://doi.org/10.1212/WNL.0b013e3182143317

Dringen, R., Brandmann, M., Hohnholt, M.C., Blumrich, E.-M., 2015. Glutathione-Dependent Detoxification Processes in Astrocytes. Neurochem. Res. 40, 2570–2582. https://doi.org/10.1007/s11064-014-1481-1

Duan, X., Wen, Z., Shen, H., Shen, M., Chen, G., 2016. Intracerebral Hemorrhage, Oxidative Stress, and Antioxidant Therapy. Oxid. Med. Cell. Longev. 2016, 1203285. https://doi.org/10.1155/2016/1203285

Dutra, F.F., Bozza, M.T., 2014. Heme on innate immunity and inflammation. Front. Pharmacol. 5, 115. https://doi.org/10.3389/fphar.2014.00115

Eid, T., Gruenbaum, S.E., Dhaher, R., Lee, T.-S.W., Zhou, Y., Danbolt, N.C., 2016. The Glutamate–Glutamine Cycle in Epilepsy, in: Advances in Neurobiology. pp. 351–400. https://doi.org/10.1007/978-3-319-45096-4_14

Eid, T., Lee, T.-S.W., Patrylo, P., Zaveri, H.P., 2018. Astrocytes and Glutamine Synthetase in Epileptogenesis. J. Neurosci. Res. https://doi.org/10.1002/jnr.24267

Emsley, H.C.A., Tyrrell, P.J., 2002. Inflammation and infection in clinical stroke. J. Cereb. Blood Flow Metab. https://doi.org/10.1097/01.WCB.0000037880.62590.28

Enatsu, R., Asahi, M., Matsumoto, M., Hirai, O., 2012. Prognostic factors of motor recovery after stereotactic evacuation of intracerebral hematoma. Tohoku J. Exp. Med. 227, 63–7.

https://doi.org/https://doi.org/10.1620/tjem.227.63

Engler-Chiurazzi, E.B., Brown, C.M., Povroznik, J.M., Simpkins, J.W., 2017. Estrogens as neuroprotectants: Estrogenic actions in the context of cognitive aging and brain injury. Prog. Neurobiol. 157, 188. https://doi.org/10.1016/J.PNEUROBIO.2015.12.008

Esposito, G., De Filippis, D., Cirillo, C., Sarnelli, G., Cuomo, R., Iuvone, T., 2006. The astroglial-derived S100β protein stimulates the expression of nitric oxide synthase in rodent macrophages through p38 MAP kinase activation. Life Sci. 78, 2707–2715. https://doi.org/10.1016/j.lfs.2005.10.023

Fang, H.-Y., Ko, W.-J., Lin, C.-Y., 2007. Inducible heat shock protein 70, interleukin-18, and tumor necrosis factor alpha correlate with outcomes in spontaneous intracerebral hemorrhage. J. Clin. Neurosci. 14, 435–441. https://doi.org/10.1016/j.jocn.2005.12.022

Ferrete-Araujo, A.M., Rodríguez-Rodríguez, A., Egea-Guerrero, J.J., Vilches-Arenas, Á., Godoy, D.A., Murillo-Cabezas, F., 2019. Brain Injury Biomarker Behavior in Spontaneous Intracerebral Hemorrhage. World Neurosurg. 132, e496–e505. https://doi.org/10.1016/j.wneu.2019.08.090

Figueiredo, R.T., Fernandez, P.L., Mourao-Sa, D.S., Porto, B.N., Dutra, F.F., Alves, L.S., Oliveira, M.F., Oliveira, P.L., Graça-Souza, A. V., Bozza, M.T., 2007. Characterization of heme as activator of toll-like receptor 4. J. Biol. Chem. 282, 20221–20229. https://doi.org/10.1074/jbc.M610737200

Fiorella, D., Zuckerman, S.L., Khan, I.S., Ganesh Kumar, N., Mocco, J., 2015. Intracerebral Hemorrhage: A Common and Devastating Disease in Need of Better Treatment. World Neurosurg. 84, 1136–1141. https://doi.org/10.1016/J.WNEU.2015.05.063

Foerch, C., Niessner, M., Back, T., Bauerle, M., De Marchis, G.M., Ferbert, A., Grehl, H., Hamann, G.F., Jacobs, A., Kastrup, A., Klimpe, S., Palm, F., Thomalla, G., Worthmann, H., Sitzer, M., BE FAST Study Group, 2012. Diagnostic Accuracy of Plasma Glial Fibrillary Acidic Protein for Differentiating Intracerebral Hemorrhage and Cerebral Ischemia in Patients with Symptoms of Acute Stroke. Clin. Chem. 58, 237–245. https://doi.org/10.1373/clinchem.2011.172676

Gao, Z., Wang, J., Thiex, R., Rogove, A.D., Heppner, F.L., Tsirka, S.E., 2008. Microglial activation and intracerebral hemorrhage. Acta Neurochir. Suppl.

105, 51–3.

Gebel, J.M., Jauch, E.C., Brott, T.G., Khoury, J., Sauerbeck, L., Salisbury, S., Spilker, J., Tomsick, T.A., Duldner, J., Broderick, J.P., 2002. Natural history of perihematomal edema in patients with hyperacute spontaneous intracerebral hemorrhage. Stroke 33, 2631–2635. https://doi.org/10.1161/01.STR.0000035284.12699.84

Gong, C., Hoff, J.T., Keep, R.F., 2000. Acute inflammatory reaction following experimental intracerebral hemorrhage in rat. Brain Res. 871, 57–65. https://doi.org/10.1016/S0006-8993(00)02427-6

Graybiel, A.M., Grafton, S.T., 2015. The striatum: where skills and habits meet. Cold Spring Harb. Perspect. Biol. 7, a021691. https://doi.org/10.1101/cshperspect.a021691

Griffin, W.S.T., Sheng, J.G., Royston, M.C., Gentleman, S.M., McKenzie, J.E., Graham, D.I., Roberts, G.W., Mrak, R.E., 2006. Glial-Neuronal Interactions in Alzheimer's Disease: The Potential Role of a 'Cytokine Cycle' in Disease Progression. Brain Pathol. 8, 65–72. https://doi.org/10.1111/j.1750-3639.1998.tb00136.x

Hanada, M., Shinjo, R., Miyagi, M., Yasuda, T., Tsutsumi, K., Sugiura, Y., Imagama, S., Ishiguro, N., Matsuyama, Y., 2014. Arundic acid (ONO-2506) inhibits secondary injury and improves motor function in rats with spinal cord injury. J. Neurol. Sci. 337, 186–192. https://doi.org/10.1016/j.jns.2013.12.008

Higashino, H., Niwa, A., Satou, T., Ohta, Y., Hashimoto, S., Tabuchi, M., Ooshima, K., 2009. Immunohistochemical analysis of brain lesions using S100B and glial fibrillary acidic protein antibodies in arundic acid- (ONO-2506) treated stroke-prone spontaneously hypertensive rats. J. Neural Transm. 116, 1209–1219. https://doi.org/10.1007/s00702-009-0278-x

Hofmann, M.A., Drury, S., Fu, C., Qu, W., Taguchi, A., Lu, Y., Avila, C., Kambham, N., Bierhaus, A., Nawroth, P., Neurath, M.F., Slattery, T., Beach, D., McClary, J., Nagashima, M., Morser, J., Stern, D., Schmidt, A.M., 1999. RAGE mediates a novel proinflammatory axis: A central cell surface receptor for S100/calgranulin polypeptides. Cell 97, 889–901. https://doi.org/10.1016/S0092-8674(00)80801-6

Hu, J., Ferreira, A., Van Eldik, L.J., 2002. S100β Induces Neuronal Cell Death

Through Nitric Oxide Release from Astrocytes. J. Neurochem. 69, 2294–2301. https://doi.org/10.1046/j.1471-4159.1997.69062294.x

Hu, J., Ferreira, A., Van Eldik, L.J., 1997. S100beta induces neuronal cell death through nitric oxide release from astrocytes. J. Neurochem. 69, 2294–301. https://doi.org/10.1046/j.1471-4159.1997.69062294.x

Hu, W., Zhou, P., Rao, T., Zhang, X., Wang, W., Zhang, L., 2015. Adrenomedullin attenuates interleukin-1β-induced inflammation and apoptosis in rat Leydig cells via inhibition of NF-κB signaling pathway. Exp. Cell Res. 339, 220–230. https://doi.org/10.1016/j.yexcr.2015.10.024

Hu, X., Tao, C., Gan, Q., Zheng, J., Li, H., You, C., 2016. Oxidative Stress in Intracerebral Hemorrhage: Sources, Mechanisms, and Therapeutic Targets. Oxid. Med. Cell. Longev. 2016, 3215391. https://doi.org/10.1155/2016/3215391

Hu, Y.-Y., Dong, X.-Q., Yu, W.-H., Zhang, Z.-Y., 2010. CHANGE IN PLASMA S100B LEVEL AFTER ACUTE SPONTANEOUS BASAL GANGLIA HEMORRHAGE. Shock 33, 134–140. https://doi.org/10.1097/SHK.0b013e3181ad5c88

Huang, M., Dong, X.-Q., Hu, Y.-Y., Yu, W.-H., Zhang, Z.-Y., 2010. High S100B levels in cerebrospinal fluid and peripheral blood of patients with acute basal ganglial hemorrhage are associated with poor outcome. World J. Emerg. Med. 1, 22–31.

Huttunen, H.J., Kuja-Panula, J., Sorci, G., Lisa Agneletti, A., Donato, R., Rauvala, H., 2000. Coregulation of Neurite Outgrowth and Cell Survival by Amphoterin and S100 Proteins through Receptor for Advanced Glycation End Products (RAGE) Activation*. https://doi.org/10.1074/jbc.M006993200

Inaji, M., Tomita, H., Tone, O., Tamaki, M., Suzuki, R., Ohno, K., 2003. Chronological changes of perihematomal edema of human intracerebral hematoma. Acta Neurochir. Suppl. 445–448. https://doi.org/10.1007/978-3-7091-0651-8_91

Ishiguro, H., Kaito, T., Hashimoto, K., Kushioka, J., Okada, R., Tsukazaki, H., Kodama, J., Bal, Z., Ukon, Y., Takenaka, S., Makino, T., Sakai, Y., Yoshikawa, H., 2019. Administration of ONO-2506 suppresses neuropathic pain after spinal cord injury by inhibition of astrocytic activation. Spine J. 19, 1434–1442. https://doi.org/10.1016/j.spinee.2019.04.006

James, M.L., Blessing, R., Phillips-Bute, B.G., Bennett, E., Laskowitz, D.T., 2009. S100B and brain natriuretic peptide predict functional neurological outcome after intracerebral haemorrhage. Biomarkers 14, 388–94. https://doi.org/10.1080/13547500903015784

James, M.L., Warner, D.S., Laskowitz, D.T., 2008. Preclinical models of intracerebral hemorrhage: A translational perspective. Neurocrit. Care 9, 139–152. https://doi.org/10.1007/s12028-007-9030-2

Jeyasingham, R.., Baird, A.L., Meldrum, A., Dunnett, S.B., 2001. Differential effects of unilateral striatal and nigrostriatal lesions on grip strength, skilled paw reaching and drug-induced rotation in the rat. Brain Res. Bull. 55, 541–548. https://doi.org/10.1016/S0361-9230(01)00557-3

Kanner, A.A., Marchi, N., Fazio, V., Mayberg, M.R., Koltz, M.T., Siomin, V., Stevens, G.H.J., Masaryk, T., Ayumar, B., Vogelbaum, M.A., Barnett, G.H., Janigro, D., Janigro, D., 2003. Serum S100beta: a noninvasive marker of blood-brain barrier function and brain lesions. Cancer 97, 2806–2813. https://doi.org/10.1002/cncr.11409

Kapural, M., Krizanac-Bengez, L., Barnett, G., Perl, J., Masaryk, T., Apollo, D., Rasmussen, P., Mayberg, M.R., Janigro, D., 2002. Serum S-100beta as a possible marker of blood-brain barrier disruption. Brain Res. 940, 102–4.

Kato, H., Kurosaki, R., Oki, C., Araki, T., 2004. Arundic acid, an astrocyte-modulating agent, protects dopaminergic neurons against MPTP neurotoxicity in mice. Brain Res. 1030, 66–73. https://doi.org/10.1016/j.brainres.2004.09.046

Keep, R.F., Hua, Y., Xi, G., 2012. Intracerebral haemorrhage: mechanisms of injury and therapeutic targets. https://doi.org/10.1016/S1474-4422(12)70104-7

Keep, R.F., Xiang, J., Ennis, S.R., Andjelkovic, A., Hua, Y., Xi, G., Hoff, J.T., 2008. Blood-brain barrier function in intracerebral hemorrhage. Acta Neurochir. Suppl. https://doi.org/10.1007/978-3-211-09469-3_15

Khaper, N., Bryan, S., Dhingra, S., Singal, R., Bajaj, A., Pathak, C.M., Singal, P.K., 2010. Targeting the Vicious Inflammation–Oxidative Stress Cycle for the Management of Heart Failure. Antioxid. Redox Signal. 13, 1033–1049. https://doi.org/10.1089/ars.2009.2930

Kim-Han, J.S., Kopp, S.A., Dugan, L.L., Diringer, M.N., 2006. Perihematomal

mitochondrial dysfunction after intracerebral hemorrhage. Stroke 37, 2457–2462. https://doi.org/10.1161/01.STR.0000240674.99945.4e

Kim, S.H., Smith, C.J., Van Eldik, L.J., 2004. Importance of MAPK pathways for microglial pro-inflammatory cytokine IL-1β production. Neurobiol. Aging 25, 431–439. https://doi.org/10.1016/S0197-4580(03)00126-X

Kim, T., Chelluboina, B., Chokkalla, A.K., 2019. Age and sex differences in the pathophysiology of acute CNS injury. Neurochem. Int. 127, 22–28. https://doi.org/10.1016/J.NEUINT.2019.01.012

Kumar, A., Kumar, P., Misra, S., Sagar, R., Kathuria, P., Vibha, D., Vivekanandhan, S., Garg, A., Kaul, B., Raghvan, S., Gorthi, S.P., Dabla, S., Aggarwal, C.S., Prasad, K., 2015. Biomarkers to enhance accuracy and precision of prediction of short-term and long-term outcome after spontaneous intracerebral haemorrhage : a study protocol for a prospective cohort study. BMC Neurol. 4–9. https://doi.org/10.1186/s12883-015-0384-3

Labovitz, D.L., Halim, A., Boden-Albala, B., Hauser, W.A., Sacco, R.L., 2005. The incidence of deep and lobar intracerebral hemorrhage in whites, blacks, and Hispanics. Neurology 65, 518–522. https://doi.org/10.1212/01.wnl.0000172915.71933.00

LeBel, C.P., Ischiropoulos, H., Bondy, S.C., 1992. Evaluation of the probe 2',7'-dichlorofluorescin as an indicator of reactive oxygen species formation and oxidative stress. Chem. Res. Toxicol. 5, 227–31.

Lei, B., Dawson, H.N., Roulhac-Wilson, B., Wang, H., Laskowitz, D.T., James, M.L., 2013. Tumor necrosis factor alpha antagonism improves neurological recovery in murine intracerebral hemorrhage, Journal of Neuroinflammation. https://doi.org/10.1186/1742-2094-10-103

Lewerenz, J., Maher, P., 2015. Chronic glutamate toxicity in neurodegenerative diseases-What is the evidence? Front. Neurosci. https://doi.org/10.3389/fnins.2015.00469

Li, X., Wang, T., Zhang, D., Li, H., Shen, H., Ding, X., Chen, G., 2018. Andrographolide ameliorates intracerebral hemorrhage induced secondary brain injury by inhibiting neuroinflammation induction. Neuropharmacology 141, 305–315. https://doi.org/10.1016/j.neuropharm.2018.09.015

Lin, S., Yin, Q., Zhong, Q., Lv, F.-L., Zhou, Y., Li, J.-Q., Wang, J.-Z., Su, B., Yang, Q.-W., 2012a. Heme activates TLR4-mediated inflammatory injury

via MyD88/TRIF signaling pathway in intracerebral hemorrhage. J. Neuroinflammation 9, 548. https://doi.org/10.1186/1742-2094-9-46

Lin, S., Yin, Q., Zhong, Q., Lv, F.-L., Zhou, Y., Li, J.-Q., Wang, J.-Z., Su, B., Yang, Q.-W., 2012b. Heme activates TLR4-mediated inflammatory injury via MyD88/TRIF signaling pathway in intracerebral hemorrhage. J. Neuroinflammation 9, 548. https://doi.org/10.1186/1742-2094-9-46

Liu, D.Z., Ander, B.P., Xu, H., Shen, Y., Kaur, P., Deng, W., Sharp, F.R., 2010. Blood-brain barrier breakdown and repair by Src after thrombin-induced injury. Ann. Neurol. 67, 526–533. https://doi.org/10.1002/ana.21924

Lue, L.-F., Walker, D.G., Brachova, L., Beach, T.G., Rogers, J., Schmidt, A.M., Stern, D.M., Yan, S. Du, 2001. Involvement of Microglial Receptor for Advanced Glycation Endproducts (RAGE) in Alzheimer's Disease: Identification of a Cellular Activation Mechanism. Exp. Neurol. 171, 29–45. https://doi.org/10.1006/exnr.2001.7732

MacLellan, C.L., Silasi, G., Auriat, A.M., Colbourne, F., 2010. Rodent models of intracerebral hemorrhage, in: Stroke. Stroke. https://doi.org/10.1161/STROKEAHA.110.594457

Maclellan, C.L., Silasi, G., Poon, C.C., Edmundson, C.L., Buist, R., Peeling, J., Colbourne, F., 2008. Intracerebral hemorrhage models in rat : comparing collagenase to blood infusion 516–525. https://doi.org/10.1038/sj.jcbfm.9600548

Mahesh, V.B., Dhandapani, K.M., Brann, D.W., 2006. Role of astrocytes in reproduction and neuroprotection. Mol. Cell. Endocrinol. 246, 1–9. https://doi.org/10.1016/j.mce.2005.11.017

Manno, E.M., 2012. Update on Intracerebral Hemorrhage. Contin. Lifelong Learn. Neurol. 18, 598–610. https://doi.org/10.1212/01.CON.0000415430.99394.3e

Mari, C., Odorcyk, F.K., Sanches, E.F., Wartchow, K.M., Martini, A.P., Nicola, F., Zanotto, C., Wyse, A.T., Gonçalves, C.A., Netto, C.A., 2019. Arundic acid administration protects astrocytes, recovers histological damage and memory deficits induced by neonatal hypoxia ischemia in rats. Int. J. Dev. Neurosci. 76, 41–51. https://doi.org/10.1016/j.ijdevneu.2019.06.003

Masada, T., Hua, Y., Xi, G., Yang, G.-Y., Hoff, J.T., Keep, R.F., 2001. Attenuation of intracerebral hemorrhage and thrombin-induced brain

edema by overexpression of interleukin-1 receptor antagonist. J. Neurosurg. 95, 680–686. https://doi.org/10.3171/jns.2001.95.4.0680

Masada, T., Hua, Y., Xi, G., Yang, G.Y., Hoff, J.T., Keep, R.F., Nagao, S., 2003. Overexpression of interleukin-1 receptor antagonist reduces brain edema induced by intracerebral hemorrhage and thrombin. Acta Neurochir. Suppl. 86, 463–7.

Matsui, T., Mori, T., Tateishi, N., Kagamiishi, Y., Satoh, S., Katsube, N., Morikawa, E., Morimoto, T., Ikuta, F., Asano, T., 2002. Astrocytic Activation and Delayed Infarct Expansion after Permanent Focal Ischemia in Rats. Part I: Enhanced Astrocytic Synthesis of S-100β in the Periinfarct Area Precedes Delayed Infarct Expansion. J. Cereb. Blood Flow Metab. 22, 711–722. https://doi.org/10.1097/00004647-200206000-00010

Mayne, M., Fotheringham, J., Yan, H.J., Power, C., Del Bigio, M.R., Peeling, J., Geiger, J.D., 2001a. Adenosine A2A receptor activation reduces proinflammatory events and decreases cell death following intracerebral hemorrhage. Ann. Neurol. 49, 727–35.

Mayne, M., Ni, W., Yan, H.J., Xue, M., Johnston, J.B., Del Bigio, M.R., Peeling, J., Power, C., 2001b. Antisense oligodeoxynucleotide inhibition of tumor necrosis factor-alpha expression is neuroprotective after intracerebral hemorrhage. Stroke 32, 240–8.

Mendelow, A.D., Gregson, B.A., Mitchell, P.M., Murray, G.D., Rowan, E.N., Gholkar, A.R., 2011. Surgical Trial in Lobar Intracerebral Haemorrhage (STICH II) Protocol. Trials 12. https://doi.org/10.1186/1745-6215-12-124

Mestriner, R.G., Pagnussat, A.S., Boisserand, L.S.B., Valentim, L., Netto, C.A., 2011. Skilled reaching training promotes astroglial changes and facilitated sensorimotor recovery after collagenase-induced intracerebral hemorrhage. Exp. Neurol. 227, 53–61. https://doi.org/10.1016/j.expneurol.2010.09.009

Metz, G.A., Whishaw, I.Q., 2002. Cortical and subcortical lesions impair skilled walking in the ladder rung walking test: A new task to evaluate fore- and hindlimb stepping, placing, and co-ordination. J. Neurosci. Methods 115, 169–179. https://doi.org/10.1016/S0165-0270(02)00012-2

Min, H., Hong, J., Cho, I.H., Jang, Y.H., Lee, H., Kim, D., Yu, S.W., Lee, S., Lee, S.J., 2015. TLR2-induced astrocyte MMP9 activation compromises the blood brain barrier and exacerbates intracerebral hemorrhage in animal

models. Mol. Brain 8. https://doi.org/10.1186/s13041-015-0116-z

Mori, T., Tateishi, N., Kagamiishi, Y., Shimoda, T., Satoh, S., Ono, S., Katsube, N., Asano, T., 2004. Attenuation of a delayed increase in the extracellular glutamate level in the peri-infarct area following focal cerebral ischemia by a novel agent ONO-2506. Neurochem. Int. 45, 381–387. https://doi.org/10.1016/j.neuint.2003.06.001

Mori, T., Town, T., Tan, J., Tateishi, N., Asano, T., 2005. Modulation of astrocytic activation by arundic acid (ONO-2506) mitigates detrimental effects of the apolipoprotein E4 isoform after permanent focal ischemia in apolipoprotein E knock-in mice. J. Cereb. Blood Flow Metab. 25, 748–762. https://doi.org/10.1038/sj.jcbfm.9600063

Mori, T., Town, T., Tan, J., Yada, N., Horikoshi, Y., Yamamoto, J., Shimoda, T., Kamanaka, Y., Tateishi, N., Asano, T., 2006. Arundic Acid ameliorates cerebral amyloidosis and gliosis in Alzheimer transgenic mice. J. Pharmacol. Exp. Ther. 318, 571–578. https://doi.org/10.1124/jpet.106.105171

Mracsko, E., Veltkamp, R., 2014. Neuroinflammation after intracerebral hemorrhage. Front. Cell. Neurosci. 8, 388. https://doi.org/10.3389/fncel.2014.00388

Nakamura, T., Keep, R.F., Hua, Y., Hoff, J.T., Xi, G., 2005. Oxidative DNA injury after experimental intracerebral hemorrhage. Brain Res. 1039, 30–36. https://doi.org/10.1016/j.brainres.2005.01.036

Nedergaard, M., Takano, T., Hansen, A.J., 2002. Beyond the role of glutamate as a neurotransmitter. Nat. Rev. Neurosci. 3, 748–755. https://doi.org/10.1038/nrn916

Neves, J.D., Aristimunha, D., Vizuete, A.F., Nicola, F., Vanzela, C., Petenuzzo, L., Mestriner, R.G., Sanches, E.F., Gonçalves, C.A., Netto, C.A., 2017. Glial-associated changes in the cerebral cortex after collagenase-induced intracerebral hemorrhage in the rat striatum. Brain Res. Bull. 134, 55–62. https://doi.org/10.1016/j.brainresbull.2017.07.002

Neves, J.D., Vizuete, A.F., Nicola, F., Da Ré, C., Rodrigues, A.F., Schmitz, F., Mestriner, R.G., Aristimunha, D., Wyse, A.T.S., Netto, C.A., 2018. Glial glutamate transporters expression, glutamate uptake, and oxidative stress in an experimental rat model of intracerebral hemorrhage. Neurochem. Int.

116, 13–21. https://doi.org/10.1016/j.neuint.2018.03.003

Nicola, F.C., Rodrigues, L.P., Crestani, T., Quintiliano, K., Sanches, E.F., Willborn, S., Aristimunha, D., Boisserand, L., Pranke, P., Netto, C.A., Nicola, F.C., Rodrigues, L.P., Crestani, T., Quintiliano, K., Sanches, E.F., Willborn, S., Aristimunha, D., Boisserand, L., Pranke, P., Netto, C.A., 2016. Human dental pulp stem cells transplantation combined with treadmill training in rats after traumatic spinal cord injury. Brazilian J. Med. Biol. Res. 49. https://doi.org/10.1590/1414-431x20165319

Nishino, A., Suzuki, M., Ohtani, H., Motohashi, O., Umezawa, K., Nagura, H., Yoshimoto, T., 1993. Thrombin may contribute to the pathophysiology of central nervous system injury. J. Neurotrauma 10, 167–79. https://doi.org/10.1089/neu.1993.10.167

Ohtani, R., Tomimoto, H., Wakita, H., Kitaguchi, H., Nakaji, K., Takahashi, R., 2007. Expression of S100 protein and protective effect of arundic acid on the rat brain in chronic cerebral hypoperfusion. Brain Res. 1135, 195–200. https://doi.org/10.1016/j.brainres.2006.11.084

Oki, C., Watanabe, Y., Yokoyama, H., Shimoda, T., Kato, H., Araki, T., 2008. Delayed treatment with arundic acid reduces the MPTP-induced neurotoxicity in mice. Cell. Mol. Neurobiol. 28, 417–430. https://doi.org/10.1007/s10571-007-9241-2

Paxinos, G., Watson, C., 2007. The rat brain in stereotaxic coordinates. Elsevier.

Pettigrew, L.C., Kasner, S.E., Albers, G.W., Gorman, M., Grotta, J.C., Sherman, D.G., Funakoshi, Y., Ishibashi, H., 2006a. Safety and tolerability of arundic acid in acute ischemic stroke. J. Neurol. Sci. 251, 50–56. https://doi.org/10.1016/j.jns.2006.09.001

Pettigrew, L.C., Kasner, S.E., Gorman, M., Atkinson, R.P., Funakoshi, Y., Ishibashi, H., 2006b. Effect of arundic acid on serum S-100β in ischemic stroke. J. Neurol. Sci. 251, 57–61. https://doi.org/10.1016/j.jns.2006.09.002

Ponath, G., Schettler, C., Kaestner, F., Voigt, B., Wentker, D., Arolt, V., Rothermundt, M., 2007. Autocrine S100B effects on astrocytes are mediated via RAGE. J. Neuroimmunol. 184, 214–222. https://doi.org/10.1016/j.jneuroim.2006.12.011

Poon, M.T.C., Fonville, A.F., Salman, R.A.S., 2014. Long-term prognosis after

intracerebral haemorrhage: Systematic review and meta-analysis. J. Neurol. Neurosurg. Psychiatry 85, 660–667. https://doi.org/10.1136/jnnp-2013-306476

Provencio, J.J., Ferreira Da Silva, I.R., Manno, E.M., 2013. Intracerebral Hemorrhage. New Challenges and Steps Forward. Neurosurg. Clin. N. Am. https://doi.org/10.1016/j.nec.2013.03.002

Qiao, H.-B., Li, J., Lv, L.-J., Nie, B.-J., Lu, P., Xue, F., Zhang, Z.-M., 2018. Eupatilin inhibits microglia activation and attenuates brain injury in intracerebral hemorrhage. Exp. Ther. Med. 16, 4005–4009. https://doi.org/10.3892/etm.2018.6699

Qu, J., Chen, W., Hu, R., Feng, H., 2016. The Injury and Therapy of Reactive Oxygen Species in Intracerebral Hemorrhage Looking at Mitochondria. Oxid. Med. Cell. Longev. 2016, 1–9. https://doi.org/10.1155/2016/2592935

Qureshi, A.I., Mendelow, A.D., Hanley, D.F., 2009. Intracerebral haemorrhage. Lancet (London, England) 373, 1632–44. https://doi.org/10.1016/S0140-6736(09)60371-8

Qureshi, A.I., Suri, M.F.K., Ostrow, P.T., Kim, S.H., Ali, Z., Shatla, A.A., Guterman, L.R., Hopkins, L.N., 2003. Apoptosis as a Form of Cell Death in Intracerebral Hemorrhage. Neurosurgery 52, 1041–1048. https://doi.org/10.1093/neurosurgery/52.5.1041

Qureshi, A.I., Tuhrim, S., Broderick, J.P., Batjer, H.H., Hondo, H., Hanley, D.F., 2001. Spontaneous intracerebral hemorrhage. N. Engl. J. Med. https://doi.org/10.1056/NEJM200105103441907

Ren, H., Kong, Y., Liu, Z., Zang, D., Yang, X., Wood, K., Li, M., Liu, Q., 2018. Selective NLRP3 (Pyrin Domain–Containing Protein 3) Inflammasome Inhibitor Reduces Brain Injury After Intracerebral Hemorrhage. Stroke 49, 184–192. https://doi.org/10.1161/STROKEAHA.117.018904

Righy, C., Bozza, M.T., Oliveira, M.F., Bozza, F.A., 2016. Molecular, Cellular and Clinical Aspects of Intracerebral Hemorrhage: Are the Enemies Within? Curr. Neuropharmacol. 14, 392–402. https://doi.org/10.2174/1570159X14666151230110058

Rosand, J., Hylek, E.M., O'Donnell, H.C., Greenberg, S.M., 2000. Warfarin-associated hemorrhage and cerebral amyloid angiopathy: A genetic and pathologic study. Neurology 55, 947–951.

https://doi.org/10.1212/WNL.55.7.947

Schlunk, F., Greenberg, S.M., 2015. The Pathophysiology of Intracerebral Hemorrhage Formation and Expansion. Transl. Stroke Res. 6, 257–263. https://doi.org/10.1007/s12975-015-0410-1

Sen, J., Belli, A., 2007. S100B in neuropathologic states: The CRP of the brain? J. Neurosci. Res. 85, 1373–1380. https://doi.org/10.1002/jnr.21211

Senn, R., Elkind, M.S. V, Montaner, J., Christ-Crain, M., Katan, M., 2014. Potential role of blood biomarkers in the management of nontraumatic intracerebral hemorrhage. Cerebrovasc. Dis. 38, 395–409. https://doi.org/10.1159/000366470

Sharp, F., Liu, D.Z., Zhan, X., Ander, B.P., 2008. Intracerebral hemorrhage injury mechanisms: Glutamate neurotoxicity, thrombin, and Src. Acta Neurochir. Suppl. https://doi.org/10.1007/978-3-211-09469-3_9

Shiratori, M., Tozaki-Saitoh, H., Yoshitake, M., Tsuda, M., Inoue, K., 2010. P2X7 receptor activation induces CXCL2 production in microglia through NFAT and PKC/MAPK pathways. J. Neurochem. 114, 810–819. https://doi.org/10.1111/j.1471-4159.2010.06809.x

Silva, Y., Leira, R., Tejada, J., Lainez, J.M., Castillo, J., Dávalos, A., Stroke Project, Cerebrovascular Diseases Group of the Spanish Neurological Society, 2005. Molecular Signatures of Vascular Injury Are Associated With Early Growth of Intracerebral Hemorrhage. Stroke 36, 86–91. https://doi.org/10.1161/01.STR.0000149615.51204.0b

Sinha, K., Das, J., Pal, P.B., Sil, P.C., 2013. Oxidative stress: the mitochondria-dependent and mitochondria-independent pathways of apoptosis. Arch. Toxicol. 87, 1157–1180. https://doi.org/10.1007/s00204-013-1034-4

Sofroniew, M. V., 2009. Molecular dissection of reactive astrogliosis and glial scar formation. Trends Neurosci. 32, 638–647. https://doi.org/10.1016/j.tins.2009.08.002

Sofroniew, M. V., Vinters, H. V., 2010a. Astrocytes: biology and pathology. Acta Neuropathol. 119, 7–35. https://doi.org/10.1007/s00401-009-0619-8

Sofroniew, M. V., Vinters, H. V., 2010b. Astrocytes: biology and pathology. Acta Neuropathol. 119, 7. https://doi.org/10.1007/S00401-009-0619-8

Sorci, G., Bianchi, R., Riuzzi, F., Tubaro, C., Arcuri, C., Giambanco, I., Donato, R., 2010. S100B protein, a damage-associated molecular pattern protein in

the brain and heart, and beyond. Cardiovasc. Psychiatry Neurol. 2010. https://doi.org/10.1155/2010/656481

Sukumari-Ramesh, S., Alleyne, C.H., Dhandapani, K.M., 2012a. Astrogliosis: a Target for Intervention in Intracerebral Hemorrhage? Transl. Stroke Res. 3, 80–87. https://doi.org/10.1007/s12975-012-0165-x

Sukumari-Ramesh, S., Alleyne, C.H., Dhandapani, K.M., 2012b. Astrocyte-Specific Expression of Survivin after Intracerebral Hemorrhage in Mice: A Possible Role in Reactive Gliosis? J. Neurotrauma 29, 2798–2804. https://doi.org/10.1089/neu.2011.2243

Takano, T., Tian, G.F., Peng, W., Lou, N., Libionka, W., Han, X., Nedergaard, M., 2006. Astrocyte-mediated control of cerebral blood flow. Nat. Neurosci. 9, 260–267. https://doi.org/10.1038/nn1623

Tanaka, Y., Marumo, T., Shibuta, H., Omura, T., Yoshida, S., 2009. Serum S100B, brain edema, and hematoma formation in a rat model of collagenase-induced hemorrhagic stroke. Brain Res. Bull. 78, 158–163. https://doi.org/10.1016/j.brainresbull.2008.10.012

Tateishi, N., Mori, T., Kagamiishi, Y., Satoh, S., Katsube, N., Morikawa, E., Morimoto, T., Matsui, T., Asano, T., 2002. Astrocytic activation and delayed infarct expansion after permanent focal ischemia in rats. Part II: suppression of astrocytic activation by a novel agent (R)-(-)-2-propyloctanoic acid (ONO-2506) leads to mitigation of delayed infarct expansion and early . J. Cereb. Blood Flow Metab. 22, 723–734. https://doi.org/10.1097/00004647-200206000-00011

Thabet, A.M., Kottapally, M., Hemphill, J.C., 2017. Management of intracerebral hemorrhage, in: Handbook of Clinical Neurology. Elsevier B.V., pp. 177–194. https://doi.org/10.1016/B978-0-444-63600-3.00011-8

Turrin, N.P., Plata-Salamán, C.R., 2000. Cytokine-cytokine interactions and the brain. Brain Res. Bull. https://doi.org/10.1016/S0361-9230(99)00203-8

Ullian, E.M., Sapperstein, S.K., Christopherson, K.S., Barres, B.A., 2001. Control of synapse number by glia. Science (80-.). 291, 657–661. https://doi.org/10.1126/science.291.5504.657

van Asch, C.J., Luitse, M.J., Rinkel, G.J., van der Tweel, I., Algra, A., Klijn, C.J., 2010. Incidence, case fatality, and functional outcome of intracerebral haemorrhage over time, according to age, sex, and ethnic origin: a

systematic review and meta-analysis. Lancet Neurol. 9, 167–176. https://doi.org/10.1016/S1474-4422(09)70340-0

Villarreal, A., Seoane, R., Torres, A.G., Rosciszewski, G., Angelo, M.F., Rossi, A., Barkert, P.A., Ramos, A.J., 2014. S100B protein activates a RAGE-dependent autocrine loop in astrocytes: Implications for its role in the propagation of reactive gliosis. J. Neurochem. 131, 190–205. https://doi.org/10.1111/jnc.12790

Vizuete, A.F., de Souza, D.F., Guerra, M.C., Batassini, C., Dutra, M.F., Bernardi, C., Costa, A.P., Gonçalves, C.-A., 2013. Brain changes in BDNF and S100B induced by ketogenic diets in Wistar rats. Life Sci. 92, 923–928. https://doi.org/10.1016/j.lfs.2013.03.004

Wajima, D., Nakagawa, I., Nakase, H., Yonezawa, T., 2013. Neuroprotective effect of suppression of astrocytic activation by arundic acid on brain injuries in rats with acute subdural hematomas. Brain Res. 1519, 127–135. https://doi.org/10.1016/j.brainres.2013.05.002

Wang, H., Zhang, L., Zhang, I.Y., Chen, X., Da Fonseca, A., Wu, S., Ren, H., Badie, S., Sadeghi, S., Ouyang, M., Warden, C.D., Badie, B., 2013. S100B promotes glioma growth through chemoattraction of myeloid-derived macrophages. Clin. Cancer Res. 19, 3764–75. https://doi.org/10.1158/1078-0432.CCR-12-3725

Wang, J., 2010. Preclinical and clinical research on inflammation after intracerebral hemorrhage. Prog. Neurobiol. https://doi.org/10.1016/j.pneurobio.2010.08.001

Wang, J., Doré, S., 2007. Inflammation after intracerebral hemorrhage. J. Cereb. Blood Flow Metab. 27, 894–908. https://doi.org/10.1038/sj.jcbfm.9600403

Wang, J., Rogove, A.D., Tsirka, A.E., Tsirka, S.E., 2003. Protective role of tuftsin fragment 1-3 in an animal model of intracerebral hemorrhage. Ann. Neurol. 54, 655–664. https://doi.org/10.1002/ana.10750

Wang, J., Tsirka, S.E., 2005. Tuftsin Fragment 1–3 Is Beneficial When Delivered After the Induction of Intracerebral Hemorrhage. Stroke 36, 613–618. https://doi.org/10.1161/01.STR.0000155729.12931.8f

Wang, S., Li, D., Huang, C., Wan, Y., Wang, J., Zan, X., Yang, B., 2018. Overexpression of adiponectin alleviates intracerebral hemorrhage-induced

brain injury in rats via suppression of oxidative stress. Neurosci. Lett. 681, 110–116. https://doi.org/10.1016/j.neulet.2018.05.050

Wang, Y.C., Zhou, Y., Fang, H., Lin, S., Wang, P.F., Xiong, R.P., Chen, J., Xiong, X.Y., Lv, F.L., Liang, Q.L., Yang, Q.W., 2014. Toll-like receptor 2/4 heterodimer mediates inflammatory injury in intracerebral hemorrhage. Ann. Neurol. 75, 876–889. https://doi.org/10.1002/ana.24159

Wasserman, J.K., Schlichter, L.C., 2007. Neuron death and inflammation in a rat model of intracerebral hemorrhage: Effects of delayed minocycline treatment. Brain Res. 1136, 208–218. https://doi.org/10.1016/j.brainres.2006.12.035

Wilson, J.X., 1997. Antioxidant defense of the brain: A role for astrocytes. Can. J. Physiol. Pharmacol. https://doi.org/10.1139/y97-146

Won, S.Y., Schlunk, F., Dinkel, J., Karatas, H., Leung, W., Hayakawa, K., Lauer, A., Steinmetz, H., Lo, E.H., Foerch, C., Gupta, R., 2013. Imaging of contrast medium extravasation in anticoagulation-associated intracerebral hemorrhage with dual-energy computed tomography. Stroke 44, 2883–2890. https://doi.org/10.1161/STROKEAHA.113.001224

Wu, H., Wu, T., Hua, W., Dong, X., Gao, Y., Zhao, X., Chen, W., Cao, W., Yang, Q., Qi, J., Zhou, J., Wang, J., 2015. PGE2 receptor agonist misoprostol protects brain against intracerebral hemorrhage in mice. Neurobiol. Aging 36, 1439–1450. https://doi.org/10.1016/j.neurobiolaging.2014.12.029

Wu, H., Zhang, Z., Hu, X., Zhao, R., Song, Y., Ban, X., Qi, J., Wang, J., 2010. Dynamic changes of inflammatory markers in brain after hemorrhagic stroke in humans: a postmortem study. Brain Res. 1342, 111–7. https://doi.org/10.1016/j.brainres.2010.04.033

Wu, J., Hua, Y., Keep, R.F., Nakamura, T., Hoff, J.T., Xi, G., 2003. Iron and Iron-Handling Proteins in the Brain after Intracerebral Hemorrhage. Stroke 34, 2964–2969. https://doi.org/10.1161/01.STR.0000103140.52838.45

Wu, J., Yang, S., Xi, G., Fu, G., Keep, R.F., Hua, Y., 2009. Minocycline reduces intracerebral hemorrhage-induced brain injury. Neurol. Res. 31, 183–8. https://doi.org/10.1179/174313209X385680

Wu, J., Yang, S., Xi, G., Song, S., Fu, G., Keep, R.F., Hua, Y., 2008. Microglial activation and brain injury after intracerebral hemorrhage. Acta Neurochir.

Suppl. 105, 59–65.

Wu, T., Wu, H., Wang, Jessica, Wang, Jian, 2011. Expression and cellular localization of cyclooxygenases and prostaglandin E synthases in the hemorrhagic brain. J. Neuroinflammation 8, 22. https://doi.org/10.1186/1742-2094-8-22

Xi, G., Keep, R., Hoff, J., 2006. Mechanisms of brain injury after intracerebral haemorrhage. Lancet Neurol. 5, 53–63.

Xi, G., Reiser, G., Keep, R.F., 2003. The role of thrombin and thrombin receptors in ischemic, hemorrhagic and traumatic brain injury: deleterious or protective? J. Neurochem. 84, 3–9.

Xiong, X.Y., Wang, J., Qian, Z.M., Yang, Q.W., 2014. Iron and Intracerebral Hemorrhage: From Mechanism to Translation. Transl. Stroke Res. https://doi.org/10.1007/s12975-013-0317-7

Xue, M., Del Bigio, M.R., 2003. Comparison of brain cell death and inflammatory reaction in three models of intracerebral hemorrhage in adult rats. J. Stroke Cerebrovasc. Dis. 12, 152–159. https://doi.org/10.1016/S1052-3057(03)00036-3

Yang, Z., Liu, Y., Yuan, F., Li, Z., Huang, S., Shen, H., Yuan, B., 2014. Sinomenine inhibits microglia activation and attenuates brain injury in intracerebral hemorrhage. Mol. Immunol. 60, 109–114. https://doi.org/10.1016/j.molimm.2014.03.005

Yang, Z., Zhong, S., Liu, Y., Shen, H., Yuan, B., 2015. Scavenger receptor SRA attenuates microglia activation and protects neuroinflammatory injury in intracerebral hemorrhage. J. Neuroimmunol. 278, 232–238. https://doi.org/10.1016/j.jneuroim.2014.11.010

Zhang, Y., Yang, Y., Zhang, G.Z., Gao, M., Ge, G.Z., Wang, Q.Q., Ji, X.C., Sun, Y.L., Zhang, H.T., Xu, R.X., 2016. Stereotactic Administration of Edaravone Ameliorates Collagenase-Induced Intracerebral Hemorrhage in Rat. CNS Neurosci. Ther. 22, 824–835. https://doi.org/10.1111/cns.12584

Zhang, Zhen, Zhang, Ze, Lu, H., Yang, Q., Wu, H., Wang, J., 2017. Microglial Polarization and Inflammatory Mediators After Intracerebral Hemorrhage. Mol. Neurobiol. 54, 1874–1886. https://doi.org/10.1007/s12035-016-9785-6

Zhou, S., Bao, J., Wang, Y., Pan, S., 2016. S100β as a biomarker for differential diagnosis of intracerebral hemorrhage and ischemic stroke. Neurol. Res.

38, 327–332. https://doi.org/10.1080/01616412.2016.1152675

Zhou, Y., Wang, Y., Wang, J., Anne Stetler, R., Yang, Q.W., 2014. Inflammation in intracerebral hemorrhage: From mechanisms to clinical translation. Prog. Neurobiol. https://doi.org/10.1016/j.pneurobio.2013.11.003

Ziai, W.C., Carhuapoma, J.R., 2018. Intracerebral Hemorrhage. Contin. Lifelong Learn. Neurol. 24, 1603–1622. https://doi.org/10.1212/CON.0000000000000672

Zou, J., Wang, Y.X., Dou, F.F., Lü, H.Z., Ma, Z.W., Lu, P.H., Xu, X.M., 2010. Glutamine synthetase down-regulation reduces astrocyte protection against glutamate excitotoxicity to neurons. Neurochem. Int. 56, 577–584. https://doi.org/10.1016/j.neuint.2009.12.021

PARTE III

5. DISCUSSÃO GERAL

A hemorragia intracerebral (HIC) corresponde a 15% de todos os acidentes vasculares cerebrais (AVC) e acomete cerca de 2 milhões de pessoas no mundo a cada ano (van Asch et al., 2010), além de ser responsável por altas taxas de morbidade e de mortalidade (Qureshi et al., 2009). A complexidade do mecanismo patofisiológico da HIC, assim como a escassez de opções terapêuticas eficazes na melhora dos desfechos clínicos dos pacientes acometidos, tornam de fundamental importância a investigação de possíveis alvos terapêuticos e de agentes com potencial neuroprotetor para auxiliar no tratamento dessa doença.

A proteína S100B, sintetizada e liberada em altos níveis pelos astrócitos reativos na HIC, demonstrou ser um biomarcador útil para o diagnóstico diferencial e prognóstico da patologia (Senn et al., 2014; Zhou et al., 2016), além de participar ativamente do mecanismo de lesão secundária. A S100B extracelular causa apoptose neuronal e ativação das células astrocitárias e microgliais (Bianchi et al., 2011) com consequente aumento na produção de citocinas inflamatórias e produtos oxidativos que contribuem para a neuroinflamação, lesão oxidativa, morte celular e agravamento da lesão (Donato et al., 2009; Sorci et al., 2010; Tanaka et al., 2009; Villarreal et al., 2014; Wajima et al., 2013). Tais evidências motivaram o estudo desta proteína como um possível alvo terapêutico para suprimir as cascatas de neuroinflamação e dano celular e, assim, melhorar os desfechos da HIC.

O ácido arúndico (AA) é um agente inibidor da síntese astrocitária de S100B que tem demonstrado efeitos benéficos e neuroprotetores em diversos

modelos experimentais de doenças do sistema nervoso central (SNC) (Hanada et al., 2014; Kato et al., 2004; Mari et al., 2019; Mori et al., 2006; Ohtani et al., 2007; Oki et al., 2008; Tateishi et al., 2002; Wajima et al., 2013), mostrando-se capaz de reduzir a morte celular, melhorar parâmetros histológicos e atenuar os déficits neurológicos causados pela lesão. Estas evidências experimentais, aliadas a segurança clínica, tolerabilidade e ausência de efeitos adversos significativos em humanos (Pettigrew et al., 2006a) nos incentivou à investigação dos efeitos da utilização do AA como tratamento no modelo experimental de HIC.

A via de administração escolhida para a infusão do AA foi a intracerebroventricular (ICV), nunca utilizada em estudos anteriores para este agente. Uma vez estabelecida a dose ideal de AA (2µg/µl), com base nos seus efeitos na redução dos níveis estriatais de S100B e GFAP, o tratamento foi administrado por meio de cirurgia estereotáxica, apenas uma vez, imediatamente antes da administração de colagenase no estriado para indução da hemorragia, e os efeitos foram observados até 7 dias após a lesão.

Conforme esperado, a HIC ocasionou aumento dos níveis de S100B tanto central (estriado e líquido cerebrospinal – LCE) quanto perifericamente (soro). A presença de concentrações elevadas de S100B no sangue pode ser atribuída à ruptura da barreira hematoencefálica (BHE) e refletir a cascata patofisiológica em andamento, bem como a liberação passiva da proteína a partir de astrócitos danificados (Kanner et al., 2003). Nossos resultados corroboram com estudos prévios que mostram que o aumento dos níveis de S100B podem ser considerados biomarcadores de lesão cerebral decorrente da HIC tanto em ratos (Neves et al., 2017; Tanaka et al., 2009) como em

humanos (Delgado et al., 2006). Estudos clínicos mostram que os níveis periféricos de S100B encontram-se aumentados em pacientes com HIC aguda, estando associados a um maior volume hemorrágico, maior severidade da lesão e, consequentemente, a piores desfechos neurológicos a curto e longo prazo, assim como elevadas taxas de mortalidade (Delgado et al., 2006; Hu et al., 2010; Huang et al., 2010; James et al., 2009). No presente estudo, o tratamento com AA inibiu a superexpressão de S100B no tecido estriatal, no soro e no LCE, em todos os pontos de tempo em que houve aumento dos níveis da proteína em animais não tratados, como verificado por meio de medidas bioquímicas e histológicas.

A redução dos níveis de S100B em processos patológicos cerebrais tem sua importância relacionada aos efeitos tóxicos exercidos por concentrações extracelulares elevadas da proteína, que resultam em neurodegeneração e aumento da resposta inflamatória. A estimulação aguda do receptor RAGE (receptor para produtos finais de glicação avançada) por altas doses de S100B causa apoptose neuronal por meio da ativação excessiva de cinases reguladas por sinal extracelular (ERK)1/2 e através da superprodução de espécies reativas de oxigênio (EROs) (Huttunen et al., 2000). Além disso, em doses relativamente altas, a S100B estimula a produção de óxido nítrico sintase induzível (iNOS) em astrócitos e micróglia, o que pode contribuir para a apoptose astrocítica e neuronal através do aumento da produção de óxido nítrico (NO) (Hu et al., 1997). Ao induzir a morte celular, a S100B estimula o estresse inflamatório, bem como a dispersão de citocinas, tais como IL-1β (interleucina-1β), IL-6 (interleucina-6) e TNF-α (fator de necrose tumoral-α) e, portanto, pode se correlacionar com a progressão da doença (Kim et al., 2004;

Ponath et al., 2007). Ainda, a proteína S100B é capaz de influenciar a atividade de células astrocitárias e microgliais, as quais expressam RAGE em sua superfície, induzindo um perfil inflamatório nesses tipos celulares, de forma a exacerbar a lesão secundária (Sorci et al., 2010).

A astrogliose reativa, que induz o aumento da síntese de S100B, também é estimulada pelos níveis aumentados da proteína, ou seja, a S100B promove um fenótipo reativo dos astrócitos, caracterizado por hipertrofia, aumento da proliferação, liberação de fatores inflamatórios, migração de astrócitos ativados para o local da lesão e aumento da expressão de RAGE em sua superfície, configurando um ciclo vicioso que potencializa e expande os efeitos da S100B (Villarreal et al., 2014). Neste sentido, o rompimento do ciclo tende a suprimir os efeitos deletérios causados pela proteína. Neste estudo, o tratamento com AA levou não somente à redução das concentrações de S100B, como também à atenuação da reatividade astrocitária no estriado, evidenciada pela manutenção dos níveis da proteína glial fibrilar ácida (GFAP) similar aos dos animais que não sofreram lesão. Dessa forma, estima-se que os diversos efeitos prejudiciais comumente exercidos pelos astrócitos reativos na HIC, tais como aumento da ruptura da BHE e do edema cerebral, assim como a secreção de citocinas inflamatórias e metaloproteinases de matriz (MMP) (Min et al., 2015) possam ser atenuados através da modulação da reatividade astrocítica, por meio da inibição da síntese de S100B.

Apesar dos conhecidos efeitos prejudiciais dos astrócitos reativos frente a uma lesão cerebral, sabe-se que estas células exercem diversas funções vitais no SNC. Uma das funções essenciais para a sobrevivência neuronal diz respeito à captação de glutamato da fenda sináptica, que além de proteger os

neurônios da excitotoxicidade, possui a função de convertê-lo em glutamina, por meio da enzima glutamina sintetase (GS), ou sintetizar glutationa (GSH), fornecendo proteção contra danos oxidativos (Dringen et al., 2015). No presente estudo, pode-se observar que os animais tratados com AA apresentaram uma redução na atividade da GS, acompanhada de um aumento no conteúdo de GSH, em 24 horas após a lesão, sugerindo que, frente a lesão cerebral aguda, o glutamato captado foi majoritariamente direcionado para atuar na proteção contra danos oxidativos.

Estudos mostram que o estresse oxidativo exerce um papel crucial na lesão cerebral após a HIC experimental (Hu et al., 2016; Nakamura et al., 2005). Em estudos clínicos, níveis sanguíneos elevados de marcadores para estresse oxidativo estão relacionados a piores desfechos funcionais (Chen et al., 2011) e à mortalidade a curto prazo (Alexandrova and Danovska, 2011). Os principais fatores que contribuem para a formação de espécies reativas e devem ser considerados neste trabalho incluem: a lise dos eritrócitos no hematoma que leva à liberação de heme, principal componente da hemoglobina, cuja degradação em ferro pela enzima heme-oxigenase gera produção abundante de EROs, resultando em neurotoxicidade; concentrações elevadas de S100B, que levam à morte celular por apoptose (Huttunen et al., 2000); a disfunção mitocondrial com consequente redução do metabolismo de oxigênio (Kim-Han et al., 2006); e, por fim, a ativação de células inflamatórias, tais como microglia/macrófagos, com consequente liberação de citocinas inflamatórias pelas mesmas, estimulando a produção de EROs (Zhang et al., 2017).

Neste trabalho, a HIC causou aumento na produção de EROs no estriado em 7 dias após a lesão, juntamente com o aumento dos níveis das citocinas inflamatórias TNF-α e IL-1β, afirmando a íntima relação existente entre inflamação e estresse oxidativo, já descrita na literatura (Duan et al., 2016), em que as EROs induzem o aumento da expressão de citocinas inflamatórias e as citocinas, por sua vez, favorecem a produção de espécies reativas, constituindo assim, mais um ciclo de *feedback* positivo (Khaper et al., 2010) que potencializa a lesão cerebral secundária, a morte neuronal e a disfunção neurológica na HIC (Duan et al., 2016). Nos animais tratados com AA, observou-se uma redução na formação de espécies reativas, associada à redução dos níveis de TNF-α e IL-1β, sugerindo ser esta uma das vias pelas quais o AA age, de forma a atenuar o estresse oxidativo e a reação inflamatória que resultam em morte neuronal após a HIC.

Sabe-se que a intensa reação inflamatória que ocorre após a HIC é marcada pela ativação da microglia residente, influxo de leucócitos no encéfalo e produção de mediadores inflamatórios, contribuindo significativamente na fisiopatologia da lesão secundária após o insulto hemorrágico (Mracsko and Veltkamp, 2014). As micróglias são as principais células responsáveis pela produção e secreção de citocinas inflamatórias no SNC. Em condições saudáveis, a microglia “em repouso” não sofre influência da S100B em níveis fisiológicos, devido à escassez ou ausência de receptores RAGE em sua superfície. Em situações de lesão cerebral, no entanto, a ativação da microglia é acompanhada pelo aumento na densidade de moléculas RAGE na superfície celular e, assim, a proteína S100B torna-se capaz de atrair quimicamente a microglia para o local da lesão, além de aumentar a produção e liberação de

citocinas inflamatórias (Lue et al., 2001). Ainda, demonstrou-se que a ligação de S100B a RAGE na microglia causa a ativação do fator de transcrição NF-κB, estimulando a atividade de transdução de RAGE e a expressão de genes pró-inflamatórios, além de regular positivamente a expressão da enzima pró-inflamatória ciclo-oxigenase 2 (COX-2) (Bianchi et al., 2010).

As análises de imunofluorescência realizadas no estriado em 72 horas e em 7 dias após a lesão para identificar microglia/macrófagos em torno da lesão, mostram um aumento dessas células em ambos os tempos nos animais não tratados. Dados da literatura indicam que este é o período de pico da ativação microglial após a HIC, a qual deve persistir por 3 a 4 semanas após o insulto (Gong et al., 2000; Wang et al., 2003; Yang et al., 2015). Além da ativação microglial, os níveis de IL-1β e TNF-α aumentaram significativamente no estriado em 7 dias após a lesão. De forma interessante, a inibição da proteína S100B através do AA preveniu a reatividade microglial no estriado parcialmente em 72 horas e completamente em 7 dias após a HIC. Corroborando com os nossos resultados, estudos prévios já haviam relatado os efeitos do AA na diminuição da ativação microglial na doença de Parkinson (Oki et al., 2008), Alzheimer (Mori et al., 2006) e glioma (Wang et al., 2013) em roedores. Ainda, no nosso estudo, a inibição da microglia foi acompanhada pela redução dos níveis de TNF-α e IL-1β em 7 dias após a lesão.

Estudos experimentais mostram que a inibição ou redução dos níveis de IL-1β e TNF-α podem diminuir os danos cerebrais e melhorar os desfechos funcionais após a HIC (Li et al., 2018; Ren et al., 2018). Tratamentos com agentes inibidores de TNF-α em ratos após HIC reduziram o volume do hematoma, o edema cerebral, a morte celular, e melhoraram os déficits

neurocomportamentais (Lei et al., 2013; Mayne et al., 2001a, 2001b). Em estudos prospectivos de coorte, pacientes com HIC que apresentaram altas concentrações plasmáticas de TNF-α foram associadas ao risco aumentado de mortalidade na unidade de terapia intensiva, à expansão do hematoma e ao mau prognóstico funcional (Fang et al., 2007; Silva et al., 2005). O aumento dos níveis de IL-1β também tem sido relacionado ao dano cerebral secundário na HIC, e a sua inibição atenuou a inflamação e a formação de edema cerebral em ratos submetidos à HIC (Masada et al., 2003, 2001).

Os efeitos do AA sobre as células microgliais confirmam que a S100B é uma forte indutora da ativação microglial e da liberação de citocinas inflamatórias na HIC, e sugerem, desta forma, que o AA possui potencial para atenuar a neuroinflamação através do rompimento do ciclo de citocinas que contribui no mecanismo de lesão cerebral secundária e resulta em aumento da morte celular e consequente agravamento da lesão (**Figura 4**).

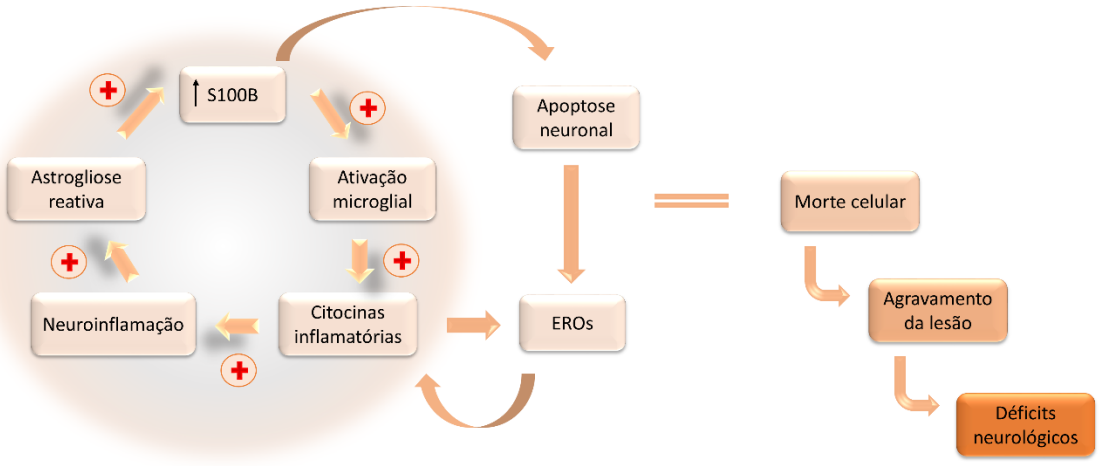

Figura 4. Representação esquemática do mecanismo de lesão secundária causado pelo aumento das concentrações extracelulares de S100B e sua influência na neuroinflamação, morte celular e aumento da severidade da hemorragia intracerebral.

A morte neuronal na HIC acontece principalmente por apoptose, necrose e autofagia (Keep et al., 2012). Neste trabalho, foi analisado o número de neurônios no estriado, assim como o número de células neuronais positivas para caspase-3 clivada, ou seja, neurônios em processo de apoptose, no sétimo dia após a HIC. Observou-se que o tratamento com AA preveniu a morte neuronal por apoptose, de forma a manter a densidade neuronal dos animais tratados semelhante à dos animais controle. Sabe-se que a ligação de S100B nos receptores RAGE dos neurônios é responsável tanto pelos seus efeitos neurotróficos (em baixas doses) quando pelos seus efeitos pró-apoptóticos (em altas doses), e que a apoptose neuronal culmina no aumento da produção de EROs (Huttunen et al., 2000). Corroborando com a literatura, este trabalho mostra que além da apoptose neuronal, também houve aumento na produção de EROs no estriado dos animais com HIC não tratados e que o AA reduziu tanto a morte neuronal como a consequente produção de EROs em 7 dias após a lesão, contribuindo para a redução de danos oxidativos e para a sobrevivência neuronal.

Como consequência da HIC, a formação do hematoma e a subsequente compressão das estruturas cerebrais levam à lesão mecânica de neurônios e células gliais, assim como à resposta inflamatória e deterioração neurológica (Enatsu et al., 2012). A expansão do hematoma ocorre principalmente durante as 3 primeiras horas após o insulto, podendo aumentar até 12 horas após o início dos sintomas (Qureshi et al., 2009). Os resultados deste trabalho sugerem que, juntos, os efeitos benéficos e neuroprotetores do AA resultaram na limitação da expansão da lesão hemorrágica estriatal e mais rápida reparação tecidual, conforme observado através das análises histológicas de

fatias cerebrais. Sabe-se que o estriado é uma estrutura relacionada ao controle da função motora (Graybiel and Grafton, 2015) e, portanto, a presença do hematoma intra-estriatal resulta em prejuízos neurológicos funcionais nos animais submetidos à HIC, conforme observado nas avaliações comportamentais realizadas neste estudo. A resolução da hemorragia observada nos animais que receberam AA possibilitou que estes apresentassem menos prejuízos funcionais do que os animais não tratados, o que foi confirmado pela preservação da funcionalidade dos membros para a marcha e prevenção da deterioração neurológica após a lesão.

6. CONCLUSÕES

O tratamento com ácido arúndico no modelo animal de hemorragia intracerebral, por meio da inibição da superexpressão de S100B, levou à atenuação da astrogliose reativa e da ativação microglial, com consequente redução dos níveis de citocinas inflamatórias e formação de espécies reativas de oxigênio, além de promover o aumento da produção de antioxidantes cerebrais pelos astrócitos. A união desses fatores culminou na prevenção da morte neuronal e na limitação da expansão do volume hemorrágico estriatal, com consequente preservação das funções motoras e prevenção da deterioração neurológica nos animais tratados.

Dessa forma, o presente trabalho torna evidente o papel deletério de níveis elevados da S100B no mecanismo de lesão secundária da HIC e a coloca como um potencial alvo terapêutico na busca de tratamentos para a doença. Neste sentido, o ácido arúndico mostrou ação neuroprotetora agindo em diferentes vias das cascatas de lesão secundária ocasionadas pela S100B, resultando na redução da severidade e na melhora dos desfechos neurológicos da HIC.

7. PERSPECTIVAS

1) Analisar os efeitos do tratamento prolongado com ácido arúndico (AA) após a hemorragia intracerebral (HIC), com maior número de administrações, via canulação intracerebroventricular.

2) Avaliar os efeitos do tratamento a longo prazo, a fim de verificar se os benefícios do AA se mantem após 4 semanas da última administração.

3) Incluir ratas fêmeas no estudo para analisar se o dimorfismo sexual influa na resposta ao tratamento.

8. REFERÊNCIAS

Abbott, N.J., Revest, P.A., Romero, I.A., 1992. Astrocyte-endothelial interaction: Physiology and pathology, in: Neuropathology and Applied Neurobiology. Neuropathol Appl Neurobiol, pp. 424–433. https://doi.org/10.1111/j.1365-2990.1992.tb00808.x

Alexandrova, M.L., Danovska, M.P., 2011. Serum C-reactive protein and lipid hydroperoxides in predicting short-term clinical outcome after spontaneous intracerebral hemorrhage. J. Clin. Neurosci. 18, 247–252. https://doi.org/10.1016/j.jocn.2010.07.125

Antonow-Schlorke, I., Ehrhardt, J., Knieling, M., 2013. Modification of the ladder rung walking task-new options for analysis of skilled movements. Stroke Res. Treat. 2013, 418627. https://doi.org/10.1155/2013/418627

Aronowski, J., Zhao, X., 2011. Molecular pathophysiology of cerebral hemorrhage: secondary brain injury. Stroke 42, 1781–6. https://doi.org/10.1161/STROKEAHA.110.596718

Asano, T., Mori, T., Shimoda, T., Shinagawa, R., Satoh, S., Yada, N., Katsumata, S., Matsuda, S., Kagamiishi, Y., Tateishi, N., 2005. Arundic acid (ONO-2506) ameliorates delayed ischemic brain damage by preventing astrocytic overproduction of S100B. Curr. Drug Targets. CNS Neurol. Disord. 4, 127–42. https://doi.org/10.2174/1568007053544084

Askenase, M.H., Sansing, L.H., Author, S.N., 2016. Stages of the Inflammatory Response in Pathology and Tissue Repair after Intracerebral Hemorrhage HHS Public Access Author manuscript. Semin Neurol 36, 288–297. https://doi.org/10.1055/s-0036-1582132

Babu, R., Bagley, J.H., Di, C., Friedman, A.H., Adamson, C., 2012. Thrombin and hemin as central factors in the mechanisms of intracerebral hemorrhage-induced secondary brain injury and as potential targets for intervention. Neurosurg. Focus 32. https://doi.org/10.3171/2012.1.FOCUS11366

Balami, J.S., Buchan, A.M., 2012. Complications of intracerebral haemorrhage. Lancet Neurol. https://doi.org/10.1016/S1474-4422(11)70264-2

Barratt, H.E., Lanman, T.A., Carmichael, S.T., 2014. Mouse intracerebral

hemorrhage models produce different degrees of initial and delayed damage, axonal sprouting, and recovery. J. Cereb. Blood Flow Metab. 34, 1463–1471. https://doi.org/10.1038/jcbfm.2014.107

Barreto, G.E., Gonzalez, J., Torres, Y., Morales, L., 2011. Astrocytic-neuronal crosstalk: Implications for neuroprotection from brain injury. Neurosci. Res. 71, 107–113. https://doi.org/10.1016/j.neures.2011.06.004

Bianchi, R., Giambanco, I., Donato, R., 2010. S100B/RAGE-dependent activation of microglia via NF-κB and AP-1: Co-regulation of COX-2 expression by S100B, IL-1β and TNF-α. Neurobiol. Aging 31, 665–677. https://doi.org/10.1016/J.NEUROBIOLAGING.2008.05.017

Bianchi, R., Kastrisianaki, E., Giambanco, I., Donato, R., 2011. S100B Protein Stimulates Microglia Migration via RAGE-dependent Up-regulation of Chemokine Expression and Release. J. Biol. Chem. 286, 7214–7226. https://doi.org/10.1074/jbc.M110.169342

Campbell, B.C.V., Khatri, P., 2020. Stroke. Lancet. https://doi.org/10.1016/S0140-6736(20)31179-X

Céspedes Rubio, Á.E., Pérez-Alvarez, M.J., Lapuente Chala, C., Wandosell, F., 2018. Sex steroid hormones as neuroprotective elements in ischemia models. J. Endocrinol. 237, R65–R81. https://doi.org/10.1530/JOE-18-0129

Chen, Y.C., Chen, C.M., Liu, J.L., Chen, S.T., Cheng, M.L., Chiu, D.T.Y., 2011. Oxidative markers in spontaneous intracerebral hemorrhage: Leukocyte 8-hydroxy-2′-deoxyguanosine as an independent predictor of the 30-day outcome: Clinical article. J. Neurosurg. 115, 1184–1190. https://doi.org/10.3171/2011.7.JNS11718

Chiu, C.-D., Yao, N.-W., Guo, J.-H., Shen, C.-C., Lee, H.-T., Chiu, Y.-P., Ji, H.-R., Chen, X., Chen, C.-C., Chang, C., 2017. Inhibition of astrocytic activity alleviates sequela in acute stages of intracerebral hemorrhage. Oncotarget 8, 94850–94861. https://doi.org/10.18632/oncotarget.22022

Cordeiro, J.L., Neves, J.D., Vizuete, A.F., Aristimunha, D., Pedroso, T.A., Sanches, E.F., Gonçalves, C.A., Netto, C.A., 2020. Arundic Acid (ONO-2506), an Inhibitor of S100B Protein Synthesis, Prevents Neurological Deficits and Brain Tissue Damage Following Intracerebral Hemorrhage in Male Wistar Rats. Neuroscience 440, 97–112. https://doi.org/10.1016/j.neuroscience.2020.05.030

Delgado, P., Alvarez Sabin, J., Santamarina, E., Molina, C.A., Quintana, M., Rosell, A., Montaner, J., 2006. Plasma S100B Level After Acute Spontaneous Intracerebral Hemorrhage. Stroke 37, 2837–2839. https://doi.org/10.1161/01.STR.0000245085.58807.ad

Diao, X., Zhou, Z., Xiang, W., Jiang, Y., Tian, N., Tang, X., Chen, S., Wen, J., Chen, M., Liu, K., Li, Q., Liao, R., 2020. Glutathione alleviates acute intracerebral hemorrhage injury via reversing mitochondrial dysfunction. Brain Res. 1727. https://doi.org/10.1016/j.brainres.2019.146514

Donato, R., Sorci, G., Riuzzi, F., Arcuri, C., Bianchi, R., Brozzi, F., Tubaro, C., Giambanco, I., 2009. S100B's double life: Intracellular regulator and extracellular signal. Biochim. Biophys. Acta - Mol. Cell Res. 1793, 1008–1022. https://doi.org/10.1016/J.BBAMCR.2008.11.009

Dowlatshahi, D., Demchuk, A.M., Flaherty, M.L., Ali, M., Lyden, P.L., Smith, E.E., 2011. Defining hematoma expansion in intracerebral hemorrhage: Relationship with patient outcomes. Neurology 76, 1238–1244. https://doi.org/10.1212/WNL.0b013e3182143317

Dringen, R., Brandmann, M., Hohnholt, M.C., Blumrich, E.-M., 2015. Glutathione-Dependent Detoxification Processes in Astrocytes. Neurochem. Res. 40, 2570–2582. https://doi.org/10.1007/s11064-014-1481-1

Duan, X., Wen, Z., Shen, H., Shen, M., Chen, G., 2016. Intracerebral Hemorrhage, Oxidative Stress, and Antioxidant Therapy. Oxid. Med. Cell. Longev. 2016, 1203285. https://doi.org/10.1155/2016/1203285

Dutra, F.F., Bozza, M.T., 2014. Heme on innate immunity and inflammation. Front. Pharmacol. 5, 115. https://doi.org/10.3389/fphar.2014.00115

Eid, T., Gruenbaum, S.E., Dhaher, R., Lee, T.-S.W., Zhou, Y., Danbolt, N.C., 2016. The Glutamate–Glutamine Cycle in Epilepsy, in: Advances in Neurobiology. pp. 351–400. https://doi.org/10.1007/978-3-319-45096-4_14

Eid, T., Lee, T.-S.W., Patrylo, P., Zaveri, H.P., 2018. Astrocytes and Glutamine Synthetase in Epileptogenesis. J. Neurosci. Res. https://doi.org/10.1002/jnr.24267

Emsley, H.C.A., Tyrrell, P.J., 2002. Inflammation and infection in clinical stroke. J. Cereb. Blood Flow Metab. https://doi.org/10.1097/01.WCB.0000037880.62590.28

Enatsu, R., Asahi, M., Matsumoto, M., Hirai, O., 2012. Prognostic factors of motor recovery after stereotactic evacuation of intracerebral hematoma. Tohoku J. Exp. Med. 227, 63–7. https://doi.org/https://doi.org/10.1620/tjem.227.63

Engler-Chiurazzi, E.B., Brown, C.M., Povroznik, J.M., Simpkins, J.W., 2017. Estrogens as neuroprotectants: Estrogenic actions in the context of cognitive aging and brain injury. Prog. Neurobiol. 157, 188. https://doi.org/10.1016/J.PNEUROBIO.2015.12.008

Esposito, G., De Filippis, D., Cirillo, C., Sarnelli, G., Cuomo, R., Iuvone, T., 2006. The astroglial-derived S100β protein stimulates the expression of nitric oxide synthase in rodent macrophages through p38 MAP kinase activation. Life Sci. 78, 2707–2715. https://doi.org/10.1016/j.lfs.2005.10.023

Fang, H.-Y., Ko, W.-J., Lin, C.-Y., 2007. Inducible heat shock protein 70, interleukin-18, and tumor necrosis factor alpha correlate with outcomes in spontaneous intracerebral hemorrhage. J. Clin. Neurosci. 14, 435–441. https://doi.org/10.1016/j.jocn.2005.12.022

Ferrete-Araujo, A.M., Rodríguez-Rodríguez, A., Egea-Guerrero, J.J., Vilches-Arenas, Á., Godoy, D.A., Murillo-Cabezas, F., 2019. Brain Injury Biomarker Behavior in Spontaneous Intracerebral Hemorrhage. World Neurosurg. 132, e496–e505. https://doi.org/10.1016/j.wneu.2019.08.090

Figueiredo, R.T., Fernandez, P.L., Mourao-Sa, D.S., Porto, B.N., Dutra, F.F., Alves, L.S., Oliveira, M.F., Oliveira, P.L., Graça-Souza, A. V., Bozza, M.T., 2007. Characterization of heme as activator of toll-like receptor 4. J. Biol. Chem. 282, 20221–20229. https://doi.org/10.1074/jbc.M610737200

Fiorella, D., Zuckerman, S.L., Khan, I.S., Ganesh Kumar, N., Mocco, J., 2015. Intracerebral Hemorrhage: A Common and Devastating Disease in Need of Better Treatment. World Neurosurg. 84, 1136–1141. https://doi.org/10.1016/J.WNEU.2015.05.063

Foerch, C., Niessner, M., Back, T., Bauerle, M., De Marchis, G.M., Ferbert, A., Grehl, H., Hamann, G.F., Jacobs, A., Kastrup, A., Klimpe, S., Palm, F., Thomalla, G., Worthmann, H., Sitzer, M., BE FAST Study Group, 2012. Diagnostic Accuracy of Plasma Glial Fibrillary Acidic Protein for Differentiating Intracerebral Hemorrhage and Cerebral Ischemia in Patients with Symptoms of Acute Stroke. Clin. Chem. 58, 237–245.

https://doi.org/10.1373/clinchem.2011.172676

Gao, Z., Wang, J., Thiex, R., Rogove, A.D., Heppner, F.L., Tsirka, S.E., 2008. Microglial activation and intracerebral hemorrhage. Acta Neurochir. Suppl. 105, 51–3.

Garton, A.L.A., Gupta, V.P., Sudesh, S., Zhou, H., Christophe, B.R., Connolly, E.S., 2020. The Intracerebral Hemorrhage Score: Changing Perspectives on Mortality and Disability. World Neurosurg. 135, e573–e579. https://doi.org/10.1016/j.wneu.2019.12.074

Gebel, J.M., Jauch, E.C., Brott, T.G., Khoury, J., Sauerbeck, L., Salisbury, S., Spilker, J., Tomsick, T.A., Duldner, J., Broderick, J.P., 2002. Natural history of perihematomal edema in patients with hyperacute spontaneous intracerebral hemorrhage. Stroke 33, 2631–2635. https://doi.org/10.1161/01.STR.0000035284.12699.84

Gong, C., Hoff, J.T., Keep, R.F., 2000. Acute inflammatory reaction following experimental intracerebral hemorrhage in rat. Brain Res. 871, 57–65. https://doi.org/10.1016/S0006-8993(00)02427-6

Graybiel, A.M., Grafton, S.T., 2015. The striatum: where skills and habits meet. Cold Spring Harb. Perspect. Biol. 7, a021691. https://doi.org/10.1101/cshperspect.a021691

Griffin, W.S.T., Sheng, J.G., Royston, M.C., Gentleman, S.M., McKenzie, J.E., Graham, D.I., Roberts, G.W., Mrak, R.E., 2006. Glial-Neuronal Interactions in Alzheimer's Disease: The Potential Role of a 'Cytokine Cycle' in Disease Progression. Brain Pathol. 8, 65–72. https://doi.org/10.1111/j.1750-3639.1998.tb00136.x

Hanada, M., Shinjo, R., Miyagi, M., Yasuda, T., Tsutsumi, K., Sugiura, Y., Imagama, S., Ishiguro, N., Matsuyama, Y., 2014. Arundic acid (ONO-2506) inhibits secondary injury and improves motor function in rats with spinal cord injury. J. Neurol. Sci. 337, 186–192. https://doi.org/10.1016/j.jns.2013.12.008

Higashino, H., Niwa, A., Satou, T., Ohta, Y., Hashimoto, S., Tabuchi, M., Ooshima, K., 2009. Immunohistochemical analysis of brain lesions using S100B and glial fibrillary acidic protein antibodies in arundic acid- (ONO-2506) treated stroke-prone spontaneously hypertensive rats. J. Neural Transm. 116, 1209–1219. https://doi.org/10.1007/s00702-009-0278-x

Hofmann, M.A., Drury, S., Fu, C., Qu, W., Taguchi, A., Lu, Y., Avila, C., Kambham, N., Bierhaus, A., Nawroth, P., Neurath, M.F., Slattery, T., Beach, D., McClary, J., Nagashima, M., Morser, J., Stern, D., Schmidt, A.M., 1999. RAGE mediates a novel proinflammatory axis: A central cell surface receptor for S100/calgranulin polypeptides. Cell 97, 889–901. https://doi.org/10.1016/S0092-8674(00)80801-6

Hu, J., Ferreira, A., Van Eldik, L.J., 2002. S100β Induces Neuronal Cell Death Through Nitric Oxide Release from Astrocytes. J. Neurochem. 69, 2294–2301. https://doi.org/10.1046/j.1471-4159.1997.69062294.x

Hu, J., Ferreira, A., Van Eldik, L.J., 1997. S100beta induces neuronal cell death through nitric oxide release from astrocytes. J. Neurochem. 69, 2294–301. https://doi.org/10.1046/j.1471-4159.1997.69062294.x

Hu, W., Zhou, P., Rao, T., Zhang, X., Wang, W., Zhang, L., 2015. Adrenomedullin attenuates interleukin-1β-induced inflammation and apoptosis in rat Leydig cells via inhibition of NF-κB signaling pathway. Exp. Cell Res. 339, 220–230. https://doi.org/10.1016/j.yexcr.2015.10.024

Hu, X., Tao, C., Gan, Q., Zheng, J., Li, H., You, C., 2016. Oxidative Stress in Intracerebral Hemorrhage: Sources, Mechanisms, and Therapeutic Targets. Oxid. Med. Cell. Longev. 2016, 3215391. https://doi.org/10.1155/2016/3215391

Hu, Y.-Y., Dong, X.-Q., Yu, W.-H., Zhang, Z.-Y., 2010. CHANGE IN PLASMA S100B LEVEL AFTER ACUTE SPONTANEOUS BASAL GANGLIA HEMORRHAGE. Shock 33, 134–140. https://doi.org/10.1097/SHK.0b013e3181ad5c88

Huang, M., Dong, X.-Q., Hu, Y.-Y., Yu, W.-H., Zhang, Z.-Y., 2010. High S100B levels in cerebrospinal fluid and peripheral blood of patients with acute basal ganglial hemorrhage are associated with poor outcome. World J. Emerg. Med. 1, 22–31.

Huttunen, H.J., Kuja-Panula, J., Sorci, G., Lisa Agneletti, A., Donato, R., Rauvala, H., 2000. Coregulation of Neurite Outgrowth and Cell Survival by Amphoterin and S100 Proteins through Receptor for Advanced Glycation End Products (RAGE) Activation*. https://doi.org/10.1074/jbc.M006993200

Inaji, M., Tomita, H., Tone, O., Tamaki, M., Suzuki, R., Ohno, K., 2003. Chronological changes of perihematomal edema of human intracerebral

hematoma. Acta Neurochir. Suppl. 445–448. https://doi.org/10.1007/978-3-7091-0651-8_91

Ishiguro, H., Kaito, T., Hashimoto, K., Kushioka, J., Okada, R., Tsukazaki, H., Kodama, J., Bal, Z., Ukon, Y., Takenaka, S., Makino, T., Sakai, Y., Yoshikawa, H., 2019. Administration of ONO-2506 suppresses neuropathic pain after spinal cord injury by inhibition of astrocytic activation. Spine J. 19, 1434–1442. https://doi.org/10.1016/j.spinee.2019.04.006

James, M.L., Blessing, R., Phillips-Bute, B.G., Bennett, E., Laskowitz, D.T., 2009. S100B and brain natriuretic peptide predict functional neurological outcome after intracerebral haemorrhage. Biomarkers 14, 388–94. https://doi.org/10.1080/13547500903015784

James, M.L., Warner, D.S., Laskowitz, D.T., 2008. Preclinical models of intracerebral hemorrhage: A translational perspective. Neurocrit. Care 9, 139–152. https://doi.org/10.1007/s12028-007-9030-2

Jeyasingham, R.., Baird, A.L., Meldrum, A., Dunnett, S.B., 2001. Differential effects of unilateral striatal and nigrostriatal lesions on grip strength, skilled paw reaching and drug-induced rotation in the rat. Brain Res. Bull. 55, 541–548. https://doi.org/10.1016/S0361-9230(01)00557-3

Kanner, A.A., Marchi, N., Fazio, V., Mayberg, M.R., Koltz, M.T., Siomin, V., Stevens, G.H.J., Masaryk, T., Ayumar, B., Vogelbaum, M.A., Barnett, G.H., Janigro, D., Janigro, D., 2003. Serum S100beta: a noninvasive marker of blood-brain barrier function and brain lesions. Cancer 97, 2806–2813. https://doi.org/10.1002/cncr.11409

Kapural, M., Krizanac-Bengez, L., Barnett, G., Perl, J., Masaryk, T., Apollo, D., Rasmussen, P., Mayberg, M.R., Janigro, D., 2002. Serum S-100beta as a possible marker of blood-brain barrier disruption. Brain Res. 940, 102–4.

Kato, H., Kurosaki, R., Oki, C., Araki, T., 2004. Arundic acid, an astrocyte-modulating agent, protects dopaminergic neurons against MPTP neurotoxicity in mice. Brain Res. 1030, 66–73. https://doi.org/10.1016/j.brainres.2004.09.046

Keep, R.F., Hua, Y., Xi, G., 2012. Intracerebral haemorrhage: mechanisms of injury and therapeutic targets. https://doi.org/10.1016/S1474-4422(12)70104-7

Keep, R.F., Xiang, J., Ennis, S.R., Andjelkovic, A., Hua, Y., Xi, G., Hoff, J.T.,

2008. Blood-brain barrier function in intracerebral hemorrhage. Acta Neurochir. Suppl. https://doi.org/10.1007/978-3-211-09469-3_15

Khaper, N., Bryan, S., Dhingra, S., Singal, R., Bajaj, A., Pathak, C.M., Singal, P.K., 2010. Targeting the Vicious Inflammation–Oxidative Stress Cycle for the Management of Heart Failure. Antioxid. Redox Signal. 13, 1033–1049. https://doi.org/10.1089/ars.2009.2930

Kim-Han, J.S., Kopp, S.A., Dugan, L.L., Diringer, M.N., 2006. Perihematomal mitochondrial dysfunction after intracerebral hemorrhage. Stroke 37, 2457–2462. https://doi.org/10.1161/01.STR.0000240674.99945.4e

Kim, S.H., Smith, C.J., Van Eldik, L.J., 2004. Importance of MAPK pathways for microglial pro-inflammatory cytokine IL-1β production. Neurobiol. Aging 25, 431–439. https://doi.org/10.1016/S0197-4580(03)00126-X

Kim, T., Chelluboina, B., Chokkalla, A.K., 2019. Age and sex differences in the pathophysiology of acute CNS injury. Neurochem. Int. 127, 22–28. https://doi.org/10.1016/J.NEUINT.2019.01.012

Kumar, A., Kumar, P., Misra, S., Sagar, R., Kathuria, P., Vibha, D., Vivekanandhan, S., Garg, A., Kaul, B., Raghvan, S., Gorthi, S.P., Dabla, S., Aggarwal, C.S., Prasad, K., 2015. Biomarkers to enhance accuracy and precision of prediction of short-term and long-term outcome after spontaneous intracerebral haemorrhage : a study protocol for a prospective cohort study. BMC Neurol. 4–9. https://doi.org/10.1186/s12883-015-0384-3

Labovitz, D.L., Halim, A., Boden-Albala, B., Hauser, W.A., Sacco, R.L., 2005. The incidence of deep and lobar intracerebral hemorrhage in whites, blacks, and Hispanics. Neurology 65, 518–522. https://doi.org/10.1212/01.wnl.0000172915.71933.00

LeBel, C.P., Ischiropoulos, H., Bondy, S.C., 1992. Evaluation of the probe 2',7'-dichlorofluorescin as an indicator of reactive oxygen species formation and oxidative stress. Chem. Res. Toxicol. 5, 227–31.

Lei, B., Dawson, H.N., Roulhac-Wilson, B., Wang, H., Laskowitz, D.T., James, M.L., 2013. Tumor necrosis factor alpha antagonism improves neurological recovery in murine intracerebral hemorrhage, Journal of Neuroinflammation. https://doi.org/10.1186/1742-2094-10-103

Lewerenz, J., Maher, P., 2015. Chronic glutamate toxicity in neurodegenerative diseases-What is the evidence? Front. Neurosci.

https://doi.org/10.3389/fnins.2015.00469

Li, X., Wang, T., Zhang, D., Li, H., Shen, H., Ding, X., Chen, G., 2018. Andrographolide ameliorates intracerebral hemorrhage induced secondary brain injury by inhibiting neuroinflammation induction. Neuropharmacology 141, 305–315. https://doi.org/10.1016/j.neuropharm.2018.09.015

Lin, S., Yin, Q., Zhong, Q., Lv, F.-L., Zhou, Y., Li, J.-Q., Wang, J.-Z., Su, B., Yang, Q.-W., 2012a. Heme activates TLR4-mediated inflammatory injury via MyD88/TRIF signaling pathway in intracerebral hemorrhage. J. Neuroinflammation 9, 548. https://doi.org/10.1186/1742-2094-9-46

Lin, S., Yin, Q., Zhong, Q., Lv, F.-L., Zhou, Y., Li, J.-Q., Wang, J.-Z., Su, B., Yang, Q.-W., 2012b. Heme activates TLR4-mediated inflammatory injury via MyD88/TRIF signaling pathway in intracerebral hemorrhage. J. Neuroinflammation 9, 548. https://doi.org/10.1186/1742-2094-9-46

Liu, D.Z., Ander, B.P., Xu, H., Shen, Y., Kaur, P., Deng, W., Sharp, F.R., 2010. Blood-brain barrier breakdown and repair by Src after thrombin-induced injury. Ann. Neurol. 67, 526–533. https://doi.org/10.1002/ana.21924

Lue, L.-F., Walker, D.G., Brachova, L., Beach, T.G., Rogers, J., Schmidt, A.M., Stern, D.M., Yan, S. Du, 2001. Involvement of Microglial Receptor for Advanced Glycation Endproducts (RAGE) in Alzheimer's Disease: Identification of a Cellular Activation Mechanism. Exp. Neurol. 171, 29–45. https://doi.org/10.1006/exnr.2001.7732

MacLellan, C.L., Silasi, G., Auriat, A.M., Colbourne, F., 2010. Rodent models of intracerebral hemorrhage, in: Stroke. Stroke. https://doi.org/10.1161/STROKEAHA.110.594457

Maclellan, C.L., Silasi, G., Poon, C.C., Edmundson, C.L., Buist, R., Peeling, J., Colbourne, F., 2008. Intracerebral hemorrhage models in rat : comparing collagenase to blood infusion 516–525. https://doi.org/10.1038/sj.jcbfm.9600548

Mahesh, V.B., Dhandapani, K.M., Brann, D.W., 2006. Role of astrocytes in reproduction and neuroprotection. Mol. Cell. Endocrinol. 246, 1–9. https://doi.org/10.1016/j.mce.2005.11.017

Manno, E.M., 2012. Update on Intracerebral Hemorrhage. Contin. Lifelong Learn. Neurol. 18, 598–610. https://doi.org/10.1212/01.CON.0000415430.99394.3e

Mari, C., Odorcyk, F.K., Sanches, E.F., Wartchow, K.M., Martini, A.P., Nicola, F., Zanotto, C., Wyse, A.T., Gonçalves, C.A., Netto, C.A., 2019. Arundic acid administration protects astrocytes, recovers histological damage and memory deficits induced by neonatal hypoxia ischemia in rats. Int. J. Dev. Neurosci. 76, 41–51. https://doi.org/10.1016/j.ijdevneu.2019.06.003

Masada, T., Hua, Y., Xi, G., Yang, G.-Y., Hoff, J.T., Keep, R.F., 2001. Attenuation of intracerebral hemorrhage and thrombin-induced brain edema by overexpression of interleukin-1 receptor antagonist. J. Neurosurg. 95, 680–686. https://doi.org/10.3171/jns.2001.95.4.0680

Masada, T., Hua, Y., Xi, G., Yang, G.Y., Hoff, J.T., Keep, R.F., Nagao, S., 2003. Overexpression of interleukin-1 receptor antagonist reduces brain edema induced by intracerebral hemorrhage and thrombin. Acta Neurochir. Suppl. 86, 463–7.

Matsui, T., Mori, T., Tateishi, N., Kagamiishi, Y., Satoh, S., Katsube, N., Morikawa, E., Morimoto, T., Ikuta, F., Asano, T., 2002. Astrocytic Activation and Delayed Infarct Expansion after Permanent Focal Ischemia in Rats. Part I: Enhanced Astrocytic Synthesis of S-100β in the Periinfarct Area Precedes Delayed Infarct Expansion. J. Cereb. Blood Flow Metab. 22, 711–722. https://doi.org/10.1097/00004647-200206000-00010

Mayne, M., Fotheringham, J., Yan, H.J., Power, C., Del Bigio, M.R., Peeling, J., Geiger, J.D., 2001a. Adenosine A2A receptor activation reduces proinflammatory events and decreases cell death following intracerebral hemorrhage. Ann. Neurol. 49, 727–35.

Mayne, M., Ni, W., Yan, H.J., Xue, M., Johnston, J.B., Del Bigio, M.R., Peeling, J., Power, C., 2001b. Antisense oligodeoxynucleotide inhibition of tumor necrosis factor-alpha expression is neuroprotective after intracerebral hemorrhage. Stroke 32, 240–8.

Mendelow, A.D., Gregson, B.A., Mitchell, P.M., Murray, G.D., Rowan, E.N., Gholkar, A.R., 2011. Surgical Trial in Lobar Intracerebral Haemorrhage (STICH II) Protocol. Trials 12. https://doi.org/10.1186/1745-6215-12-124

Mestriner, R.G., Pagnussat, A.S., Boisserand, L.S.B., Valentim, L., Netto, C.A., 2011. Skilled reaching training promotes astroglial changes and facilitated sensorimotor recovery after collagenase-induced intracerebral hemorrhage. Exp. Neurol. 227, 53–61. https://doi.org/10.1016/j.expneurol.2010.09.009

Metz, G.A., Whishaw, I.Q., 2002. Cortical and subcortical lesions impair skilled walking in the ladder rung walking test: A new task to evaluate fore- and hindlimb stepping, placing, and co-ordination. J. Neurosci. Methods 115, 169–179. https://doi.org/10.1016/S0165-0270(02)00012-2

Min, H., Hong, J., Cho, I.H., Jang, Y.H., Lee, H., Kim, D., Yu, S.W., Lee, S., Lee, S.J., 2015. TLR2-induced astrocyte MMP9 activation compromises the blood brain barrier and exacerbates intracerebral hemorrhage in animal models. Mol. Brain 8. https://doi.org/10.1186/s13041-015-0116-z

Mori, T., Tateishi, N., Kagamiishi, Y., Shimoda, T., Satoh, S., Ono, S., Katsube, N., Asano, T., 2004. Attenuation of a delayed increase in the extracellular glutamate level in the peri-infarct area following focal cerebral ischemia by a novel agent ONO-2506. Neurochem. Int. 45, 381–387. https://doi.org/10.1016/j.neuint.2003.06.001

Mori, T., Town, T., Tan, J., Tateishi, N., Asano, T., 2005. Modulation of astrocytic activation by arundic acid (ONO-2506) mitigates detrimental effects of the apolipoprotein E4 isoform after permanent focal ischemia in apolipoprotein E knock-in mice. J. Cereb. Blood Flow Metab. 25, 748–762. https://doi.org/10.1038/sj.jcbfm.9600063

Mori, T., Town, T., Tan, J., Yada, N., Horikoshi, Y., Yamamoto, J., Shimoda, T., Kamanaka, Y., Tateishi, N., Asano, T., 2006. Arundic Acid ameliorates cerebral amyloidosis and gliosis in Alzheimer transgenic mice. J. Pharmacol. Exp. Ther. 318, 571–578. https://doi.org/10.1124/jpet.106.105171

Mracsko, E., Veltkamp, R., 2014. Neuroinflammation after intracerebral hemorrhage. Front. Cell. Neurosci. 8, 388. https://doi.org/10.3389/fncel.2014.00388

Nakamura, T., Keep, R.F., Hua, Y., Hoff, J.T., Xi, G., 2005. Oxidative DNA injury after experimental intracerebral hemorrhage. Brain Res. 1039, 30–36. https://doi.org/10.1016/j.brainres.2005.01.036

Nedergaard, M., Takano, T., Hansen, A.J., 2002. Beyond the role of glutamate as a neurotransmitter. Nat. Rev. Neurosci. 3, 748–755. https://doi.org/10.1038/nrn916

Neves, J.D., Aristimunha, D., Vizuete, A.F., Nicola, F., Vanzela, C., Petenuzzo, L., Mestriner, R.G., Sanches, E.F., Gonçalves, C.A., Netto, C.A., 2017.

Glial-associated changes in the cerebral cortex after collagenase-induced intracerebral hemorrhage in the rat striatum. Brain Res. Bull. 134, 55–62. https://doi.org/10.1016/j.brainresbull.2017.07.002

Neves, J.D., Vizuete, A.F., Nicola, F., Da Ré, C., Rodrigues, A.F., Schmitz, F., Mestriner, R.G., Aristimunha, D., Wyse, A.T.S., Netto, C.A., 2018. Glial glutamate transporters expression, glutamate uptake, and oxidative stress in an experimental rat model of intracerebral hemorrhage. Neurochem. Int. 116, 13–21. https://doi.org/10.1016/j.neuint.2018.03.003

Nicola, F.C., Rodrigues, L.P., Crestani, T., Quintiliano, K., Sanches, E.F., Willborn, S., Aristimunha, D., Boisserand, L., Pranke, P., Netto, C.A., Nicola, F.C., Rodrigues, L.P., Crestani, T., Quintiliano, K., Sanches, E.F., Willborn, S., Aristimunha, D., Boisserand, L., Pranke, P., Netto, C.A., 2016. Human dental pulp stem cells transplantation combined with treadmill training in rats after traumatic spinal cord injury. Brazilian J. Med. Biol. Res. 49. https://doi.org/10.1590/1414-431x20165319

Nishino, A., Suzuki, M., Ohtani, H., Motohashi, O., Umezawa, K., Nagura, H., Yoshimoto, T., 1993. Thrombin may contribute to the pathophysiology of central nervous system injury. J. Neurotrauma 10, 167–79. https://doi.org/10.1089/neu.1993.10.167

Ohtani, R., Tomimoto, H., Wakita, H., Kitaguchi, H., Nakaji, K., Takahashi, R., 2007. Expression of S100 protein and protective effect of arundic acid on the rat brain in chronic cerebral hypoperfusion. Brain Res. 1135, 195–200. https://doi.org/10.1016/j.brainres.2006.11.084

Oki, C., Watanabe, Y., Yokoyama, H., Shimoda, T., Kato, H., Araki, T., 2008. Delayed treatment with arundic acid reduces the MPTP-induced neurotoxicity in mice. Cell. Mol. Neurobiol. 28, 417–430. https://doi.org/10.1007/s10571-007-9241-2

Paxinos, G., Watson, C., 2007. The rat brain in stereotaxic coordinates. Elsevier.

Pettigrew, L.C., Kasner, S.E., Albers, G.W., Gorman, M., Grotta, J.C., Sherman, D.G., Funakoshi, Y., Ishibashi, H., 2006a. Safety and tolerability of arundic acid in acute ischemic stroke. J. Neurol. Sci. 251, 50–56. https://doi.org/10.1016/j.jns.2006.09.001

Pettigrew, L.C., Kasner, S.E., Gorman, M., Atkinson, R.P., Funakoshi, Y.,

Ishibashi, H., 2006b. Effect of arundic acid on serum S-100β in ischemic stroke. J. Neurol. Sci. 251, 57–61. https://doi.org/10.1016/j.jns.2006.09.002

Ponath, G., Schettler, C., Kaestner, F., Voigt, B., Wentker, D., Arolt, V., Rothermundt, M., 2007. Autocrine S100B effects on astrocytes are mediated via RAGE. J. Neuroimmunol. 184, 214–222. https://doi.org/10.1016/j.jneuroim.2006.12.011

Poon, M.T.C., Fonville, A.F., Salman, R.A.S., 2014. Long-term prognosis after intracerebral haemorrhage: Systematic review and meta-analysis. J. Neurol. Neurosurg. Psychiatry 85, 660–667. https://doi.org/10.1136/jnnp-2013-306476

Provencio, J.J., Ferreira Da Silva, I.R., Manno, E.M., 2013. Intracerebral Hemorrhage. New Challenges and Steps Forward. Neurosurg. Clin. N. Am. https://doi.org/10.1016/j.nec.2013.03.002

Qiao, H.-B., Li, J., Lv, L.-J., Nie, B.-J., Lu, P., Xue, F., Zhang, Z.-M., 2018. Eupatilin inhibits microglia activation and attenuates brain injury in intracerebral hemorrhage. Exp. Ther. Med. 16, 4005–4009. https://doi.org/10.3892/etm.2018.6699

Qu, J., Chen, W., Hu, R., Feng, H., 2016. The Injury and Therapy of Reactive Oxygen Species in Intracerebral Hemorrhage Looking at Mitochondria. Oxid. Med. Cell. Longev. 2016, 1–9. https://doi.org/10.1155/2016/2592935

Qureshi, A.I., Mendelow, A.D., Hanley, D.F., 2009. Intracerebral haemorrhage. Lancet (London, England) 373, 1632–44. https://doi.org/10.1016/S0140-6736(09)60371-8

Qureshi, A.I., Suri, M.F.K., Ostrow, P.T., Kim, S.H., Ali, Z., Shatla, A.A., Guterman, L.R., Hopkins, L.N., 2003. Apoptosis as a Form of Cell Death in Intracerebral Hemorrhage. Neurosurgery 52, 1041–1048. https://doi.org/10.1093/neurosurgery/52.5.1041

Qureshi, A.I., Tuhrim, S., Broderick, J.P., Batjer, H.H., Hondo, H., Hanley, D.F., 2001. Spontaneous intracerebral hemorrhage. N. Engl. J. Med. https://doi.org/10.1056/NEJM200105103441907

Ren, H., Kong, Y., Liu, Z., Zang, D., Yang, X., Wood, K., Li, M., Liu, Q., 2018. Selective NLRP3 (Pyrin Domain–Containing Protein 3) Inflammasome Inhibitor Reduces Brain Injury After Intracerebral Hemorrhage. Stroke 49, 184–192. https://doi.org/10.1161/STROKEAHA.117.018904

Righy, C., Bozza, M.T., Oliveira, M.F., Bozza, F.A., 2016. Molecular, Cellular and Clinical Aspects of Intracerebral Hemorrhage: Are the Enemies Within? Curr. Neuropharmacol. 14, 392–402. https://doi.org/10.2174/1570159X14666151230110058

Rosand, J., Hylek, E.M., O'Donnell, H.C., Greenberg, S.M., 2000. Warfarin-associated hemorrhage and cerebral amyloid angiopathy: A genetic and pathologic study. Neurology 55, 947–951. https://doi.org/10.1212/WNL.55.7.947

Schlunk, F., Greenberg, S.M., 2015. The Pathophysiology of Intracerebral Hemorrhage Formation and Expansion. Transl. Stroke Res. 6, 257–263. https://doi.org/10.1007/s12975-015-0410-1

Sen, J., Belli, A., 2007. S100B in neuropathologic states: The CRP of the brain? J. Neurosci. Res. 85, 1373–1380. https://doi.org/10.1002/jnr.21211

Senn, R., Elkind, M.S. V, Montaner, J., Christ-Crain, M., Katan, M., 2014. Potential role of blood biomarkers in the management of nontraumatic intracerebral hemorrhage. Cerebrovasc. Dis. 38, 395–409. https://doi.org/10.1159/000366470

Sharp, F., Liu, D.Z., Zhan, X., Ander, B.P., 2008. Intracerebral hemorrhage injury mechanisms: Glutamate neurotoxicity, thrombin, and Src. Acta Neurochir. Suppl. https://doi.org/10.1007/978-3-211-09469-3_9

Shiratori, M., Tozaki-Saitoh, H., Yoshitake, M., Tsuda, M., Inoue, K., 2010. P2X7 receptor activation induces CXCL2 production in microglia through NFAT and PKC/MAPK pathways. J. Neurochem. 114, 810–819. https://doi.org/10.1111/j.1471-4159.2010.06809.x

Silva, Y., Leira, R., Tejada, J., Lainez, J.M., Castillo, J., Dávalos, A., Stroke Project, Cerebrovascular Diseases Group of the Spanish Neurological Society, 2005. Molecular Signatures of Vascular Injury Are Associated With Early Growth of Intracerebral Hemorrhage. Stroke 36, 86–91. https://doi.org/10.1161/01.STR.0000149615.51204.0b

Sinha, K., Das, J., Pal, P.B., Sil, P.C., 2013. Oxidative stress: the mitochondria-dependent and mitochondria-independent pathways of apoptosis. Arch. Toxicol. 87, 1157–1180. https://doi.org/10.1007/s00204-013-1034-4

Sofroniew, M. V., 2009. Molecular dissection of reactive astrogliosis and glial scar formation. Trends Neurosci. 32, 638–647.

https://doi.org/10.1016/j.tins.2009.08.002

Sofroniew, M. V., Vinters, H. V., 2010a. Astrocytes: biology and pathology. Acta Neuropathol. 119, 7–35. https://doi.org/10.1007/s00401-009-0619-8

Sofroniew, M. V., Vinters, H. V., 2010b. Astrocytes: biology and pathology. Acta Neuropathol. 119, 7. https://doi.org/10.1007/S00401-009-0619-8

Sorci, G., Bianchi, R., Riuzzi, F., Tubaro, C., Arcuri, C., Giambanco, I., Donato, R., 2010. S100B protein, a damage-associated molecular pattern protein in the brain and heart, and beyond. Cardiovasc. Psychiatry Neurol. 2010. https://doi.org/10.1155/2010/656481

Sukumari-Ramesh, S., Alleyne, C.H., Dhandapani, K.M., 2012a. Astrogliosis: a Target for Intervention in Intracerebral Hemorrhage? Transl. Stroke Res. 3, 80–87. https://doi.org/10.1007/s12975-012-0165-x

Sukumari-Ramesh, S., Alleyne, C.H., Dhandapani, K.M., 2012b. Astrocyte-Specific Expression of Survivin after Intracerebral Hemorrhage in Mice: A Possible Role in Reactive Gliosis? J. Neurotrauma 29, 2798–2804. https://doi.org/10.1089/neu.2011.2243

Takano, T., Tian, G.F., Peng, W., Lou, N., Libionka, W., Han, X., Nedergaard, M., 2006. Astrocyte-mediated control of cerebral blood flow. Nat. Neurosci. 9, 260–267. https://doi.org/10.1038/nn1623

Tanaka, Y., Marumo, T., Shibuta, H., Omura, T., Yoshida, S., 2009. Serum S100B, brain edema, and hematoma formation in a rat model of collagenase-induced hemorrhagic stroke. Brain Res. Bull. 78, 158–163. https://doi.org/10.1016/j.brainresbull.2008.10.012

Tateishi, N., Mori, T., Kagamiishi, Y., Satoh, S., Katsube, N., Morikawa, E., Morimoto, T., Matsui, T., Asano, T., 2002. Astrocytic activation and delayed infarct expansion after permanent focal ischemia in rats. Part II: suppression of astrocytic activation by a novel agent (R)-(-)-2-propyloctanoic acid (ONO-2506) leads to mitigation of delayed infarct expansion and early . J. Cereb. Blood Flow Metab. 22, 723–734. https://doi.org/10.1097/00004647-200206000-00011

Thabet, A.M., Kottapally, M., Hemphill, J.C., 2017. Management of intracerebral hemorrhage, in: Handbook of Clinical Neurology. Elsevier B.V., pp. 177–194. https://doi.org/10.1016/B978-0-444-63600-3.00011-8

Turrin, N.P., Plata-Salamán, C.R., 2000. Cytokine-cytokine interactions and the

brain. Brain Res. Bull. https://doi.org/10.1016/S0361-9230(99)00203-8

Ullian, E.M., Sapperstein, S.K., Christopherson, K.S., Barres, B.A., 2001. Control of synapse number by glia. Science (80-.). 291, 657–661. https://doi.org/10.1126/science.291.5504.657

van Asch, C.J., Luitse, M.J., Rinkel, G.J., van der Tweel, I., Algra, A., Klijn, C.J., 2010. Incidence, case fatality, and functional outcome of intracerebral haemorrhage over time, according to age, sex, and ethnic origin: a systematic review and meta-analysis. Lancet Neurol. 9, 167–176. https://doi.org/10.1016/S1474-4422(09)70340-0

Villarreal, A., Seoane, R., Torres, A.G., Rosciszewski, G., Angelo, M.F., Rossi, A., Barkert, P.A., Ramos, A.J., 2014. S100B protein activates a RAGE-dependent autocrine loop in astrocytes: Implications for its role in the propagation of reactive gliosis. J. Neurochem. 131, 190–205. https://doi.org/10.1111/jnc.12790

Vizuete, A.F., de Souza, D.F., Guerra, M.C., Batassini, C., Dutra, M.F., Bernardi, C., Costa, A.P., Gonçalves, C.-A., 2013. Brain changes in BDNF and S100B induced by ketogenic diets in Wistar rats. Life Sci. 92, 923–928. https://doi.org/10.1016/j.lfs.2013.03.004

Wajima, D., Nakagawa, I., Nakase, H., Yonezawa, T., 2013. Neuroprotective effect of suppression of astrocytic activation by arundic acid on brain injuries in rats with acute subdural hematomas. Brain Res. 1519, 127–135. https://doi.org/10.1016/j.brainres.2013.05.002

Wang, H., Zhang, L., Zhang, I.Y., Chen, X., Da Fonseca, A., Wu, S., Ren, H., Badie, S., Sadeghi, S., Ouyang, M., Warden, C.D., Badie, B., 2013. S100B promotes glioma growth through chemoattraction of myeloid-derived macrophages. Clin. Cancer Res. 19, 3764–75. https://doi.org/10.1158/1078-0432.CCR-12-3725

Wang, J., 2010. Preclinical and clinical research on inflammation after intracerebral hemorrhage. Prog. Neurobiol. https://doi.org/10.1016/j.pneurobio.2010.08.001

Wang, J., Doré, S., 2007. Inflammation after intracerebral hemorrhage. J. Cereb. Blood Flow Metab. 27, 894–908. https://doi.org/10.1038/sj.jcbfm.9600403

Wang, J., Rogove, A.D., Tsirka, A.E., Tsirka, S.E., 2003. Protective role of

tuftsin fragment 1-3 in an animal model of intracerebral hemorrhage. Ann. Neurol. 54, 655–664. https://doi.org/10.1002/ana.10750

Wang, J., Tsirka, S.E., 2005. Tuftsin Fragment 1–3 Is Beneficial When Delivered After the Induction of Intracerebral Hemorrhage. Stroke 36, 613–618. https://doi.org/10.1161/01.STR.0000155729.12931.8f

Wang, S., Li, D., Huang, C., Wan, Y., Wang, J., Zan, X., Yang, B., 2018. Overexpression of adiponectin alleviates intracerebral hemorrhage-induced brain injury in rats via suppression of oxidative stress. Neurosci. Lett. 681, 110–116. https://doi.org/10.1016/j.neulet.2018.05.050

Wang, Y.C., Zhou, Y., Fang, H., Lin, S., Wang, P.F., Xiong, R.P., Chen, J., Xiong, X.Y., Lv, F.L., Liang, Q.L., Yang, Q.W., 2014. Toll-like receptor 2/4 heterodimer mediates inflammatory injury in intracerebral hemorrhage. Ann. Neurol. 75, 876–889. https://doi.org/10.1002/ana.24159

Wasserman, J.K., Schlichter, L.C., 2007. Neuron death and inflammation in a rat model of intracerebral hemorrhage: Effects of delayed minocycline treatment. Brain Res. 1136, 208–218. https://doi.org/10.1016/j.brainres.2006.12.035

Wilson, J.X., 1997. Antioxidant defense of the brain: A role for astrocytes. Can. J. Physiol. Pharmacol. https://doi.org/10.1139/y97-146

Won, S.Y., Schlunk, F., Dinkel, J., Karatas, H., Leung, W., Hayakawa, K., Lauer, A., Steinmetz, H., Lo, E.H., Foerch, C., Gupta, R., 2013. Imaging of contrast medium extravasation in anticoagulation-associated intracerebral hemorrhage with dual-energy computed tomography. Stroke 44, 2883–2890. https://doi.org/10.1161/STROKEAHA.113.001224

Wu, H., Wu, T., Hua, W., Dong, X., Gao, Y., Zhao, X., Chen, W., Cao, W., Yang, Q., Qi, J., Zhou, J., Wang, J., 2015. PGE2 receptor agonist misoprostol protects brain against intracerebral hemorrhage in mice. Neurobiol. Aging 36, 1439–1450. https://doi.org/10.1016/j.neurobiolaging.2014.12.029

Wu, H., Zhang, Z., Hu, X., Zhao, R., Song, Y., Ban, X., Qi, J., Wang, J., 2010. Dynamic changes of inflammatory markers in brain after hemorrhagic stroke in humans: a postmortem study. Brain Res. 1342, 111–7. https://doi.org/10.1016/j.brainres.2010.04.033

Wu, J., Hua, Y., Keep, R.F., Nakamura, T., Hoff, J.T., Xi, G., 2003. Iron and

Iron-Handling Proteins in the Brain after Intracerebral Hemorrhage. Stroke 34, 2964–2969. https://doi.org/10.1161/01.STR.0000103140.52838.45

Wu, J., Yang, S., Xi, G., Fu, G., Keep, R.F., Hua, Y., 2009. Minocycline reduces intracerebral hemorrhage-induced brain injury. Neurol. Res. 31, 183–8. https://doi.org/10.1179/174313209X385680

Wu, J., Yang, S., Xi, G., Song, S., Fu, G., Keep, R.F., Hua, Y., 2008. Microglial activation and brain injury after intracerebral hemorrhage. Acta Neurochir. Suppl. 105, 59–65.

Wu, T., Wu, H., Wang, Jessica, Wang, Jian, 2011. Expression and cellular localization of cyclooxygenases and prostaglandin E synthases in the hemorrhagic brain. J. Neuroinflammation 8, 22. https://doi.org/10.1186/1742-2094-8-22

Xi, G., Keep, R., Hoff, J., 2006. Mechanisms of brain injury after intracerebral haemorrhage. Lancet Neurol. 5, 53–63.

Xi, G., Reiser, G., Keep, R.F., 2003. The role of thrombin and thrombin receptors in ischemic, hemorrhagic and traumatic brain injury: deleterious or protective? J. Neurochem. 84, 3–9.

Xiong, X.Y., Wang, J., Qian, Z.M., Yang, Q.W., 2014. Iron and Intracerebral Hemorrhage: From Mechanism to Translation. Transl. Stroke Res. https://doi.org/10.1007/s12975-013-0317-7

Xue, M., Del Bigio, M.R., 2003. Comparison of brain cell death and inflammatory reaction in three models of intracerebral hemorrhage in adult rats. J. Stroke Cerebrovasc. Dis. 12, 152–159. https://doi.org/10.1016/S1052-3057(03)00036-3

Yang, Z., Liu, Y., Yuan, F., Li, Z., Huang, S., Shen, H., Yuan, B., 2014. Sinomenine inhibits microglia activation and attenuates brain injury in intracerebral hemorrhage. Mol. Immunol. 60, 109–114. https://doi.org/10.1016/j.molimm.2014.03.005

Yang, Z., Zhong, S., Liu, Y., Shen, H., Yuan, B., 2015. Scavenger receptor SRA attenuates microglia activation and protects neuroinflammatory injury in intracerebral hemorrhage. J. Neuroimmunol. 278, 232–238. https://doi.org/10.1016/j.jneuroim.2014.11.010

Zhang, Y., Yang, Y., Zhang, G.Z., Gao, M., Ge, G.Z., Wang, Q.Q., Ji, X.C., Sun, Y.L., Zhang, H.T., Xu, R.X., 2016. Stereotactic Administration of Edaravone

Ameliorates Collagenase-Induced Intracerebral Hemorrhage in Rat. CNS Neurosci. Ther. 22, 824–835. https://doi.org/10.1111/cns.12584

Zhang, Zhen, Zhang, Ze, Lu, H., Yang, Q., Wu, H., Wang, J., 2017. Microglial Polarization and Inflammatory Mediators After Intracerebral Hemorrhage. Mol. Neurobiol. 54, 1874–1886. https://doi.org/10.1007/s12035-016-9785-6

Zhou, S., Bao, J., Wang, Y., Pan, S., 2016. S100β as a biomarker for differential diagnosis of intracerebral hemorrhage and ischemic stroke. Neurol. Res. 38, 327–332. https://doi.org/10.1080/01616412.2016.1152675

Zhou, Y., Wang, Y., Wang, J., Anne Stetler, R., Yang, Q.W., 2014. Inflammation in intracerebral hemorrhage: From mechanisms to clinical translation. Prog. Neurobiol. https://doi.org/10.1016/j.pneurobio.2013.11.003

Ziai, W.C., Carhuapoma, J.R., 2018. Intracerebral Hemorrhage. Contin. Lifelong Learn. Neurol. 24, 1603–1622. https://doi.org/10.1212/CON.0000000000000672

Zou, J., Wang, Y.X., Dou, F.F., Lü, H.Z., Ma, Z.W., Lu, P.H., Xu, X.M., 2010. Glutamine synthetase down-regulation reduces astrocyte protection against glutamate excitotoxicity to neurons. Neurochem. Int. 56, 577–584. https://doi.org/10.1016/j.neuint.2009.12.021